FEATURE EXTRACTION STRATEGIES BASED ON MATHEMATICAL MORPHOLOGY FOR THE ANALYSIS OF REMOTELY SENSED IMAGERY

Thesis

Submitted in partial fulfillment of the requirements for the degree of

DOCTOR OF PHILOSOPHY

by

RISHIKESHAN C A

(Reg. No: 148037 AM14F06)

DEPARTMENT OF APPLIED MECHANICS AND HYDRAULICS

NATIONAL INSTITUTE OF TECHNOLOGY KARNATAKA

SURATHKAL, MANGALURU – 575 025

AUGUST 2019

FEATURE EXTRACTION STRATEGIES BASED ON MATHEMATICAL MORPHOLOGY FOR THE ANALYSIS OF REMOTELY SENSED IMAGERY

Thesis

Submitted in partial fulfillment of the requirements for the degree of

DOCTOR OF PHILOSOPHY

by

RISHIKESHAN C A

(Reg. No: 148037 AM14F06)

DEPARTMENT OF APPLIED MECHANICS AND HYDRAULICS

NATIONAL INSTITUTE OF TECHNOLOGY KARNATAKA

SURATHKAL, MANGALURU – 575 025

AUGUST 2019

DECLARATION
by the Ph.D. Research scholar

I hereby *declare* that the Research Thesis entitled "**Feature Extraction Strategies Based on Mathematical Morphology for the Analysis of Remotely Sensed Imagery**" which is being submitted to the **National Institute of Technology Karnataka, Surathkal** in partial fulfilment of the requirements for the award of the Degree of **Doctor of Philosophy** in the **Department of Applied Mechanics and Hydraulics** is a *bonafide report of the research work carried out by me*. The material contained in this Research Thesis has not been submitted to any University or Institution for the award of any degree.

148037 AM14F06, RISHIKESHAN C A

(Register Number, Name & Signature of the Research Scholar)

Department of Applied Mechanics and Hydraulics

National Institute of Technology Karnataka, Surathkal

Place: NITK-Surathkal

Date: 20|08|2019

C E R T I F I C A T E

This is to *certify* that the Research Synopsis entitled "**Feature Extraction Strategies Based on Mathematical Morphology for the Analysis of Remotely Sensed**" submitted by **Rishikeshan C A** (Register Number: 148037 AM14F06) as the record of the research work carried out by him, is *accepted as the Research Thesis submission* in partial fulfilment of the requirements for the award of degree of **Doctor of Philosophy**.

20/08/2019

Dr. H. Ramesh

(Research Guide)

Prof. Amba Shetty

(Chairperson - DRPC)

Chairman (DRPC)
Department of Applied Mechanics & Hydraulics
National Institute of Technology Karnataka Surathkal
Mangalore -575025, Karnataka,INDIA

DEPARTMENT OF APPLIED MECHANICS AND HYDRAULICS

NATIONAL INSTITUTE OF TECHNOLOGY KARNATAKA,

SURATHKAL, MANGALURU – 575 025

ACKNOWLEDGEMENTS

Rishikeshan C A

ABSTRACT

The thesis evolves on the development of novel feature extraction methods for the analysis of remotely sensed images which are enabled to enhance the robustness and the generalization properties of the feature extraction system. Recent developments in optical data sensors mounted on-board of both space-borne and airborne earth observation platforms have led to increasing volume, acquisition speed and a variety of sensed images. Therefore the feature extraction from remotely sensed imageries is a major concern and challenge for the photogrammetry, remote sensing, and GIS communities. The extensive survey of literatures expose the shortcomings overlooked for the existing approaches utilized in the feature extraction of remote sensing images. The automated extraction of features from the remotely sensed images has been an active area of research for over a decade due to its substantial role in several application areas viz. urban planning, transportation navigation, traffic management, emergency handling, etc. Although the concept of feature extraction is relatively simple, the reliability and accuracy remains a major challenge.

With advanced imaging technologies, there is an augmented demand for developing new approaches which can exhaustively explore the information embedded in remote sensing images. The past studies evidenced mathematical morphological tools as best suited for the potential exploitation of the spatial information in the remote sensing imageries. Priorly, mathematical morphology was applied only for the interpretation of binary images. However, it was extended to analyze grey scale and colour images. The thesis presents different spatial feature extraction methods which are developed based on mathematical morphology for the analysis of remote sensing optical images addressing to different applications such as urban feature detection, waterbody extraction, crop field boundary extraction and shoreline extraction. The morphology based feature extraction algorithms developed are effective and contribute to the interpretation of high resolution remotely sensed images.This automatic, scalable, and parallel processing methods can be used to analyze colossal remote sensing data within the selected classification schemes of remote sensing image system. The proposed methodologies contribute to the operational use of remote sensing datasets in many

practical applications related to monitoring and management of environmental resources.

In this thesis, a novel approach is presented for extracting shoreline from remotely sensed images. Shoreline extraction is inevitable for several studies such as coastal zone management, coastline erosion monitoring, GIS database updating, watershed definition, flood plain mapping and the evaluation of water resources. Multiple techniques are proposed for the extraction of different types of waterbodies such as lakes, rivers and glacier lakes. MM techniques have been exploited for the extraction of crop field boundaries from multiple satellite imageries. UAV driven images are beneficial as they facilitate a comprehensive description of the scenes, and concurrently require pertinent image processing techniques to exploit the geometrical information from the image datasets. This study introduces two innovative feature extraction methods for UAV and satellite images

The novel feature extraction techniques proposed in the thesis have been investigated and experimented in different datasets to test their degree of performance. The experimental investigation performed with the developed techniques for analysis of remotely sensed images are noted for its improved accuracy when compared against other state of the art methods.

Keywords: Remote sensing, image processing, computer vision, mathematical morphology, classification, shoreline detection, waterbody extraction, crop field boundary delineation, building extraction, UAV, VHR images, urban features.

CONTENTS

LIST OF FIGURES

LIST OF TABLES

ABBREVIATIONS

ANN	Artificial Neural Network
AoI	Area of Interest
AP	Attribute profiles
DMP	Differential Morphological Profiles
DN	Digital Number
EAP	Extended Attribute profiles
ECHO	Extraction and Classification of Homogeneous Objects
ETM	Enhanced Thematic Mapper
GIS	Geographic Information System
LISS	Linear Imaging Self-Scanning System
MCC	Matthews Correlation Coefficient
ML	Maximum Likelihood
MM	Mathematical Morphology
MNDWI	Modified Normalized Difference Water Index
MSS	Multispectral Scanner Systems.
NDVI	Normalized Difference Vegetation Index
NDWI	Normalized Difference Water Index
NIR	Near Infrared
PAN	Panchromatic
RGB	Red-Green-Blue
RoI	Region of Interest
RS	Remote Sensing
SDC	SDC information systems
SVM	Support Vector Machines
SE	Structuring Element
TM	Thematic Mapper
UAV	Unmanned Aerial Vehicle
VHR	Very High Resolution

CHAPTER 1

INTRODUCTION

This chapter introduces the relevance of the thesis and defines the objectives therein. The proposed study lays out its interest in feature extraction techniques based on mathematical morphology for the analysis of remotely sensed images. The background of remote sensing imaging systems and the image processing of the remotely sensed images are concisely presented with particular emphasis to the feature extraction techniques, and a brief elucidation of fundamental concepts of mathematical morphology is provided. The chapter closes with a description of the structural framework of the thesis.

1.1 OVERVIEW ON REMOTE SENSING IMAGING SYSTEMS

Remote sensing is a potentially revolutionary technology with significant methodological and theoretical implications, which monitors the changes in the Earth's environment and surface features continuously in an objective way (Blumberg and Jacobsen, 1997). Generally, the term 'remote sensing' refers to the method that employs electromagnetic radiation (e.g. light, heat and radio waves) as the means of detecting and measuring target characteristics (Sabins, 1997). A basic assumption in remote sensing is that specific targets such as diverse soil types, water with varying degrees of impurities, rocks of differing lithologies, vegetation of several species etc. have an individual and characteristic manner of interacting with incident radiation that is described by the spectral response of that target (Mather, 2004). The current progress of remote sensing systems, based on airborne and space borne platforms and comprising active and passive sensors, offers an unprecedented wealth of information about the Earth's surface for environmental monitoring, sustainable resource management, disaster prevention, emergency response and defense (Moser et al. 2018). A detailed understanding of remote sensing and digital image interpretation is available in Jensen (1986), Lillesand & Kiefer (1994), Robert (2007), Zhu et al. (2017), Moser et al.(2018).

Feature Extraction Strategies Based on Mathematical Morphology for the Analysis of Remotely Sensed Imagery, PhD Thesis, 2019, NITK Surathkal, India.

1

Remote sensing has advanced from balloon photography to hyper-spectral satellite imaging. Last decades witnessed rapid technological advancement in the field of remote sensing and offers an increasingly wide array of imagery with a broad variety of spectral and spatial resolution (Fisher et al. 2017). The remote sensing data promotes an increased prospect to assess, monitor and predict the dynamics of land-covers, anthropologic processes, and influence to the environments (Huang et al. 2017). The rapid accumulation of gigabytes worth of satellite and aerial data on a daily basis has rendered scalable, robust and automated tools, designed for their management, search, and retrieval, and essential for their effectual exploitation (Bosilj et al. 2016). Broader and increasingly interdisciplinary applications are driven by the evolving technological characteristics of remote sensing systems, widespread availability of remotely sensed imagery, and developing of wide range of data processing and analysis techniques (Fugate, 2010). Human visual perception makes quantification of the true spectral composition of an object difficult, in contrast, artificial vision systems (imagers) such as RGB (red-green-blue) cameras, satellite sensors, and spectrometers allow a much more precise quantification of the spectral properties, which are directly linked to the chemical composition of the object of interest (Brydegaard et al. 2009). It is clearly understood from Figure 1.1
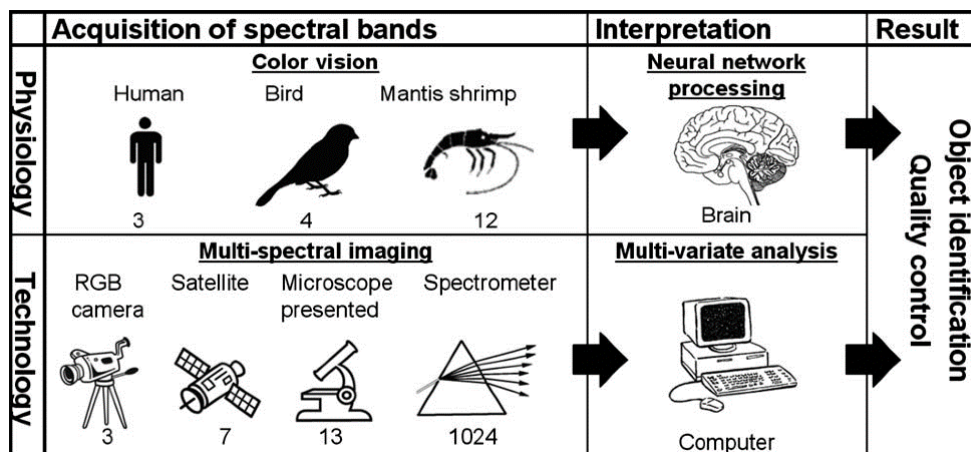
Figure 1.1 Relation between colour vision, multispectral imaging, multivariate analysis, and spectral bands of various species or spectral instruments (Source: Brydegaard et al. 2009)

The repetitive and consistent view of the earth acquired from imaging systems, particularly those on board satellites has been utilized in various remote sensing applications such as urban sprawl analysis, deforestation and crop monitoring, weather prediction, land use land cover mapping etc. (Fonseca, 2009).The spectral imaging systems acquiring data in contiguous 10-nm-wide bands, can generate data with adequate resolution for the direct identification of those materials with diagnostic spectral features (Goetz et al. 1985).

The concept of spectral imaging for remote sensing of terrestrial features and objects emerge as an alternative to high-spatial-resolution, large-aperture satellite imaging systems; it is conceptualized in Figure 1.2. An airborne or space-borne imaging sensor concurrently samples multiple spectral wavebands over a large area in a ground-based scene. After suitable processing, each pixel in the resulting image comprises a sampled spectral measurement of reflectance, which can be interpreted to recognize the material present in the scene. The graphs in the figure illustrate the spectral variation in reflectance for soil, water, and vegetation (Shaw and Burke, 2003).
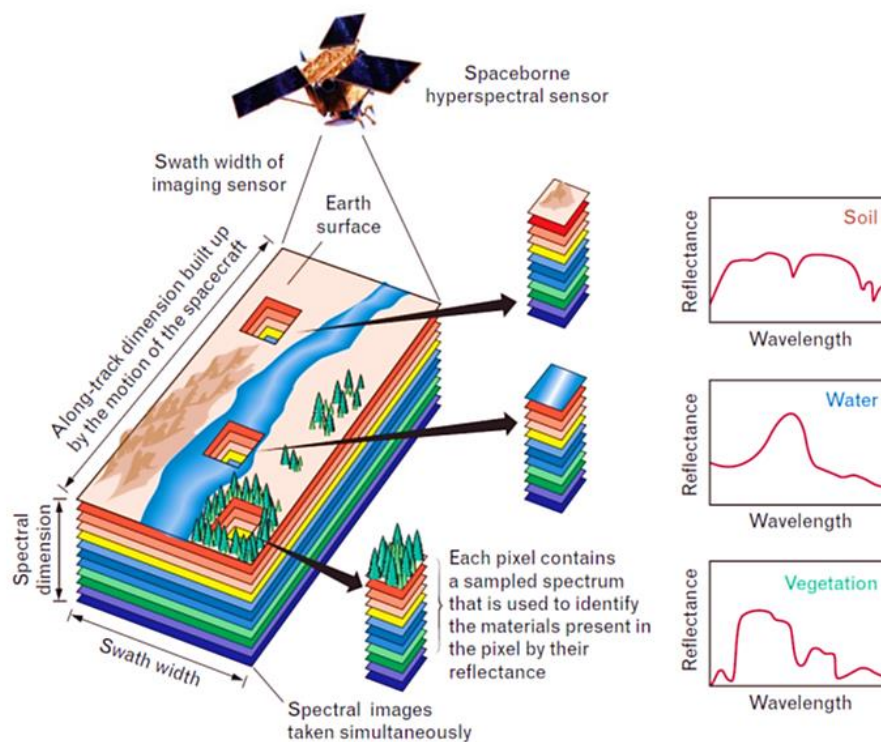
Figure 1.2 The concept of imaging spectroscopy (source: Shaw and Burke, 2003).

Feature Extraction Strategies Based on Mathematical Morphology for the Analysis of Remotely Sensed Imagery, PhD Thesis, 2019, NITK Surathkal, India.

3

The modern earth remote sensing technology from satellites unfolded in 1972, when the Landsat Multispectral Scanner System (MSS) provided for the first time, a consistent set of synoptic, high-resolution earth images to the world scientific community (Robert, 2007). The Earth's surface is represented in great detail with very high spatial resolution satellite datasets since 1999 (Carleer, 2005). Multi- and Hyper spectral technologies have supported remote sensing Earth Observation (EO) to stride forward in the last decades (Transon, 2018). Multispectral remote sensing technologies, in a single observation, collect data from several spectral bands from the visible and near-infrared region of the electromagnetic spectrum, over the past 2 decades, the development of airborne and satellite hyperspectral sensor technologies has overcome the limitations of multispectral sensors (Govender, 2008). Figure 1.3 brings a basic comparison between the multispectral and hyper-spectral imaging.
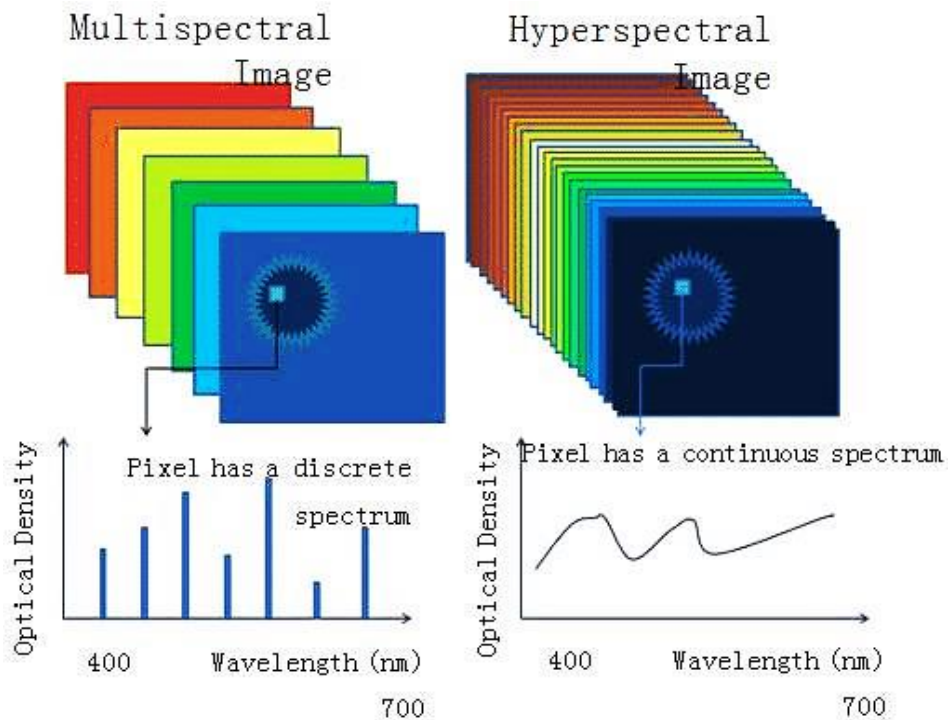
Figure 1.3 Comparison between Multispectral Imaging and Hyperspectral Imaging (Source: Aboras et al. 2015).

One of the potential game-changing opportunities in earth observation has come through advances in the technology associated with unmanned aerial vehicles (McCabe et al. 2017). Unmanned Aerial Vehicles (UAV) have arose as a fast, low-cost and

flexible data acquisition system and produce high-resolution imagery which has enabled a new approach for defining property boundaries (Crommelinck et al. 2016).

The availability of very high resolution commercial satellite data has ignited much interest to extract man-made objects from such imagery (Xiao et al. 2004). For application of remote sensing on different sectors, it is necessary to develop a specific methodology to extract information from the image data. Image Processing and Analysis can be defined as the "act of examining images for the purpose of identifying objects and judging their significance". The remotely sensed data is analyzed and experimented through logical process in detecting, identifying, classifying, measuring and evaluating the significance of physical and cultural objects, their patterns and spatial relationship (Babar, 2006). The applications of the high-resolution remote sensing image processing mainly include the following aspects: city remote sensing, basic geographic mapping, environmental monitoring and assessment, precision agriculture, and public information service, etc. (Wang et al. 2016). Digital imaging process encompass a wide variety of techniques and mathematical tools, and each application involves a sequence of processing steps (Hord, 1982). The identification of a procedure based on image processing techniques that is more adequate to the problem solution is essential to develop a methodology (Fonseca, 2009). The fundamental steps involved in an image processing are depicted in the flowchart shown in Figure 1.4 and reported as the idealized sequence for image processing.

Pre-processing comprises set of operations that prepare data for successive analysis that correct or compensate for systematic errors and subsequently, the analyst may use feature extraction to decrease the dimensionality of the data. The next step image enhancement is fundamentally improving the interpretability or perception of information in imagery for end users and providing improved input for other automated image processing techniques (Maini and Aggarwal, 2010). Image enhancement accepts a digital image as input and produce an enhanced image as output by increasing or decreasing the contrast, removing and introducing geometric distortions, edge

---

Feature Extraction Strategies Based on Mathematical Morphology for the Analysis of Remotely Sensed Imagery, PhD Thesis, 2019, NITK Surathkal, India.

5

sharpening or smoothing or altering the image in some respect that facilitates the interpretation of its information content (Hord, 1982).
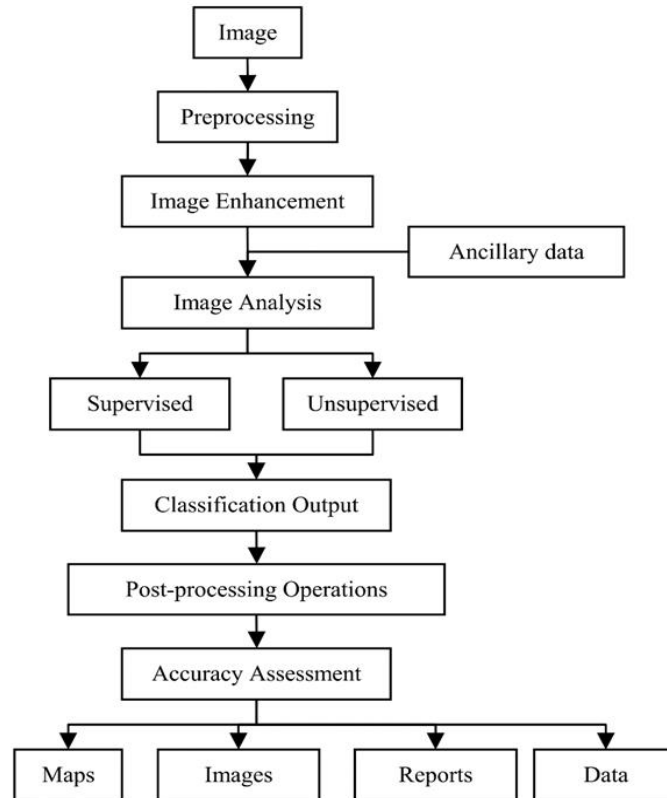
Figure 1.4. Fundamental steps in remote sensing image processing

(Source: Fonseca, 2009).

The different land cover categories in an image can be differentiated with image classification algorithms by spectral features, i.e. the brightness and "colour" information contained in each pixel; the classification procedures can be "supervised", "unsupervised" (Kar and Kelkar, 2013) or "semi-supervised". Selecting suitable variables is a critical step for successfully implementing an image classification (Lu and Weng, 2007). Usually multispectral remote sensing imagery have numerous bands, and might have large redundant information so it becomes difficult to extract the key features of the image. Therefore, it is necessary to study the methods regarding how to extract the desired features from the image effectively (Tian et al. 2005). In the context of remote sensing, feature extraction can be expressed as an image processing technique to recognize and classify mutual relationships between image regions (Baatz et al. 2000;

Feature Extraction Strategies Based on Mathematical Morphology for the Analysis of Remotely Sensed Imagery, PhD Thesis, 2019, NITK Surathkal, India.

6

Momm and Easson, 2011). The present study has focused in detail on the feature extraction techniques for the image processing of remotely sensed images.

1.2 FEATURE EXTRACTION IN SATELLITE IMAGERY

Image segmentation and feature extraction are two major components of modern computerized image analysis or "machine vision (Sklansky, 1978). Feature extraction in image processing is a method of transforming large redundant data into a reduced data representation (Athira and Sreekumar, 2014). Several successful feature extraction methods have been developed in the past decade to this end (Aptoula, 2014). The evolutionary algorithms for remote sensing feature extraction are discussed in Momm and Easson (2011). The efficiency of feature extraction method enhances further processing of an image to a great extent (Goel et al. 2016). Feature extraction strategies include traditional pixel-driven remote sensing image classification procedures in which each distinct pixel is independently assessed and allotted to one class (Lillesand & Kiefer, 2000). In contrast, image segmentation methods create a continuous boundary, however it requires more post segmentation processing steps to delineate the boundary pixels, and encounter difficulties of determining a reliable threshold in thresholding algorithms, and formulating homogeneous criteria in region growing, and region splitting and merging algorithms (Liu and Jezek, 2004). There are two fundamentally different strategies for image segmentation, i.e., edge detection and region growing (Benediktsson et al. 2003). Edge (boundary) based methods are segmentation methods based on discontinuity where abrupt changes in the intensity value are found and facilitates higher level image analysis (Saini and Arora, 2014). If the edges of images are identified precisely, all of the objects can be located and the basic parameters such as area, perimeter and shape can be measured (Joshi and Koju, 2012). Among the two major types, one is the first derivative-based edge detection operator which detect image edges by computing the image gradient values, such as Roberts operator, Sobel operator, Prewitt operator and the other is the second derivative-based edge detection operator, by seeking in the second derivative zero-crossing to edge detection, such as LOG operator, Canny operator (Bin and Yeganeh, 2012). However, edge detection methods suffer from the fact that the edge pixels

produced by edge detectors are quite discontinuous and hardly characterize any linear features completely (Lee and Jurkevich 1990; Mason and Davenport 1996).

Benediktsson et al (2003) investigated the use of two feature extraction methods and a simple feature selection approach. The considered approaches were decision boundary feature extraction for neural networks, discriminant analysis feature extraction, and simple feature selection based on sorting the indexes of the DMP (Differential Morphological Profiles) using the value of the discrete derivative. Major research and developmental efforts are put on the automated extraction of man-made structures, like roads and buildings from digital aerial and space imagery, the approaches range from manual methods, to semi-automated and automated feature extraction methods from single and multiple image frames and digital surface models (Gulch, 2000). Consequently, the significance of designing and implementing flexible automated feature extraction practices to advance the information extraction procedures have been highlighted in the previous studies.

The theoretical concepts and workflow involved in feature extraction techniques are described subjectively in the following chapters. Over the past decade, the incorporation of spatial information has drawn increasing attention in multispectral and hyperspectral data analysis (Wang et al, 2016). In the last decades there has been a constant increase in geometrical resolution of Earth observation sensors. The spatial information provides an ever increasing contribution to interpret the remote sensing imagery, as it characterizes the remotely sensed landscape in a complementary way with respect to the spectral signatures of the land covers (Mura, 2011). The mathematical models for image processing and analysis play fundamental roles, by effectively exploiting the potential conveyed by the availability of remote sensing data that requires automatic or semi-automatic techniques capable of suitably characterizing and extracting thematic information of interest while minimizing the need for user intervention (Moser et al, 2018). In this scenario of the modelling of the spatial information, mathematical morphology (MM) plays a pivotal role as it consists of powerful set of tools for analyzing the spatial domain (Soille et al, 1998; Soille and

----
Feature Extraction Strategies Based on Mathematical Morphology for the Analysis of Remotely Sensed Imagery, PhD Thesis, 2019, NITK Surathkal, India.

8

Pesaresi 2002).It can extract or suppress desired image features by using set operators such as union, intersection, and complementation with a set of meticulously selected (for both shape and size) structuring elements (SEs) (Wang et al, 2016). It has indeed motivated this study to further advance the robustness and accuracy of feature extraction techniques for the effective analysis of spatial structures in remote sensing images based on mathematical morphology. The fundamental theory and concepts of mathematical morphology (MM) are described in the following section.

1.3 MATHEMATICAL MORPHOLOGY: THEORETICAL BACKGROUND

Mathematical morphology was first introduced in 1964 through the collaboration of Georges Matheron and Jean Serra who established its basic concepts and tools (Matheron, 1975). It contributes a wide range of operators to image processing domain, all deal with a few mathematical concepts from set theory (Serra, 1982). MM is a tool for extracting image components that are useful for representation and description. Morphological procedures usually probe an image with a template or shape known as a structuring element (SE) or kernel. The SE is placed at all possible places in the image and is matched with the equivalent neighbourhood of pixels. These set theory based operations have been broadly reviewed and discussed in image processing texts of Parker (1997) Soille, (1999), Seul et al. (2001) and Gonzalez and Woods (2002). Dilation and erosion are the two primary morphological operations. The erosion operation X Θ B is denoted by εB (X) in a functional form (Serra, 1982). Similarly, the dilation operation X ⊕ B is denoted by δB (X) in a functional form.

Erosion is a Minkowski subtraction, which is the intersection of translated point sets (Eq. 1.1). Erosion combines two sets using vector subtraction of set elements (Eq. 1.2). The image X eroded by the structuring element B is the intersection of all translations of the image X by vector −b ∈ B (Figure 1.5).

$$X \ominus B = \bigcap_{b \in B} X_{-b} \tag{1.1}$$

$$\varepsilon B\,(X) = X \ominus B = \{p \in Z^2 : p = x + b \in X \text{ for every } b \in B\} \tag{1.2}$$

Feature Extraction Strategies Based on Mathematical Morphology for the Analysis of Remotely Sensed Imagery, PhD Thesis, 2019, NITK Surathkal, India.

9

This formula says that every point p from the image is tested; the result of the erosion is given by those points p for which all possible p + b are in X
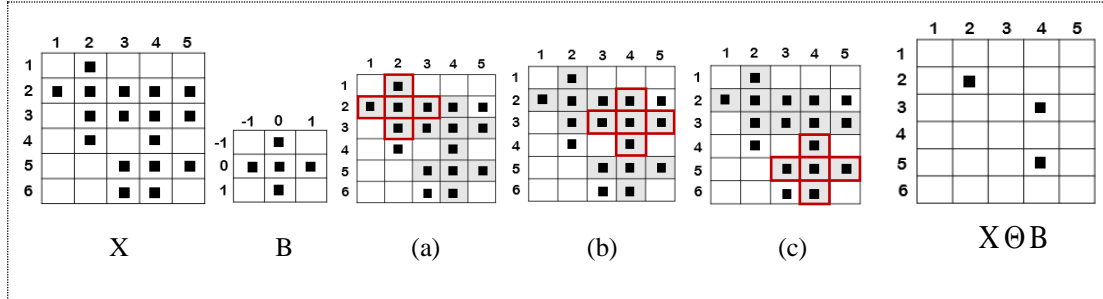
Figure 1.5 Illustration of an erosion operation. Where, X is input image, B is the structuring element, (a) – (c) are the intermediate processing stage and X ⊖ B is the final eroded image.

Dilation is a Minkowski addition, which can be expressed as a union of translated point sets ((Eq. 1.3). Dilation X ⊕ B is the point set of all the possible vector additions of pairs of elements, one from each of the sets X and B (Figure 1.6).

$$\delta_B (X) = X \oplus B = \{p \in Z^2 : p = x + b, x \in X \text{ and } b \in B\} \tag{1.3}$$

Similarly, it can be expressed as a union of translated point sets (Eq. 1.4). Every point p from the image is tested; the result of the Dilation is given by those points p for which all possible p + b are in X

$$X \oplus B = \bigcup_{b \in B} X_b \tag{1.4}$$
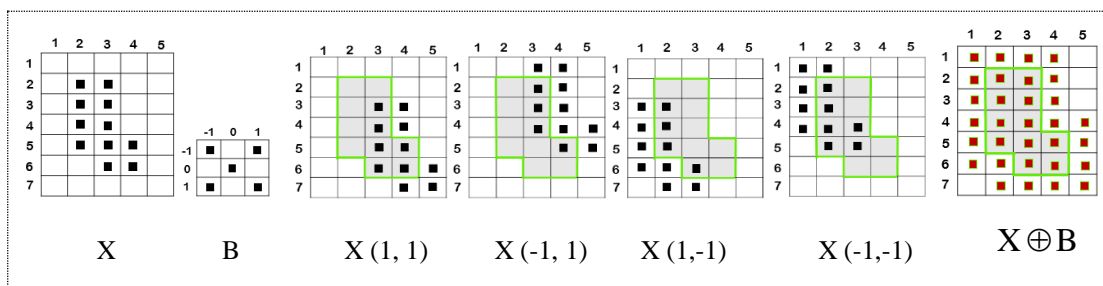
Figure 1.6. Illustration of a dilation operation. Where, X is input image, B is the structuring element, (a) – (c) are the intermediate translations of the image, and X ⊕ B is the final dilated image.

The erosion and dilation can be extended to include grayscale images: The formulae

----
Feature Extraction Strategies Based on Mathematical Morphology for the Analysis of Remotely Sensed Imagery, PhD Thesis, 2019, NITK Surathkal, India.

10

for erosion ε and dilation δ of a grayscale image f with a structuring element B is as follows (Eq. 1.5 and Eq. 1.6 respectively):

$$(\in (f))(x) = \underset{b \in B}{\min} \; f(x+b) \tag{1.5}$$

$$(\delta (f))(x) = \underset{b \in B}{\max} \; f(x+b) \tag{1.6}$$

Morphologic opening γ (f) and closing φ (f) operation for gray-scale image is in equations 1.7 and 1.8 respectively (Figure 1.7).

$$\text{Opening: } \gamma (f) = \delta (\varepsilon (f)) = f \circ B = (f \ominus B) \oplus B \tag{1.7}$$

$$\text{Closing: } \varphi (f) = \varepsilon (\delta (f)) = f \bullet B = (f \oplus B) \ominus B \tag{1.8}$$
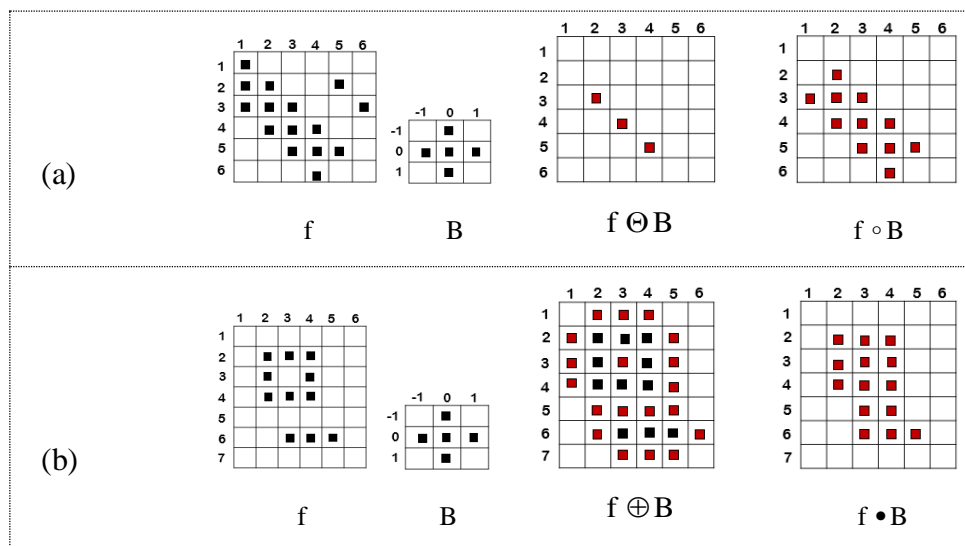
Figure 1.7. Illustration of an (a) Opening and (b) Closing operation. Where f is input image, B is the structuring element, f ∘ B is the opened image, and f • B is the closed image.

Top-hat and Bot-hat transforms are applied to improve the contrast of images by using morphological methods (Serra, 1982). They are referred as Open Top-hat (White Top-hat) and Close Top-hat (Black Top-hat) respectively. Top-Hat transform is achieved by subtracting the Opening of the image from its original image (Eq. 1.9), and Bot-hat transforms achieved by subtracting the original image from its closing (Eq. 1.10).

$$T_{hat}(f) = f - (f \circ B)$$

(1.9)

$$B_{hat}(f) = (f \bullet B) - f$$

(1.10)

One major application of these transforms is in eliminating the objects that do not fit in the image by making use of a structuring element in the opening and closing (Li, et al. 2014). Top-hat is used for light objects on a dark background and Bottom-hat for dark objects on a light background (Dougherty and Lotufo, 2003). One of the main application of top-hat transformation is in correcting the effects of non-uniform illumination (Wang et al. 2017).

Reconstruction is based on geodesic dilation or erosion (Figure 1.8). The geodesic dilation (Eq. 1.11) repeated n times is expressed and given by

$$\delta_g^{(n)}(f) = \delta_g^{(n-1)}(f)$$

(1.11)

Reconstruction by dilation Rg (f) is given by equation 1.12 (where g is a mask image, f is a marker Image)

$$R_g(f) = \delta_g^{(i)}(f)$$

(1.12)

Where, $\delta_g^{(i)}(f) = \delta_g^{(i+1)}(f)$

(a) (b) (c) (d) (e) (f)
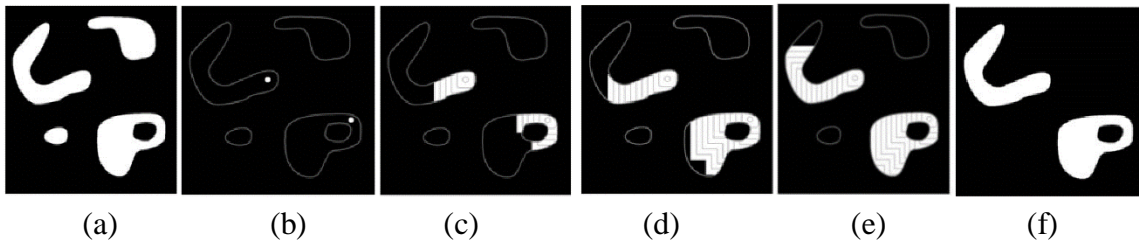
Figure 1.8. Illustration of a Morphological reconstruction. (a) Original image (the mask) (b) Marker image. (c) - (e) Intermediate result after 100, 200 and 300 iterations respectively. (f) Final result. (Gonzalez et al. 2009).

Likewise, the Opening by Reconstruction (Eq. 1.13) and Closing by Reconstruction (Eq. 1.14) can be expressed as (where, n is the size and f is the mask image),

$$O_R^{(n)}(f) = R_f^D [f \ominus nB]$$

(1.13)

$$C_R^{(n)}(f) = R_f^E [f \oplus nB]$$

(1.14)

Morphological reconstruction can be utilized for the extraction of meaningful information about shapes in an image. But is a little-utilized method in this context (Gonzalez and Woods 2002). The processing repeats until stability is attained, which means the image no longer changes. The processes include unique properties such as processing by two images; a mask and a marker, rather than a structuring element and one image. Morphological reconstruction can be used to detect bright regions surrounded by dark pixels, image border touching objects, object holes, spurious high or low points filter, marked objects extraction and so on.

1.4 RATIONALE OF THE STUDY

Feature extraction is one of the significant steps in image processing and thereby it is essential to develop novel approaches for enhancing the robustness of the feature extraction system over the existing methods. Currently considerable efforts have been put forth to advance the feature extraction techniques in remotely sensed images. The proposed approaches exploit the operators included in the mathematical morphology framework to perform analysis at region-level through image segmentation and simplification operations. The shape-oriented processing capability of the MM methods has rendered it popular with remote sensing imageries for different applications. In several cases, single segmentation of the scene is insufficient for the consistent representation of the objects in the scene. By exploiting the efficient MM algorithms based on hierarchical data structures, it would be possible to extract the spatial information of different resolution images through a dynamic multiscale representation, rather than a unique segmentation or classification.

1.5 RESEARCH OBJECTIVES

The proposed work aims at developing novel feature extraction techniques based on core mathematical morphology for the analysis of remotely sensed images. This study emphasizes the use of morphological operators in feature extraction methods for different remote sensing applications.

The specific objectives of the present study are:

1. Development of a novel algorithm for shoreline extraction from satellite images.
2. Development of an algorithm for
   - Water body extraction from satellite images.
   - Glacial lakes extraction from satellite images.
   - ANN assisted hybrid algorithm for lake extraction from satellite images.
3. The application and effectiveness analysis of an MM algorithm for irregular crop field boundary delineation from high-resolution remote sensing images.
4. Development of an algorithm to test the efficacy of MM assisted approaches for the extraction of urban features from UAV and satellite datasets.

1.6 ORGANIZATION OF THE THESIS

This thesis is organized into eight chapters.

Chapter 1 is a compendium of remote sensing systems, which includes the advancements of remote sensing systems, techniques and tools used in digital image processing. The significance of image feature extraction is described with particular emphasis on the mathematical morphology aided feature extraction. The rationale of the study, objectives of the thesis and the organizational framework of the thesis are presented.

Chapter 2 covers the state-of-the-art methods for feature extraction (in both computer vision and remote sensing) from remotely sensed images. Moreover, a survey of significant techniques appeared in the literatures based on the morphological profiles is

also presented. The formulation of the research problem is also described.

Chapter 3 deals with the materials and methods of the present experimental investigation and addressed to the satellite and aerial datasets, the software tools and aids, and validation strategies

In chapter 4, a novel shoreline extraction approach from the remotely sensed images is presented. Chapter 5 introduces multiple approaches for extraction of different types of waterbodies (such as lakes, rivers, and glacier lakes). In Chapter 6, a MM based efficient approach exploited for the extraction of crop field boundaries from multiple satellite imageries is discussed. Chapter 7 discusses two innovative feature extraction methods for UAV and satellite images.

Based on the analysis and the experiments carried out in the framework of this thesis, some interesting avenues of research as future directions of this work are reported in Chapter 8.

CURRENT STATE OF KNOWLEDGE

2.1. GENERAL

Past decade has witnessed extensive research efforts to extract the features and objects from moderate and high-resolution satellite images. Feature extraction from raster imageries is pertinent for many GIS activities such as GIS updating, geo-referencing, and geospatial data integration. This process depends heavily on human effort, which makes GIS database development, an expensive and time-consuming operation when executed manually. The automated feature extraction can significantly reduce the time and cost of data acquisition and update, database development and turnaround time. Henceforth, the scientists and researchers have identified the significance of developing more flexible semi-automated or automated feature extraction practices to advance the information extraction procedures.

Feature extraction strategies includes traditional pixel-driven remote sensing image classification procedures in which each, distinct pixel is independently assessed and allotted to one class (Lillesand & Kiefer, 2000). Many of the techniques reported in the literature combine strategies from a variety of approaches, and categorizing such approaches become a challenge. In this chapter, the literature review for the extraction of features and objects and the corresponding background information regarding the fields involved are specified. Especially the following sections present the different techniques (algorithms) involved in automatically or semi automatically extracting features from different sets of imageries.

2.2. FEATURE EXTRACTION IN COMPUTER VISION, AIRBORNE AND SPACE-BORNE REMOTE SENSING

"A picture is worth a thousand words." As human beings, we are able to tell a story from a picture based on what we see and our background knowledge, likewise a

----

computer program can discover semantic concepts from images, and few researchers has addressed this problem in the last decades (Ping Tian, 2013). Since the advent of the field of computer vision, researchers have been developing various techniques which can enable a computer program to understand digital images (Azayev, 2016). Remote sensing techniques, different from the exhaustive and expensive field evaluations have prominent advantages of being macroscopic, comprehensive, high frequency, dynamic, and low-cost (Addo et al. 2011). During the last decade, very high-resolution images have become available for civilians and researchers, opening new possibilities and challenges for remote sensing studies (Brito and Quintanilha, 2012). Lillesand & Kiefer, (2000) stated that the objective of image classification procedures is to automatically (or semi-automatically) order entire pixels in an image into classes centered on multidimensional spectral likenesses of electromagnetic quantities at several wavelengths. With the increase of the spatial resolution, the homogeneous structures in the scene has become generally larger than the size of a pixel. Pixel-based classification methods are less effective for very high-resolution images. In order to deal with these issues, spatial contextual classification methods can exploit the correlation among the spectral signature of pixels included in a subset of the spatial domain (Cavallaro, 2016). The following sections describe and compare the various methods involved in automated or semi-automated feature extraction.

2.2.1. Methodologies for Feature Extraction

Research in feature extraction is still very diverse and object extraction is a fundamental computer vision operator (Mohammadzadeha et al. 2004). The purpose of the feature extraction procedure is to identify homogeneous clusters of pixels (Gairns, 1993). The extraction of objects from imagery is generally based on two characteristics of the pixel values (digital number): a) the similarity and b) the difference of adjacent pixel values, in other words how the discontinuity of pixel grey values is treated and when the abruptions of the intensity values based on certain criteria are significant or not to indicate a boundary between different image features (Armenakis and Savopol, 2004). Feature extraction routines tend to focus on a single feature, for example roads, which

----

reduces the confusion matrix to a report of a total count of the feature detected and errors of commission and omission (Quackenbush, 2004). Its application has been proved in diverse fields (Fan et al. 2009; Ershad et al. 2012; Rathi and Palani, 2012, Hecher et al. 2013). Quackenbush (2004) reviewed the studies on linear feature extraction, where the procedures of various techniques involved are described, and also assessed the qualitative and quantitative accuracy of these methods. Time evolved approaches on the spectral-spatial feature extraction are summarized in Table 2.1.

Table 2.1: Summary of spectral-spatial feature extraction methods.

(Source: Liang, 2016)

Year	Method / Approach	Author
2002	Markov Random Field	Q.Jackson et al.
2003	ECHO Classifier	D.A. Landgrebe
2005	Extended Morphological Profile	Benediktsson et al.
2006	Composite Kernels	G. Camps-Valls et al.
2009	Spatial Regulation based on Segmentation	Y. Tarabalka et al.
2010	Directional MM (for road network)	S.Valero et al.
2011	Dictionary-based Sparse Representation	Y. Chen et al.
2011	Extended Attribute Profile	M. Dalla Mura et al.
2011	3D Gabor Wavelet	L. Shen et al.
2013	3D Discrete Wavelet Transform	Y. Qian et al.
2013	Tensor Discriminative Locality Alignment	L. Zhang et al.
2013	3D Gray Level Co-occurrence	T. Fuai et al.
2014	Super-pixel Representation	W. Duan et al.
2014	Spectral-Spatial Constraint	R. Ji et al.
2015	3D Local Derivative Pattern	J. Liang et al.
2015	Multiple Feature Combination	J. Li et al.
2016	Spectral-Spatial Classification	G. Cavallaro

Feature Extraction Strategies Based on Mathematical Morphology for the Analysis of Remotely Sensed Imagery, PhD Thesis, 2019, NITK Surathkal, India.

18

Numerous methods have been proposed by different researchers so far. Table 2.2 summarizes few important techniques (Quackenbush, 2004; Igbinosa, 2013; Buddhiraju et al. 2010; Gonzales and Woods, 2002; Castro and Centeno 2010) emphasizing its benefits and drawbacks. Feature extraction is highly important for classification of remote-sensing (RS) images however, extraction of comprehensive spatial features from high-resolution imagery is still challenging, leading to many misclassifications in various applications (Zhang et al. 2012).

Table 2.2 Advantages and Disadvantages of feature extraction methods

(Source: Quackenbush, 2004; Igbinosa, 2013; Buddhiraju et al. 2010; Gonzales and Woods, 2002; Castro and Centeno 2010)

Algorithm / Methods	Advantages	Disadvantages
Hough Transform (HT)	• Detects lines with some fragmentation and reasonably unaffected by random noise. • Reduces the problem of searching for lines in the image space to searching for peaks in the parameter space.	• Requires pre-processing to threshold the input image to a binary layer. • It can give misleading results when objects happen to be aligned by chance.
Multi-Resolution Techniques	• Simple concept • Doesn't requires fine resolution data.	• Many multi-resolution approaches generate lower resolution imagery by degrading a high-resolution source. • Less successful in urban areas
Template Matching	• A template describing the general characteristics of the feature of interest is defined. • Incorporate both spatial and spectral information.	• Depended on template. • Normalization with regard to size, shape, and orientation may require. • difficult to represent the third dimension (depth) with template matching
Dynamic Programming	• Optimization through a recursive search. • Computational cost is less	• Applicable only if a function can be expressed in terms of relationships between neighboring pixels alone and involves a sequential decision making process

Feature Extraction Strategies Based on Mathematical Morphology for the Analysis of Remotely Sensed Imagery, PhD Thesis, 2019, NITK Surathkal, India.

19

Current State of Knowledge

Pixel Swapping	• Clouds were eliminated by dilating areas that were identified as inner regions	• The effect of swapping intensity values among pixels matters
Knowledge Integration	• Combines rules from a variety of sources, including human intuition, can combine a variety of local image feature operators • Overcome the limitations of any single operator	• May become complex, depends on multiple modules
Classification based Feature Extraction	• Classification is useful as a pre-processing step in feature extraction. • Directly applied to solving the problem of linear feature extraction	• Depends on training and algorithm involved
Active contour models	• Achieve sub-pixel accuracy of object boundaries. • Easily formulated under a principled energy minimization framework • Allow incorporation of prior knowledge, for robust image segmentation. • Provide smooth and closed contours as segmentation result • Readily used for further applications viz. Shape analysis and recognition.	• Region-based active contour models tend to rely on intensity homogeneity in each of the regions to be segmented.
ANN, SVM, Cloud Basis Functions (CBFs)	• Better accuracy. • ANN classifiers have much less parameters, and the number of parameters is easy to control. • Less storage and Computations than SVMs	• Complex computation • SVM learning often results in a large number of SVs
Sobel, Prewitt, Robert Cross	• Simplicity • Detection of edges and their orientations	• Sensitivity to noise • Inaccurate.

Canny	• Use probability for finding error rate, localization and response, • Improving signal to noise ratio & better detection, • Insensitive to noise	• Expensive computation • False zero crossing • Time consuming • Complex
Mathematical Morphology	• Powerful tools • Less turnaround time • Shape-oriented processing capability • Better accuracy when well programmed • Easy to adopt, implementation cost is less. • Wide sets of image processing tools available. • Provides with an image processing technique complementary to those based on the analysis of spectral signature of pixels.	• Sensitive to structuring elements shape and size.

2.2.2. Advancement in Feature Extraction Techniques

With the rapid increase of remote sensing data on a gigabytes scale at daily basis, the need for robust and automated tools for retrieval, management, and processing the data for effective exploitation has also increased (Aptoula, 2014). The manual investigation of huge geography and numerous images are expensive and time consuming (Munyati, 2000). Therefore, past few decades witnessed rigorous research to accomplish the complex task of automatic extraction of features (Castro and Centeno, 2010). Automatic feature extraction from satellite imagery is cost effective and fast, an essential issue in this context is the degree of accuracy for thematic correctness obtainable through common pixel-based and object-oriented classification algorithms (Hecher et al. 2013). The implementation of higher level of automation in the mapping operations is highly desirable to reduce both the production time and the cost involved, especially when dealing with the vast size (Armenakis and Savopol, 2004). It can also update database effectively with minimal turnaround time. A thorough analysis of various studies for comparing the automatic against manual extraction exposes the requirement to significantly improve reliability of the automated systems

----
Feature Extraction Strategies Based on Mathematical Morphology for the Analysis of Remotely Sensed Imagery, PhD Thesis, 2019, NITK Surathkal, India.

21

(Quackenbush, 2004). Sebari and Dong-Chen (2013) presented a better automated method for object extraction from high-resolution satellite imageries based on Object Based Image Analysis (OBIA). They combined both segmentation primitives and fuzzy rule sets for image interpretation. Singh and Garg (2013) introduced a hybrid technique comprises of improved marker-controlled watershed transforms and a nonlinear derivative method to overcomes the disadvantages of existing region-based and edge-based methods. Sharma et al. (2008) attempted to automate the process of extracting feature boundaries from satellite imagery. That process was intended to eventually replace manual digitization by computer assisted boundary detection and conversion to a vector layer in GIS. Another potential application is to be able to use the extracted linear features in image matching algorithms. Similarly, Ohlhof et al. (2004) developed an operational software system for the semi-automatic extraction of line and zone features in 2D as well as 3D from aerial images and high-resolution satellite imagery. Tian (2013) studied the latest development in image feature extraction, provided a comprehensive survey on image feature representation techniques, and discussed the future potential research directions.

Soft computing has been experimented in feature extraction by several researchers. Li et al. (2015) proposed a strong framework based on conditional random field (CRF) for building extraction in visible band images. The CRF formulation to attain precise rooftops extraction, which incorporates pixel-level information and segment-level information for the identification of rooftops. Ghamisi and Benediktsson (2015) proposed a novel feature selection method that is based on the combination of a particle swarm optimization and genetic algorithm. Chen et al. (2014) identified that Deep convolutional neural networks (DNNs) can learn rich features from the training data automatically and has achieved state-of-the-art performance in many image classification databases. Forestier et al. (2008) studied the scope of genetic algorithms (GA) for optimal search for ontology rules for effectively segmenting satellite images.

The development of image segmentation algorithms for RS images has been drastically increased after the availability of VHR images and the failure of pixel-based approaches (Blaschke, 2010). The main objective of image segmentation is to determine the

----

suitable homogeneity measure which can discriminate the objects from each other (Cavallaro, 2016). In (Dey et al. 2010) the image segmentation methods for optical RS are categorized into three main classes. The first class of approaches is image driven. The image driven approach extracts objects based on the statistical features of the image derived from the pixels. This includes most of the edge based segmentation techniques (Canny, 1986). The second category of approaches is model driven. The most significant models that have been used are: a threshold model (Weszka, 1978; Rosenfield and Davis, 1979; Otsu, 1979), neural network based models such as Markov Random Field (MRF) (Geman and Geman, 1984), Conditional Random Field (CRF) (Lafferty et al. 2001) and Spatial Point Processes (SPP) (Hahn, et al. 2003)), Multi-resolution model (Woodcock and Strahler, 1987), Watershed Model (Vincent and Soille, 1991; Beucher, 1992) and Fuzzy Model (Zadeh, 1965). The last class of techniques use the different possible homogeneity measures of image features shape and size (Beveridge, 1989), Spectral and textural (Haralick, et al. 1973; Kettig and Landgrebe 1976), context (Thakur and Dikshit, 1997) and prior knowledge (Richards and Jia, 2013) The final performance of the segmentation-based classification is always determined by the selected homogeneity measure, which exposes image segmentation to two types of errors: under-segmentation and over-segmentation (Moller et al. 2007; Cavallaro, 2016).

By increasing the level of abstraction in the analysis it is possible to extract and exploit more spatial information, e.g., at object-level (Cavallaro, 2016). OBIA is relatively new class of algorithms that have been built on older segmentation, edge-detection, feature extraction and classification concepts that has been used in RS image analysis for decades. A detailed study on object based image analysis for remote sensing datasets were performed (Blaschke, 2010). Several studies have shown the advantages of object-based classification over pixel-based classification, nevertheless less attention has been paid to its potential limitations (Hay and Castilla, 2008; Kampouraki et al. 2008; Blaschke, 2010). The advantages and limitations of an object-based approach for remote sensing image classification relative to a pixel-based approach was assessed (Liu and Xia, 2010). Two categories of errors often found in image segmentation are

----

over-segmentation and under-segmentation (Möller et al. 2007; Kampouraki et al. 2008). Segmentation accuracy and the overall effect of object-based classification are both dependent on the scale of image segmentation (Addink et al. 2007; Benz et al. 2004; Kim et al. 2009). That is one of the typical limitations of object-based methods.

Over the time, UAVs have developed as a fast, efficient, low-cost and suitable data acquisition system for remote sensing applications (Colomina, 2014). The acquired data can be of high accuracy and resolution, for a precision varying from a sub-meter to a few centimetres (Gerke, et al. 2016). Crommelinck et al. (2016) in their review states that UAVs have advanced as a flexible acquisition system that acts as a feasible tool in cadastral mapping. A workflow that automatically extracts boundary features from UAV data could increase the pace of current mapping procedures. Aerial remote sensing and its mapping, for some years now, have been delivering the necessities of large-scale, low-altitude imaging for geospatial data users and has led to the crafting of an industry of its own (Cho et al. 2013; Mayr, 2013; Petrie, 2013). Mohajerin et al. (2014) carried out the classification of UAV versus non-UAV tracks based on a mixture of bird, aircraft and simulated UAV tracks.

2.2.3. Miscellaneous Application of Feature Extraction Methods

Mokhtarzade, (2007) utilized ANN for road network extraction. The proposed novel road extraction approach by Sghaier and Lepage, (2016) using texture analysis and multi-scale reasoning based on the beamlet transform is able to efficiently extract roads and reduce computation time. Mena et al. (2003) surveyed the state of the art on automatic road extraction for GIS update from aerial and satellite imagery. Hu and Tao (2007) adopted hierarchical grouping policy to automatically extract main road centerlines from high-resolution satellite imagery. Wang et al. (2016) briefed the road extraction techniques from remotely sensed images researched in recent years and highlighted the areas overlooked in the past studies. They have discussed a few points that can be included in the future works, the first is the requisite for a multi-model to model challenging phenomena for roads such as discontinuities, occlusion or shadows, near-parallel boundaries with constancy in width, and sharp bends; and suggested that

----
Feature Extraction Strategies Based on Mathematical Morphology for the Analysis of Remotely Sensed Imagery, PhD Thesis, 2019, NITK Surathkal, India.

24

the texture feature (Kuldeep & Garg, 2014) would improve the detection accuracy rather than adopting one kind of road features; also raised the need for developing a complete automated road extraction technique.

Automatic building detection from satellite/aerial imagery involves various problems related to computer vision, as there are many other subjects in close proximity such as trees, power lines vehicles, and parking lots and these subjects may occlude the building's rooftops (Bhadauria et al. 2013). The urban land cover mapping and automated extraction of building boundaries is a crucial step in generating 3D city models (Ramiya et al. 2015). Ghanea et al. (2014) proposed an automatic algorithm for the extraction of 2D buildings from PS-MS GeoEye imagery. Their study has compared the algorithm with other approaches and it was found to operate best in areas of high building density.

Remote sensing, as a suitable, fast, efficient, and timely earth observation practice, can provide increasing potential for information extraction such as water bodies (Kumar, 2002; Huang, et al. 2015; Kumar & Reshmidevi, 2013). With the development of high spatial as well as temporal resolution satellite imageries for disaster monitoring, it is possible to utilise the remotely sensed data to monitor and predict the lake dynamics and outburst potential (Cenderelli and Wohl, 2001; Mergili, et al. 2011; Song et al. 2014; Huang, et al., 2015). Jawak, et al. (2015) focused on the comprehensive evaluation of existing methods for extraction of lake or water body features from remotely sensed optical data. They briefed pixel-based, object-based, hybrid, spectral index based, target and spectral matching methods employed in extracting lake features in urban and cryospheric environments. Song et al. (2014) reported the advances in application of remote sensing methods for various lake environment monitoring, including lake surface extent and water level, glacial lake and potential outburst floods, with particular emphasis on the trends and magnitudes of lake area and water-level change and their spatially and temporally heterogeneous patterns. McFeeters (1996) proposed an NDWI assisted approach for waterbody extraction using raw DN (digital Number) values of satellite imagery. Later on Xu revised this approach as modified

NDWI by altering the spectral band employed in the NDWI method. These methods require reflectance in green and NIR bands for NDWI and green and MIR bands for MNDWI respectively. So, the single band imagery from CARTOSAT series, worldview-1 cannot be tested with these approaches. Nevertheless, the supervised technique requires sufficiently large spectral training data sets and is not a fully automated method and it does not take into account the spatial features of the objects (Mishra, & Prasad, 2015). Spectral based classification approaches are highly dependent on the spectral information and neglect some important information from high spatial resolution images, such as spatial features.

A texture analysis based water extraction method without using spectral characteristics of water proposed by Wang et al. (2008) works well for high-resolution panchromatic imagery and it is noted that the changes in spatial resolution influences its performance. Zanin, et al. (2013) defined and tested a method to perform feature extraction in remote sensing images for the extraction of rivers in orbital images for areas that are seasonally flooded, i.e., large zones containing more water bodies besides the river. Feyisa, et al. (2014) devised an index that consistently improves the water extraction accuracy in the presence of various sorts of environmental noise and simultaneously offers a stable threshold value. Consequently, they introduced a new Automated Water Extraction Index (AWEI) improving the classification accuracy in areas that include shadow and dark surfaces, which the other classification methods have failed to classify correctly. Duong, (2012) proposed an application of spectral pattern analysis for water body extraction using spectral bands green, red, near infrared (NIR) and short wave infrared (SWIR). This algorithm not only extracts waterbodies but also assess the quality of water. Kääb and Leprincegive, (2014) gave the first systematic summary of the methods and matters involved in using near-simultaneous satellite and airborne acquisitions, their study proved that the movement of river ice debris, sea ice flows or suspended sediments cloud motion vector fields and vehicle trajectories, detect motion of fast vehicles, such as cars and airplanes, or ocean waves. A brief review on remote sensing methods used for lake feature extraction has been given by Jawak et al. (2015), and they also marked that misclassification of dark pixels in feature extraction accounts for

----

inaccuracies in lake extraction. Similarly, Song et al. (2014) discussed the factors leading to inaccuracy of detecting lake area and water-level variations from multisource satellite imageries and studied the current uncertainties in mapping characteristics of glacial lakes by means of remote sensing strategies.

2.3. ROLE OF MATHEMATICAL MORPHOLOGY IN FEATURE EXTRACTION.

Mathematical Morphology is the fundamental theory for several image-processing algorithms, which can extract image shape features by employing various shape-structuring elements (Shih et al. 1995, Kupidura 2013). It provides an alternative move towards image processing based on shape concept rooted from set theory (Naegel, 2007) rather than traditional mathematical modelling and analysis. Mathematical morphology (MM) was first introduced in 1964 through the collaboration of Georges Matheron and Jean Serra who established its basic concepts and tools, coined the name in 1966, and set up in 1968, the "Centre de Morphologie Mathématique" Fontainebleau site of the Paris School of mines (Ronse et al. 2005). It is not only a theory, but also a powerful image analysis technique; it is called morphology because it aims at analysing the shape and form of objects; it is mathematical in the sense that the analysis is based on the set theory, integral geometry, and lattice algebra (Heijmans, 1994; Giada et al. 2003). The keyword for morphology is shape: unlike, e.g., an averaging filter that averages grey values, a morphological operator does not look at the grey values in the first place, but uses geometrical features of objects in an image (Ledda, 2007). Originally it was applied for analysing images from geological or biological specimen, however its rich theoretical framework, algorithmic efficiency, easy implementability on special hardware and suitability for many shape oriented problems have propelled its widespread diffusion and adoption by many academic and industry groups in many countries as one among the dominant image analysis methodologies (Maragos et al. 1996). Serra, 1988; Soille and Pesaresi, 2002; soille, 2003; Najman and Talbot, 2010 have discussed the role of mathematical morphology on image processing.

The tools of mathematical morphology have become part of the mainstream image

----
Feature Extraction Strategies Based on Mathematical Morphology for the Analysis of Remotely Sensed Imagery, PhD Thesis, 2019, NITK Surathkal, India.

27

----

analysis and image processing technologies. It can be applied to any field of image processing where shape plays certain role. This can be object extraction, noise filtering, edge enhancement, segmentation, texture analysis, classification, shape description, and so on (Ledda, A. 2007). Last decades witnessed the appearance of many techniques involving MM for the analysis of remote sensing images, strengthening the mutual connection between remote sensing and MM (Soille, 2009; Mura et al. 2011). The growth of popularity is due to the development of powerful techniques, like granulometries and the pattern spectrum analysis, that provide insights into shapes, and tools like the watershed or connected operators that segment an image. Besides that, its acceptance in industrial applications is also due to the discovery of fast algorithms that make mathematical morphology competitive with linear operations in terms of computational speed (Droogenbroeck & Buckley, 2005). This processing technique has been demonstrated as a powerful tool for several computer-vision tasks in binary and grey scale images, such as edge detection, skeletonization, noise suppression, image enhancement and pattern recognition (Ortiz, et al. 2002). As the performance of classic edge detectors degrades with noise, morphological edge detector has been studied (Lee et al. 1987). The shape-oriented processing capability of the mathematical morphology toolbox has rendered it popular with remote sensing images (Stankov and He, 2013; Soille and Pesaresi, 2002).

Ononye, et al. (2007) described a sequence of image processing tools such as multi-band image gradient calculation, NDWI along with basic morphological approaches are used to recognise and constrain the fire propagation parameters from multispectral infrared imageries. Benediktsson et al. (2005) introduced a method based on MM techniques and principal component analysis for pre-processing of hyperspectral data. A morphological profile (MP) is constructed based on the repetitive use of opening and closing operation with a structuring element of increasing size, beginning with one original image. Similarly, Plaza et al. (2005) explained series of extended morphological transformations for filtering and classification of high-dimensional hyperspectral datasets. In addition, object-based morphological profiles (OMPs) concept introduced to encode shape-related, topological, and hierarchical properties of image objects in an

exhaustive way (Geiß et al. 2016). The proposed OMPs allow for significant improvements with respect to classification accuracy compared to standard MPs (i.e., obtained by paired sequences of erosion, dilation, opening, closing, opening by top-hat, and closing by top-hat operations). Bellens et al. (2008) proposed the usage of operators based on "partial reconstruction" in place of the conventional geodesic reconstruction to minimize the "leakage effect." It can be seen that the addition of the line-based MP provides a considerable enhancement of the classification result. The concept of attribute profile (AP), proposed by Mura et al. (2010) was used for modelling the structural information of the scene to enhance the effectiveness of classification and building extraction. Ghamisi et al. (2015) discussed about the morphological profile, as a powerful tool to model spatial information (e.g., contextual relations) of the image. The concept of AP and its extensions EAP (Extended Attribute Profile) and EMAP (Extended Multi-Attribute Profile) have proven to be effective in the analysis of remote sensing images. Similarly, a set of powerful image processing operators have been defined in the mathematical morphology framework (Cavallaro et al. 2016). Among those, connected operators [e.g., attribute filters (AFs)] have proven their effectiveness in processing very high-resolution images. Cavallaro et al. (2016) considered the definition of minimum (min), maximum (max), direct and subtractive filter rules for the computation of attribute filters over the tree of shapes representation and studied their performance on the classification of remotely sensed images and compared over the tree of shapes with the results obtained when the same rules are applied on the component trees.

The mathematical morphology assisted remote sensing application range includes texture analysis (Huang et al. 2009) simplification (Soille, 2008) and segmentation (Tarabalka et al. 2010). In addition, morphological approaches have been used broadly for spatial structure extraction problems, e.g., building detection and extraction (Ouzounis et al. 2011), road network delineation (Valero et al. 2007), rubble detection (Ouzounis et al. 2011), target detection (Velasco-Forero and Angulo 2010), etc. Daryal and Kumar (2010) used the mathematical morphology to extract lines and developed a program in the MATLAB platform. Kumar et al. (2014) also used morphological

Feature Extraction Strategies Based on Mathematical Morphology for the Analysis of Remotely Sensed Imagery, PhD Thesis, 2019, NITK Surathkal, India.

29

operations to refine road fragments detection from high-resolution images. Frigato and Silva (2008) compared the result of morphology with other techniques and presented itself as the best routine for extraction of highways. Gonzales and Woods (2002) has discussed the role of mathematical morphology techniques for automating the feature extraction and highlighted its emphasis on the area that studies the geometric properties of objects in the images which allows the extraction of image components that are beneficial in the representation and description of the shape of a region, such as skeletons and borders. Bagli and Soille (2003) proposed a new approach for extracting automatically the coastline with better accuracy and demonstrated its application to the entire European continent. Giada et al. (2003) adopted automatic image analysis methods for a quick and reliable identification of refugee tents as well as their spatial magnitude.

In the recent years, morphology has shown its need to the researchers in the realization of several topics like image enhancement, image segmentation, image restoration, edge detection, texture analysis, feature generation, skeletonization, shape analysis, image compression, component analysis, curve filling, general thinning, feature detection and noise reduction (Gaurav, 2009). It provides a nonlinear approach to the processing of images, which is based on geometrical shape (Haralick et al. 1987). There is a general consensus that mathematical morphology is an excellent basis to extract the features of interest in the digital images (Stroppa et al. 2010). Morphology is commonly applied in remote sensing because of its ability to process image, de-noising and segmentation of objects of different texture and completing edges, which is very promising and potentially helpful for extracting features in photogrammetry (Kowalczyk, 2008). A close survey of the past literatures reveals that there is immense scope for the utilization of MM on diverse fields and possibility for further expansion on its theoretical end. This thesis focuses only on the applicability of several morphological tools in feature extraction from high-resolution satellite images.

Feature Extraction Strategies Based on Mathematical Morphology for the Analysis of Remotely Sensed Imagery, PhD Thesis, 2019, NITK Surathkal, India.

30

2.4. SUMMARY AND RESEARCH GAP

- The literature survey elicits the scope of morphological methods over image processing. As it provides numerous tools for image analysis, it is extensively used in digital image processing activities. Therefore, the MM techniques can be applied on UAV and satellite imageries as well. However, the use of morphological methods on the satellite imageries has been very sparse when compared to its application on digital images.

- It has been revealed that numerous scientists and researchers have stressed the importance of developing reliable, effective and fast automated or semi-automated feature extraction techniques. Automated or semi-automated feature extraction techniques improve the information extraction process from bulk volume of satellite imageries.

- Several studies are available on the development of hybrid approaches utilizing the soft computing tools combined with other methods to produce better results, but quite a few researchers coupled soft computing tools with the MM techniques.

- Remote sensing applications necessitate explicit coding or programming for good results, due to the different aspects such as variation in sensor, spectral and spatial resolutions, changes in environmental conditions between images and the feature of interest to be extracted.

2.5. PROBLEM FORMULATION

In the view of above aspects, it is crucial to propose new algorithms for efficient and fast extraction of geospatial features from the satellite imageries. Hence the present work aims to bridge the knowledge gap by developing novel algorithms to extract the geospatial features from satellite and aerial imageries by using core mathematical morphological techniques supported by different image thresholding schemes and soft computing approaches. It focusses to provide wider flexibility and scope in terms of accuracy and speed.

Feature Extraction Strategies Based on Mathematical Morphology for the Analysis of Remotely Sensed Imagery, PhD Thesis, 2019, NITK Surathkal, India.

31

MATERIALS AND METHODS

This chapter is about the important data sets used, research methodologies applied and software aids utilized for the present study.

3.1 STUDY AREA AND DATA COLLECTION

This research uses a wide set of cloud-free open-source and procured satellite and aerial imagery to identify how well the proposed approach performs. Satellite images of different resolution including high resolution CARTOSAT series and LISS IV sensor imageries are acquired from NRSC data center. Different open source images including LISS-III and Landsat images were downloaded from NRSC Bhuvan and USGS archives respectively. This study uses single spectral band (for CARTOSAT 1 and 2, PAN band is used whereas for multispectral imagery both Red and NIR band gives similar results and the present study uses red band). This study also uses a set of noise free UAV driven aerial imageries to identify how well the proposed approach performs. Apart from this, standard data sets (used by various researchers globally) obtained from different data archives are also used to test the efficacy of the algorithms. The details of all the important data sets used for the present investigation procured from various sources and agencies with different spatial resolutions are summarized in Table 3.1.

Table 3.1 Specification of datasets used

Sl. No	Satellite and Sensor	Spatial Resolution (Meters)	Source / Agency	ROI
1.	Cartosat 2, PAN	0.8	NRSC[1]*	Mangalore, India
2.	Cartosat 1, PAN	2.5	NRSC	Bhopal, India.

3.	IRS P6 LISS IV	5.8	NRSC	Mangalore, India
3.	IRS P6 LISS III	23.5	NRSC	Mangalore, India
4.	Landsat 5, TM	30	Intergraph Corp.[2*] ERDAS IMAGINE Remote Sensing sample data sets	Lake Lanier, Georgia, USA
5.	Color- IR aerial images (4-3 imagery subset)	High (> 2m)	Intergraph Corp. ERDAS RS sample data sets	Eastern Illinois, USA
6.	NITK, Aerial Dataset	Very high (> 1m)	UAV Lab, Applied Mechanics Dept. NITK, India	NITK campus, Mangalore, India
7.	UC Merced Land Use Dataset	High	UC Merced-Dataset[3*] (Yang et al. 2010)	Not Available

[1]*National Remote Sensing Centre, Govt. of India.

[2]*ERDAS IMAGINE Remote Sensing sample data sets licensed to N.I.T.K.

[3]*UC Merced Land Use Dataset, URL:http://vision.ucmerced.edu/datasets/landuse.html

3.2 METHODOLOGY

This research work proposes novel algorithms by using core mathematical morphological techniques in assistance with different image thresholding schemes and soft computing approach to extract the geospatial features from satellite and aerial imageries. It will provide wider flexibility and scope in terms of innovative results using different set of remotely sensed data sets. The methodology adopted for the present research work is explained in this chapter and the flow chart of methodology is depicted in Figure 3.1.

Several diverse approaches has been proposed in the present investigation to address the feature extraction task for different features of interest, using different data sets and in various geographical locations. Initially, a preliminary study of the existing

----

Feature Extraction Strategies Based on Mathematical Morphology for the Analysis of Remotely Sensed Imagery, PhD Thesis, 2019, NITK Surathkal, India.

33

approaches is carried out and their weakness and strength are identified. All the required input imageries were collected and radiometric and geometric corrections were applied.

Different algorithmic approaches to extract shoreline, different types of waterbodies (such as ponds rivers, glacier lakes), crop field boundaries and urban features (building extraction) as shown in Figure 3.1 are developed. Detailed description of each of the proposed algorithm and their performance or efficacy analysis are presented in the following subsequent chapters. The complete pseudocodes of each proposed algorithms are included in the Appendix-I .The extraction outcome should be validated using appropriate metrics, standard data sets. The results of the proposed approach are compared with that of existing methods. The metrics used such as, Precision, Accuracy, F-score and MCC for the assessment is discussed in detail in the following subsections.
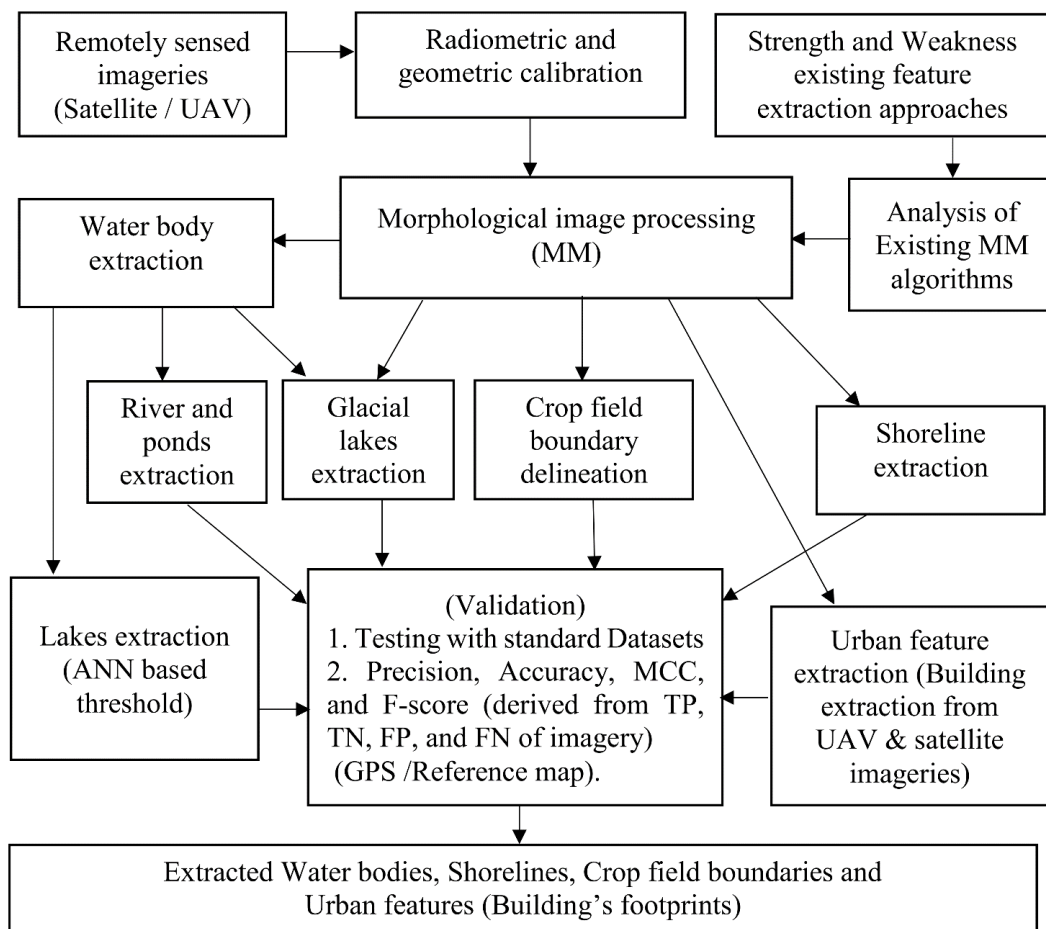
Figure 3.1. Overall methodology

3.3 SOFTWARE USED

The image processing scripts are developed using SDC Morphology toolbox and Image Processing toolbox in association with MATLAB programming environment.

3.3.1   MATLAB

MATLAB (Matrix Laboratory) is a multi-paradigm numerical computing software and one of the leading programming languages which provides a flexible platform for technical computing, particularly for mathematical computing, visualization and command language. For specific usage it has specific companion. MATLAB features are incorporated with additional application specific solutions, so-called toolboxes that are inevitable to the users who are involved in advance research. These extensive collections of MATLAB functions (M-files) enhances the MATLAB competence to expound specific kind of problems (MathWorks, 2011). Toolboxes are available in different areas viz.signal processing, control systems, fuzzy logic, neural networks, wavelets, simulation etc. There is an inbuilt Image Processing Toolbox developed by MathWorks, Inc. which is available with MATLAB package. It is a collection of several image processing functions that are capable of improving the versatility of MATLAB numeric computing environment. This toolbox supports image processing operations such as spatial image transformations, neighborhood & block operations, linear filtering and filter, image analysis & enhancement etc. (MathWorks, 2010) and also the fundamental morphological operations, which is an image processing method based on shapes, is also incorporated.

3.3.2   SDC MM toolbox

The SDC Morphology Toolbox encompasses a powerful set of latest state-of-the-art gray-scale morphological tools, which can be applied to image segmentation, non-linear filtering, and pattern recognition and image analysis. It delivers high precision and accuracy for processing and determining the data from the image (e.g. object counting and granulometry). Although, the image processing toolbox exhibit good

precision and accuracy, the precision is not as much of what is acquired in SDC Morphology toolbox (Mustafa, 2002). SDC Mathematical Morphology toolbox is used for the compilation and execution of computer source code of the proposed algorithm.

Each operator that pertains to the SDC Morphology Toolbox starts with 'mm' and so aids the user to distinguish the operators by its name that is different from the others in MATLAB software (User's Guide, 2001). One of the best feature in SDC Morphology Toolbox are the functions. Every function has its description or help manual that can be read by typing 'help function name' in the MATLAB command window. The SDC Morphology Toolbox for MATLAB V1.6 release (12 Aug 2011) is used in the present study.

3.4 METRICS FOR VALIDATION AND ACCURACY ASSESSMENT

It is important to validate the developed algorithms, so it should be tested and verified with different data sets including GPS driven ground truth information and Digitized sketches from reliable sources. The ground truths are prepared collectively combining the knowledge of the user via field visit and manual digitization. Apart from this Google earth verification and correction at pixel and object level in an iterative fashion to obtain maximum possible accuracy is performed. Comparison of extracted features and manually delineated features are carried out by pixel-by-pixel basis.

In the image, the pixels are categorized into four types: True Positive (TP): both manual and extracted result corresponds to feature, True Negative (TN): both manual and extracted result corresponds to background, False Positive (FP): in the extracted result, the pixel is incorrectly labelled as feature, and False Negative (FN): the extracted result, the pixel is incorrectly labelled as background. The calculation of Precision, F-score, Accuracy and MCC (Complete, Correct, Rank and Distance) parameters are carried out based on reference data (Zhou et al, 2014).

Precision (3.1), F-Score (3.2), Accuracy (3.3) and Matthew's Correlation Coefficient (MCC) (3.4) are the metrics used to evaluate the system performance. F-score takes both false positives and false negatives into account. Intuitively it is not as easy to

----

understand as accuracy, but F-score is usually more useful than accuracy, especially if you have an uneven class distribution (Powers, 2007). Accuracy works best if false positives and false negatives have similar cost. Accuracy is the most intuitive performance measure and it is simply a ratio of correctly predicted observation to the total observations. One may think that, if we have high accuracy then our model is best. Yes, accuracy is a great measure but only when you have symmetric datasets where values of false positive and false negatives are almost same. The formulae for these metrics is as follows:

$$\text{Precision} \quad = \quad TP/(TP + FP) \tag{3.1}$$

$$\text{F-score} \quad = \quad 2TP/(FP + TP + P) \tag{3.2}$$

$$\text{Accuracy} \quad = \quad \frac{TP + TN}{P + N} \tag{3.3}$$

$$\text{MCC} \quad = \frac{TP * TN - FP * FN}{\sqrt{((TP + FP) * (TP + FN) * (TN + FP) * (TN + FN))}} \tag{3.4}$$

MCC takes into account true and false positives and negatives and is generally regarded as a balanced measure which can be used even if the classes are of very different sizes (Boughorbel, 2017). The MCC is in essence a correlation coefficient between the observed and predicted binary classifications; it returns a value between −1 and +1. A coefficient of +1 represents a perfect prediction, 0 no better than random prediction and −1 indicates total disagreement between prediction and observation. While there is no perfect way of describing the confusion matrix of true and false positives and negatives by a single number, the MCC is generally regarded as being one of the best method for performance assessment (Powers, 2011).

Feature Extraction Strategies Based on Mathematical Morphology for the Analysis of Remotely Sensed Imagery, PhD Thesis, 2019, NITK Surathkal, India.

37

ALGORITHM FOR SHORELINE EXTRACTION

4.1 GENERAL

Shoreline extraction is fundamental and inevitable for several studies. Determining the precise location of the shoreline is crucial for coastal regulatory zone management (CRZM). Recently, the need for using remote sensing data to accomplish the complex task of automatic extraction of features has considerably increased. Automated feature extraction can drastically minimize the time and cost of data acquisition and database updation. Rapid and effective approaches are necessary to monitor coastline retreat and update shoreline maps. In the present chapter, a novel mathematical morphology driven approach for shoreline extraction algorithm from satellite imageries is presented. The noticeable features of this work are the preservation of actual size and shape of the shoreline, runtime SE definition, semi-automation, faster processing and single band adaptability. The proposed approach is tested with various sensor driven images with low to high resolutions. The accuracy of the developed methodology has been assessed with manually prepared ground truths of the study area and compared with an existing supervised shoreline classification approach. This approach is found successful in shoreline extraction from a wide variety of satellite images based on the results drawn from visual and quantitative assessments.

4.2 BACKGROUND AND RELATED WORKS

Delineation and extraction of coastlines from remote sensing imagery is a vital task and is useful for various application fields such as coastal regulatory zone management, coastline erosion/accretion monitoring, GIS database updating, watershed definition, flood and other disaster management and the evaluation of water resources. Recently, the need for using remote sensing data to perform the task of automated extraction of

features has increased significantly. Automated feature extraction can drastically minimize the time and cost of data acquisition and database update. Remote sensing techniques, different from the exhaustive and expensive field evaluations have prominent advantages being macroscopic, comprehensive, high frequency, dynamic, and low-cost (Addo et al. 2011). The collection of this information is difficult, complex and time consuming when using conventional ground survey methods. Moreover, it is highly dependent on the morphological characteristics of the coastline (like rock cliffs, sandy beaches). So rapid and reliable techniques are required to monitor coastline retreat or aggradation and update coastline maps (Puissant et al. 2008).

To locate the position of shoreline optimally and reliably, numerous researchers have proposed variety of methods. These include the application of supervised classification (Hoeke et al. 2001; Nguyen, et al. 2013, Hoonhout et al. 2015), unsupervised classification (Guariglia et al. 2006; Ekercin, 2007, Huang et al. 2014) and several thresholding assisted methods (White & El Asmar, 1999; Jishuang & Chao, 2002; Liu & Jezec, 2004; Bayram et al. 2008; Kuleli et al. 2011; Maiti & Bhattacharya, 2009). Approaches focused on hard classification renders each pixel as either sea or land. These approaches are less effective in delineating the shoreline and in several instances, a large proportion of misclassification may occur. Huang et al. (2014) conducted a detailed comparative study of unsupervised and supervised methods and showed that some unsupervised feature extraction methods have the potential to provide better results than the supervised ones.

The current status of the use of remote sensing for the detection, extraction, and monitoring of coastlines have been reviewed extensively (Gens 2015). Also, an overview of shoreline indicators and the remote sensing techniques used for coastline monitoring was provided in the study. Liu and Jezek (2004) performed delineation of the complete coastline of Antarctica using SAR imagery. The DN value of the threshold is obtained with a simple geometric equation (La Monica et al. 2008; Braga et al. 2013). All the pixels lesser than the designated threshold were classified as water; all the pixels

----

Feature Extraction Strategies Based on Mathematical Morphology for the Analysis of Remotely Sensed Imagery, PhD Thesis, 2019, NITK Surathkal, India.

39

higher than the designated threshold were classified as land and finally extracted the rough shoreline with the edge detection technique, based on the identified threshold.

Texture is another salient property of an imagery for shoreline extraction. A texture analysis based technique for shoreline extraction from remotely sensed imageries has been proposed (Bo et al. 2001). Di et al. (2003) adopted the image segmentation algorithm proposed by Comaniciu and Meer (2002) to detect shoreline. Automated high-resolution satellite images extraction of the coastline is more complex because of the reduced pixel dimensions that require greater attention to distinguish different classes such as sea and soil (Giannini et al. 2015). They also proposed an object-based approach for instantaneous coastline extraction from QuickBird dataset. Bagli and Soille, (2003) introduced an automated morphological segmentation assisted method for coastline extraction. A sea–land separation method was designed, and then a shoreline detection method was proposed for interpreting multispectral remote sensing images by considering both spectral attributes and texture attributes (Wang et al. 2010). Huang et al. (2016) proposed scale-span differential profiles, i.e., generalized differential morphological profiles (GDMPs), to obtain the complete differential profiles. GDMPs can describe the complete shape spectrum and quantify the difference between arbitrary scales, which is more appropriate for representing the multiscale characteristics and complex landscapes of remote sensing image scenes.

In this research, an attempt has been put forth to propose an MM based efficient approach for the extraction of shoreline from higher and moderate resolution imageries. In an MM approach, the value of each pixel in the resultant image is based on an assessment of the matching pixel in the input image with its neighbors. By choosing the shape and size of the neighborhood, it is possible to make a morphology-assisted operation that is useful to particular shapes (such as shoreline) in a given image. A set of powerful MM driven operations such as Opening, Closing, Top-hat, Bot-hat and reconstruction-driven operations were applied at multiple times and multiple instances to delineate shoreline.

Feature Extraction Strategies Based on Mathematical Morphology for the Analysis of Remotely Sensed Imagery, PhD Thesis, 2019, NITK Surathkal, India.

40

4.3 DATA AND METHODS FOR SHORELINE EXTRACTION

The present study uses multiple sets of satellite imageries to identify how well the proposed approach is performing with datasets including very high-resolution panchromatic (PAN) data of 0.8 meter, moderate resolution Resourcesat-2 LISS IV 5.8 meter data and low-resolution Landsat ETM+ 30 meter data. The important datasets used for this investigation is procured from various sources and agencies listed in Table 4.1.

Table 4.1. Specification of datasets for the present study

Sl. No	Satellite and Sensor	Spatial Resolution	Source / Agency	Area of Interest	Date of procurement
1.	Cartosat-2, PAN	0.8 m	NRSC	Mangalore, India	12-NOV-2008
2.	Cartosat 1, PAN (Tile-532-338)	2.5 m	NRSC	Mangalore southern coast, India	16-FEB-2012
3.	Cartosat 1, PAN (Tile-530-334)	2.5 m	NRSC	Mangalore northern coast, India	14-NOV-2014
4	Resourcesat-2, LISS IV	5.8 m	NRSC	Mangalore, India	6-FEB-2016
5	Landsat 8, ETM+	30 m	USGS	Mangalore northern coast, India	11-JAN-2015

4.3.1 Methodology

The methodological flowchart of the present investigation is presented in Figure 4.1. The acquired cloud free image was initially pre-processed for various operations to rectify radiometric and geometric errors. Median filtering is applied to suppress nonlinear objects and noises such as salt and pepper, etc. The SE, threshold declaration (SE1 to SE3) and initialization, which governs important processing activities, are performed before the execution of the algorithm. Moreover, the initialized SEs and

----
Feature Extraction Strategies Based on Mathematical Morphology for the Analysis of Remotely Sensed Imagery, PhD Thesis, 2019, NITK Surathkal, India.

41

threshold values have a greater significance; their slight variation changes the entire shoreline extraction result and accuracy. The application of erosion followed immediately by dilation using the same structuring elements is called opening. This binary operation attempts to open small gaps between touching objects in an image. In addition, it can be explained as a process that destroys edges. This concept is directly applied to the analyzed coastal image to get rid of the edges present in land while preserving the coastline. In addition, the application of a dilation procedure immediately followed by erosion using the same structuring element is called closing. As its name indicates, it closes or fills the gaps between objects. Opening will act over neighbouring pixels, destroying the edges in the touching objects of the image. Then the image is smoothed while the strongest edges remain. A series of MM operations were applied, starting with powerful MM computation of matching Top-hat and Bot-hat algebra and opening by reconstruction, followed by thresholding operations either automatically or manually. The structuring elements employed are SE1 for Top-hat and Bot-hat algebraic operation. SE2 for opening by reconstruction, and SE3 for closing by reconstruction. Then the algorithm aims to isolate unwanted objects that are irrelevant in shoreline delineation through closing by reconstruction and Binary Area Open (with P pixel size) operation with the threshold image. The details of these operations are outlined in algorithm steps of the present section. The theoretical and mathematical background of these MM operations is explained in detail in section 1.3 of chapter 1.

MM reconstruction is advantageous, and it is a good exercise for extracting substantial details about shapes in an image (Gonzalez and Woods, 2002). Since the study use MM reconstruction-driven operations, the actual size and shape of the objects in the outcome remain unchanged. The distinctive properties of such processing are based on two images; a marker image and a mask rather than a single image and SE. The execution repeats until stability attains, i.e., until the image no longer alters. One can apply MM reconstruction to detect and delineate marked objects, find bright areas bounded by dark pixels, detect or eliminate objects touching the image boundary, find or fill in object gaps, filter out spurious high or low points and execute many other operations.

Feature Extraction Strategies Based on Mathematical Morphology for the Analysis of Remotely Sensed Imagery, PhD Thesis, 2019, NITK Surathkal, India.

42
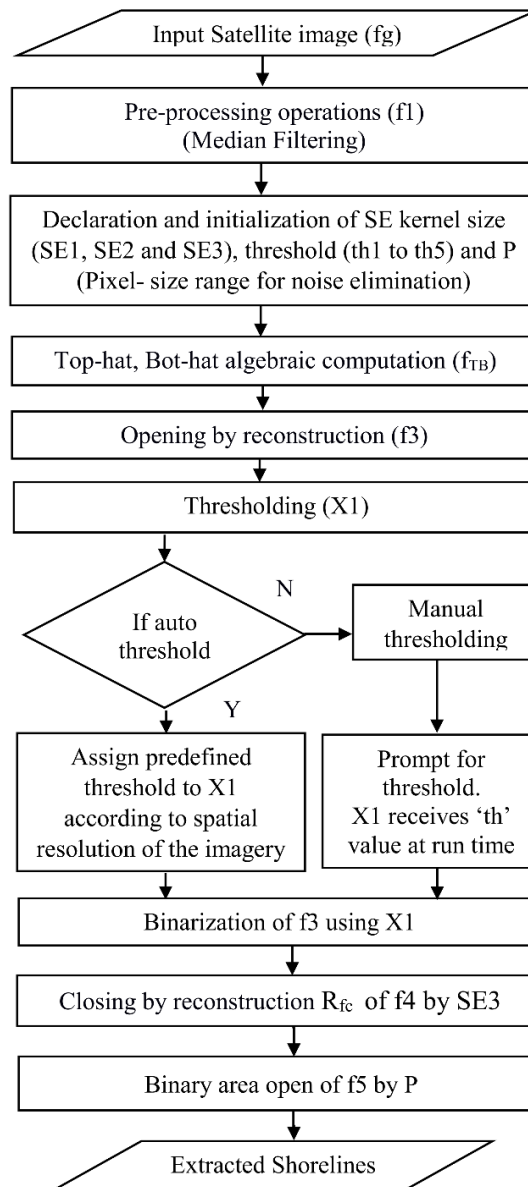
Figure 4.1. Flowchart of the proposed MM approach for shoreline extraction.

The ground truths are prepared collectively combining the knowledge of the user via field visit and manual digitization. Apart from this Google earth verification and correction at pixel and object level in an iterative fashion to obtain maximum possible accuracy is performed. A supervised maximum likelihood (ML) classification was performed using shore and non-shore signatures. The signatures were grouped as either

---
Feature Extraction Strategies Based on Mathematical Morphology for the Analysis of Remotely Sensed Imagery, PhD Thesis, 2019, NITK Surathkal, India.

43

non-shore or shore region. Sufficient numbers of signatures for shore regions and non-shore regions were collected to ensure better classification accuracy.

4.3.2 Algorithm development

This section describes the stepwise algorithm development of the flowchart shown in figure 4.1.

Input: An N x N matrix sized satellite input image (f1).

Output: An N x N matrix sized extracted output image (X).

1- Start

2- Procurement and registration of the satellite image.

3- Pre-processing operations such as Median filtering (f1 = Mf (fg, [3, 3])) to suppress nonlinear objects and noises such as salt and pepper.

4- SE (SE1 to SE3), P (to remove noises /non-shore objects) and threshold (th1 to th5) declarations & initializations for processing activities.

5- Prompt for spatial resolution of input satellite images: Input 1 for Very high (>1m), 2 for high (1-5m), 3 if moderate (5-25m), 4 if sparse (>25)

6- Computation of matching Top-hat and Bot-hat algebra;

(f2 = f1+ Top-hat (f1, SE1)) – Bot-hat (f1, SE1)).

7- Opening by reconstruction; (f3 = Rfo (f2, SE2)).

8. Thresholding

If (auto threshold) then

switch Res

case '1' :X1 = im2bw (f3, th1);
case '2' : X1 = im2bw (f3, th2);
case '3' : X1 = im2bw (f3, th3);
case '4' : X1 = im2bw (f3, th4);
otherwise
 X1 = im2bw (f3, th5);

End

Else (manual threshold)

prompt = 'Please enter threshold value'

X1 = input (prompt);

X1 = im2bw (f3, X1);

9-   Closing by reconstruction; (X = Rfc (X1, SE3, mmsebox)).

10-   Binary area open; bwareaopen (X, P), noise removal (non-shores)

11-   Display extracted outcome and save resultant imagery.

12-   End.

4.4 RESULTS AND DISCUSSION

The proposed approach is tested with imageries of different region of interest (RoI) with varying areal coverage, images acquired from several sensors with different acquisition dates and spatial resolution were used. This section describes the results drawn from different sets of the input imageries including visual, qualitative and quantitative assessments. The results of this analysis were also compared with the results of the traditional ML classifier result.

The performance of the proposed MM approach and ML shoreline classification approach is tabulated in Table 4.2 and Table 4.3 respectively.

Table 4.2. Statistics of accuracy assessment of proposed MM approach

Sensor and AOI	TP (feature)	FP	TN (background)	FN	F-score	MCC	Accuracy
Cartosat-2, PAN	470275	47498	52904280	60929	0.89663	0.89568	0.99797
Cartosat 1, Tile:532-338	285895	17426	36154604	14335	0.94737	0.94695	0.99912
Cartosat 1, Tile530-334	240917	71419	86907650	10794	0.85424	0.85878	0.99905
Resourcesat-2, LISS IV	74394	6292	19993870	16324	0.86805	0.86899	0.99887
Landsat 8, ETM+	36497	48011	27884335	3613	0.58574	0.62619	0.99815

Feature Extraction Strategies Based on Mathematical Morphology for the Analysis of Remotely Sensed Imagery, PhD Thesis, 2019, NITK Surathkal, India.

45

Shoreline Extraction

Table 4.3. Statistics of Accuracy assessment of ML shoreline classification approach.

Sensor and AOI	TP (feature)	FP	TN (background)	FN	F-score	MCC	Accuracy
Cartosat-2, (PAN)	509278	966121	51985657	21926	0.50760	0.56941	0.98152
Cartosat 1, Tile:532-338	256139	328471	35843559	44091	0.57894	0.60727	0.98978
Cartosat 1, Tile:530-334	216435	893029	86086040	35276	0.85985	0.40668	0.98935
Resourcesat-2, LISS IV	68414	207940	19792222	22304	0.37275	0.42811	0.98853
Landsat 8, ETM+	37263	246138	27686208	2847	0.23036	0.21575	0.97489

The figure numbered 4.2 to 4.6 (a) – (e) illustrates different input datasets, ground truth image, MM algorithm processing stage, results drawn from ML classification approach and output drawn from proposed MM approach. Figure 4.2 (d) and 4.2(e) illustrates the performance of an ML classification approach and the proposed MM algorithm with Cartosat-1 (Tile-532-338) imagery. The proposed algorithm extracts shoreline with better accuracy of 99.91% as compared to the accuracy of 98.97 % of shoreline classification approach. The MCC (0.94695) and F-score (0.94737) values are also marginally better than the traditional ML classification approach.

Figure 4.3(e) illustrates the algorithm performance with Cartosat-2 imagery covering Mangalore sea shore and Nethravathi river segments. Here, the proposed algorithm can extract shoreline with 99.79% accuracy. The statistics such as MCC (0.89568) and F-score (0.89663) values were found satisfactory. Even though traditional shoreline classification approach has an accuracy of 98.15 %, its MCC and F-score values are lower than that of 0.6 due to misclassifications. Figure 4.4(e) illustrates the performance of the algorithm with LISS IV imagery of coastal regions of northern Mangalore. Here, 99.88% accuracy is achieved by the proposed algorithm and an accuracy of 98.85% by

----
Feature Extraction Strategies Based on Mathematical Morphology for the Analysis of Remotely Sensed Imagery, PhD Thesis, 2019, NITK Surathkal, India.

46

ML classification approach. MCC and F-score values of 0.8689 and 0.8680 are observed for the proposed algorithm, and for the ML classification approach, it is observed to be 0.3727 and 0.4281.Thus the proposed MM based approach proved to be more efficient.

| (a) | (b) | (c) | (d) | (e) |
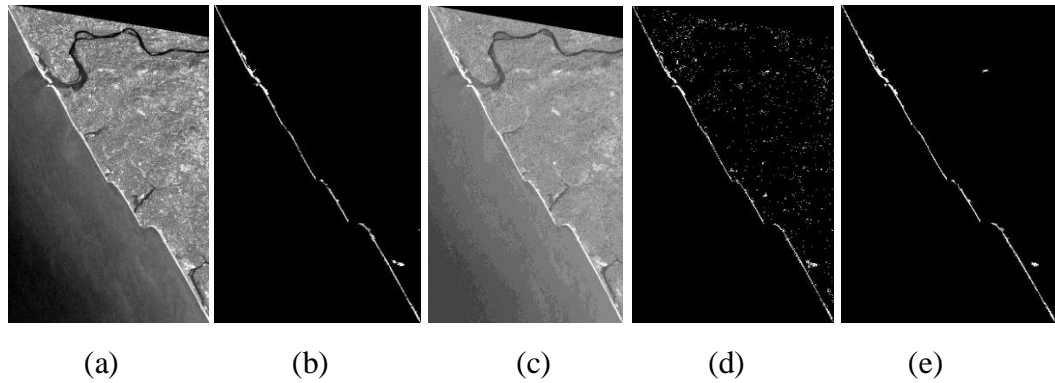
Figure 4.2. (a) – (e). Illustration of results with Cartosat-1 (PAN) image (Tile-532-338). (a) Original image (b) Ground truth (c) MM processed image (intermediate stage) (d) ML Classification result (e) Proposed MM algorithm result

| (a) | (b) | (c) |

| (d) | (e) |
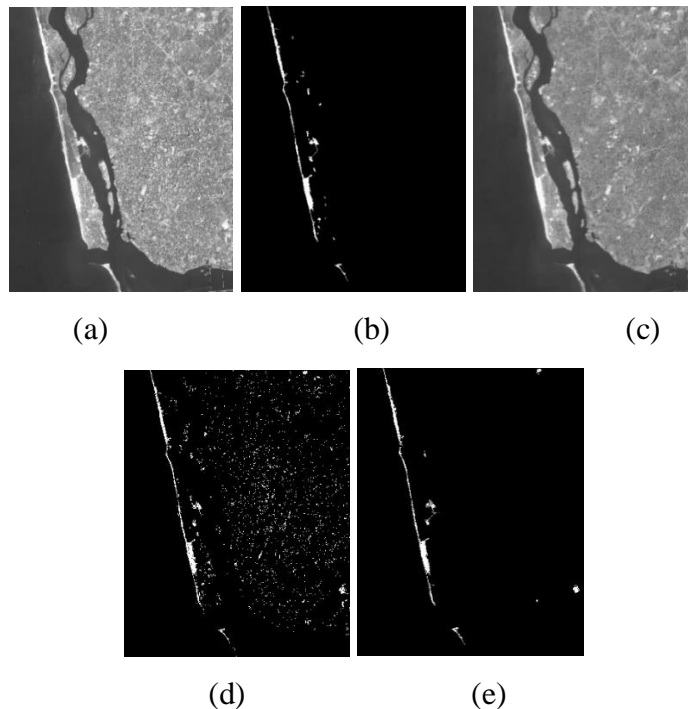
Figure 4.3. (a) – (e). Illustration of results with Cartosat-2 imagery (a) Original image (b) Ground truth (c) MM processed image (intermediate stage) (d) ML Classification result (e) Proposed MM algorithm outcome.

<div align="center">(a)   (b)   (c)   (d)   (e)</div>
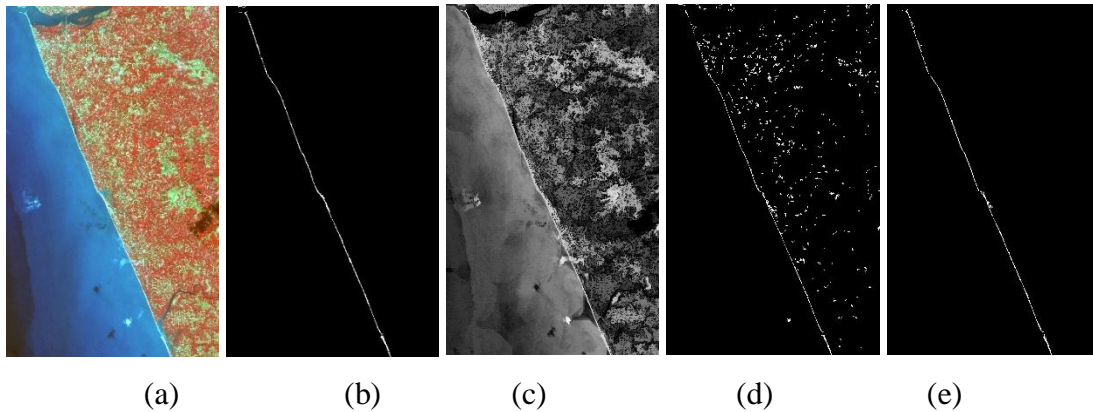
Figure 4.4 (a) – (e). Illustration of results with Resourcesat-2, LISS IV imagery (a) Original image (b) Ground truth (c) MM processed image (intermediate stage) (d) ML Classification result (e) Proposed MM algorithm outcome.

Figure 4.5(a)–(e) illustrates the performance of the algorithm with Cartosat-1 imagery of northern coastal regions of Mangalore. In this case, the algorithm can detect shoreline with 99.90 percentile accuracy. The statistic MCC and F-score values are 0.85878 and 0.85424 respectively recorded. Similarly, figure 4.6 (a)–(e) illustrates the performance of the algorithm with Landsat 8, ETM+ imagery. The proposed MM algorithm extracts shoreline with an accuracy of 99.81% as compared to the accuracy of 97.48% of traditional shoreline classification approach. Since the areal extent is large, visually the shoreline appears very thin. In addition, it is found that, numerous other objects with reflections resembling shoreline pixels are present in the imagery. These pixels led to a reduction of other performance statistics such as F-score and MCC. The traditional shoreline classification approach shows a lesser amount of MCC and F-score values of 0.21575 and 0.23036 respectively.

<div align="center">(a)   (b)   (c)</div>

Feature Extraction Strategies Based on Mathematical Morphology for the Analysis of Remotely Sensed Imagery, PhD Thesis, 2019, NITK Surathkal, India.

48
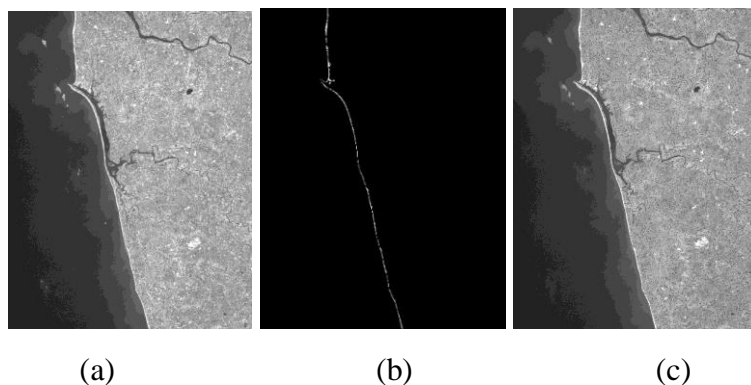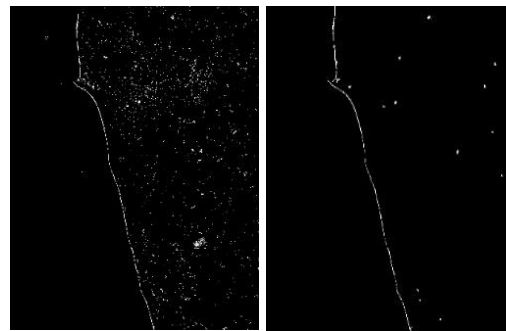
(d)   (e)

Figure 4.5. (a) – (e). Illustration of results with Cartosat 1, PAN (Tile-530-334). (a) Original image (b) Ground truth (c) MM processed image (intermediate stage) (d) ML Classification result (e) Proposed MM algorithm result
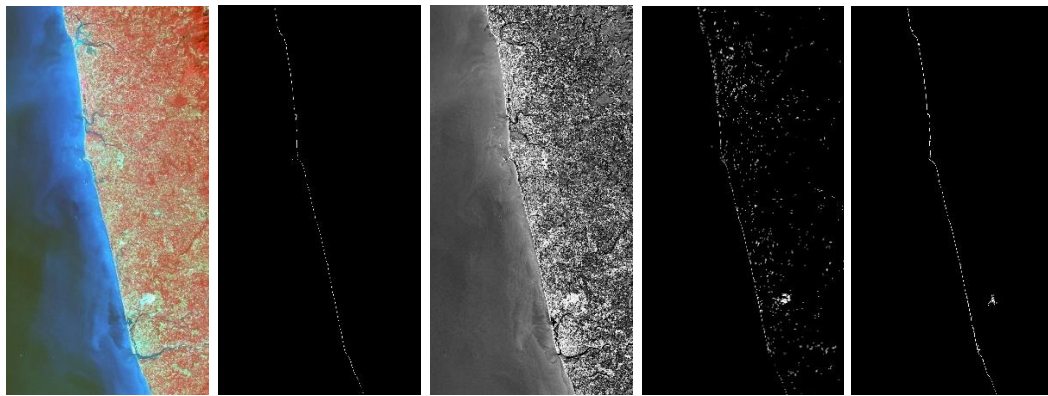
(a)   (b)   (c)   (d)   (e)

Figure 4.6. (a) – (e). Illustration of results with Landsat imagery (a) Original image (b) Ground truth (c) MM processed image (intermediate stage) (d) ML Classification result (e) Proposed MM algorithm result.

As compared to the proposed MM approach, there is an increased number of False Positive and decreased True Positive pixels in the ML classification method. Similarly, True positive pixels recorded a marginal lower count as compared to proposed MM approach. Among all the datasets employed except Cartosat-2 PAN imagery, the proposed MM algorithm performs better in TP pixels. The Cartosat 1 (Tile-532-338) imagery shows highest overall performance (above 0.9) regarding accuracy, MCC, and F-score. Among other datasets, Cartosat 2 imagery also shows the similar value of accuracy with better MCC and F-scores values. The lowest performance observed is

Feature Extraction Strategies Based on Mathematical Morphology for the Analysis of Remotely Sensed Imagery, PhD Thesis, 2019, NITK Surathkal, India.

49

----

with Landsat 8 imagery with MCC and F-score values of 0.62619 and 0.58574 respectively, which are very low as compared to other datasets. The reduction in F-score and MCC values might be due to the presence of objects with same reflections (pixels) resembling shoreline pixels in the imagery. Similarly, larger areal coverage is also accounted for the reduction in performance of Landsat 8 imagery. Here, slight variations in spatial resolution of imagery do not deteriorate the performance; whereas, large variations affect the performance on a larger scale since the shoreline appears very thin in moderate and coarse resolution imageries. As compared to the manual digitization, the proposed algorithm takes very less time for processing. The turnaround time is only a few minutes, whereas it takes hardly few minutes for very small coastal stretches.

4.5 CONCLUSION

Shoreline extraction is inevitable for several studies such as coastal regulatory zone management, coastline erosion monitoring, GIS database updating, watershed definition, flood prediction and the evaluation of water resources. For short stretches of coast, it is easy to trace the shoreline manually, whereas, it is practically difficult when the shoreline becomes very wide, long, complex and inaccessible regions. So automated and reliable techniques play a vital role in updating coastline maps, to evaluate the spatial and temporal alterations due to natural and anthropogenic events, especially for large areas. In this research, the applications and effectiveness of mathematical morphology assisted approach for the extraction of shoreline from different satellite images have been studied. The accuracy of the developed methodology has been assessed with manually prepared ground truths, which reveal that the proposed MM algorithm performs better with different satellite imagery in comparison with an ML classifier result. Therefore, it is concluded that the proposed MM algorithm could be effectively used for updating shoreline maps.

Feature Extraction Strategies Based on Mathematical Morphology for the Analysis of Remotely Sensed Imagery, PhD Thesis, 2019, NITK Surathkal, India.

50

ADAPTIVE APPROACHES FOR WATER BODY EXTRACTION

5.1 GENERAL

Water is one of the most active and inevitable natural resources for the environment, which plays a vital role in social development, human life, and climatic variation. Fast and accurate delineation of water body from satellite images is of great importance due to its utility in several applications such as water resources development, land use planning, wetland protection, lake change detection, flood prediction, and evaluation. Extraction and mapping of glacial lakes from satellite imagery is very important and valuable for many GIS activities such as disaster prediction, critical zone identification, impact assessment (outbursts floods and debris flows), monitoring, etc. Thus, glacial inventory maps of potential areas have to be updated periodically. Most of the strategies proposed until now are based on geography, spectral and spatial characteristics or the category of the feature to be extracted rather than a general approach.

In this chapter, the application and effectiveness of mathematical morphology assisted approach for the extraction of waterbodies from several satellite images with different spatial resolution are elucidated. This chapter focused more on different types of waterbody extraction strategies for ponds, lakes, rivers, and glacier lakes. Different image threshold techniques are used in each method.

5.2 AUTOMATED ALGORITHM FOR WATER BODY EXTRACTION

5.2.1 Introduction

Detection and extraction of water body from satellite imageries are very important and useful for many GIS activities such as riverbank erosion mapping, areal extent calculation, watershed management etc. Methods like normalized difference water index (NDWI) cannot be implemented in the absence of either green or near infrared

(NIR) bands of the satellite imagery. Moreover, some commonly used approaches may even tend to fail or underperform when the resolution of the imagery varies substantially. In this regard, mathematical morphological techniques for image processing have been employed for feature extraction.

This section proposes a flexible MM driven approach which is very effective and useful for the extraction of water bodies from several varieties of satellite images with different spatial resolution. The accuracy of proposed methodology has been assessed with ground truths of the study area. This approach is found successful in water body extraction from different satellite images based on the results drawn from visual and qualitative assessments and in comparison with wellknown methods.

5.2.2   Background and previous research

In recent times, the need for using remote sensing data to accomplish the intricate task of automatic extraction of features has significantly increased (de Castro and Centeno, 2010). With the rapid increase of remote sensing data on a gigabytes scale at daily basis, the need for robust and automated tools for retrieval, management, and processing the data for effective exploitation has also increased (Aptoula, 2014). However, manual investigation of the huge spatial extent and numerous images are expensive and time consuming (Munyati, 2000). Automated feature extraction can significantly reduce the time and cost of data acquisition and can update database effectively with minimal turnaround time. It is primarily significant in remote sensing applications because of varying attributes like sensor fluctuations, changes in spectral and spatial resolutions, alteration of atmospheric conditions among images, and targeted feature of interest. The improved availability and accessibility of remote sensing platforms with varying spatial and temporal resolutions at minimal financial expenditure worldwide gives the prospective of monitoring lake water locations at bigger spatial coverage and wider timescales (Song et al. 2014).

A brief review of RS methods used for lake feature extraction has been given by Jawak et al. (2015) and highlighted that misclassification of dark pixels in feature extraction

accounts for inaccuracies in lake extraction. It is observed particularly in rough terrains such as mountain shadows which acts as dark pixels. Similarly, Song et al. (2014) studied the factors leading to inaccuracy of detecting lake area and water-level variations from multisource satellite imageries and the current uncertainties in mapping characteristics of glacial lakes using remote sensing strategies. A texture analysis based water extraction method without using spectral characteristics of water was proposed by Wang et al. (2008). This algorithm works well for high-resolution panchromatic imagery and the changes in spatial resolution affects its performance. A complex, robust oscillatory network-based algorithm proposed for water body extraction (Li et al. 2011). Similarly, Luo et al. (2010) used Landsat TM images and presented an approach comprising of classification, whole-scale, and local-scale segmentation, water index computation in water extraction yielding better results.

An NDWI assisted approach (McFeeters,1996) in equation 5.1 was suggested for surface water extraction using raw DN (digital number) of Landsat imagery by imposing a threshold value of zero, where all negative NDWI values were categorized as non-water and positive values as water. However, Xu (2006) later on suggested that the NDWI cannot efficiently suppress the radiations from built-up surfaces and an NDWI threshold of zero does not correctly enable in discriminating water pixels from built-up surfaces. Therefore, Xu modified the NDWI assisted approach of McFeeters (1996) by altering NIR band (0.77-0.90 µm) by MIR band (1.55 to 1.75 µm) of Landsat imagery and kept the Green band (0.52-0.60 µm) unchanged, referred to as Modified NDWI (MNDWI) in equation 5.2. Among the existing methods, this modified MNDWI is one of the most widely used water indices for diverse applications.

$$NDWI = \frac{\text{Green - NIR}}{\text{Green + NIR}} \tag{5.1}$$

$$MNDWI = \frac{\text{Green - MIR}}{\text{Green + MIR}} \tag{5.2}$$

A novel Automated Water Extraction Index (AWEI) had been proposed to refine the accuracy of classification containing dark and shadow regions in the imagery in which existing classification strategies fail to classify suitably (Feyisa, et al. 2014).

Feature Extraction Strategies Based on Mathematical Morphology for the Analysis of Remotely Sensed Imagery, PhD Thesis, 2019, NITK Surathkal, India.

53

Performance of the classifier was matched with that of the MNDWI and Maximum Likelihood (ML) classifiers. Duong (2012) specified that the application of red, green, shortwave infrared (SWIR) and NIR band's spectral pattern examination is very useful for water body extraction. Harini and Anil (2013) employed a line driven feature extraction and demonstration strategy and captured the spatial and structural patterns in the scene. A tiered analysis scheme was used to address the computational challenges involved in representation for large-scale image analysis. An approach for river extraction has been defined and tested by researcher Zanin et al. (2013) for the orbital images of those areas found seasonally flooded.

A generalized differential morphological profiles (GDMPs) are developed to obtain the complete differential profiles (Huang et al. 2016). GDMPs can describe the complete shape spectrum and quantify the difference between arbitrary scales, which is more appropriate for representing the multi-scale characteristics and complex landscapes of remote sensing image scenes. Gonzales and Woods (2002) described the use of mathematical morphology techniques in automated feature extraction task. They also pointed out that the MM theory emphasises on the area that studies the geometric properties of features or objects in the images which allow the extraction of image components that are beneficial in the representation and description of the shape of a region, such as skeletons and borders. Compared to traditional pixel based algorithm for object-oriented classification of remote sensing data, Kupidura (2013) showed that mathematical morphology operations provided better accuracy. However the algorithm lacked provision to feed the most sensitive structuring element kernel size at runtime which could affect the results from an input with substantially varying spatial resolution.

Most of the strategies proposed are based on geography, satellite imagery or the category of the feature to be extracted rather than a general approach. Existing approaches may tend to fail or underperform when the resolution of the imagery considerably varies and may require specific spectral bands such as NIR or Green bands of the satellite imagery. In the traditional classification (except object-based

---

classifications) only digital number of pixels are considered, but with the MM strategies, one could additionally consider shape, neighborhood, size and other features of the object. Moreover, state-of-the-art MM based approaches do not give the flexibility to work with any resolution imageries and an option to feed SE size dynamically. The present study aims to develop an MM based algorithm on a single spectral band during execution, rendering flexibility and adaptability, minimal turnaround time with highest possible accuracy. The proposed MM algorithm intends to facilitate core mathematical morphological concepts by providing flexibility to work with any satellite imageries by preserving actual size and shape of the objects in the extracted outcome.

5.2.3 Data

This investigation uses a large set of satellite imageries to identify how well the proposed approach is working towards all these datasets (including very high-resolution Panchromatic (PAN) data of 0.8 meter). The important data sets used for this investigation are procured from various sources and agencies presented in Table 5.1.

Table 5.1. Specification of datasets used

Sl. No	Satellite and Sensor	Spatial Resolution (Meters)	Source / Agency	Region of Interest (ROI)	Date of procurement
1.	CARTOSAT 2, PAN	0.8	NRSC	Mangalore, India	12 NOV 2008
2.	CARTOSAT 1, PAN	2.5	NRSC	Bhopal, India.	06 APR 2006
3.	IRS P6 LISS III	23.5	NRSC	Mangalore, India	22 FEB 2012
4.	Landsat 5, Thematic Mapper	30	Intergraph Corp.	Lake Lanier, Georgia, USA	-

---

Feature Extraction Strategies Based on Mathematical Morphology for the Analysis of Remotely Sensed Imagery, PhD Thesis, 2019, NITK Surathkal, India.

55

5.2.4 Methodology

The acquired images are cloud free, preprocessed to rectify radiometric and geometric errors. The methodological flowchart of the present investigation is presented in Figure 5.1.
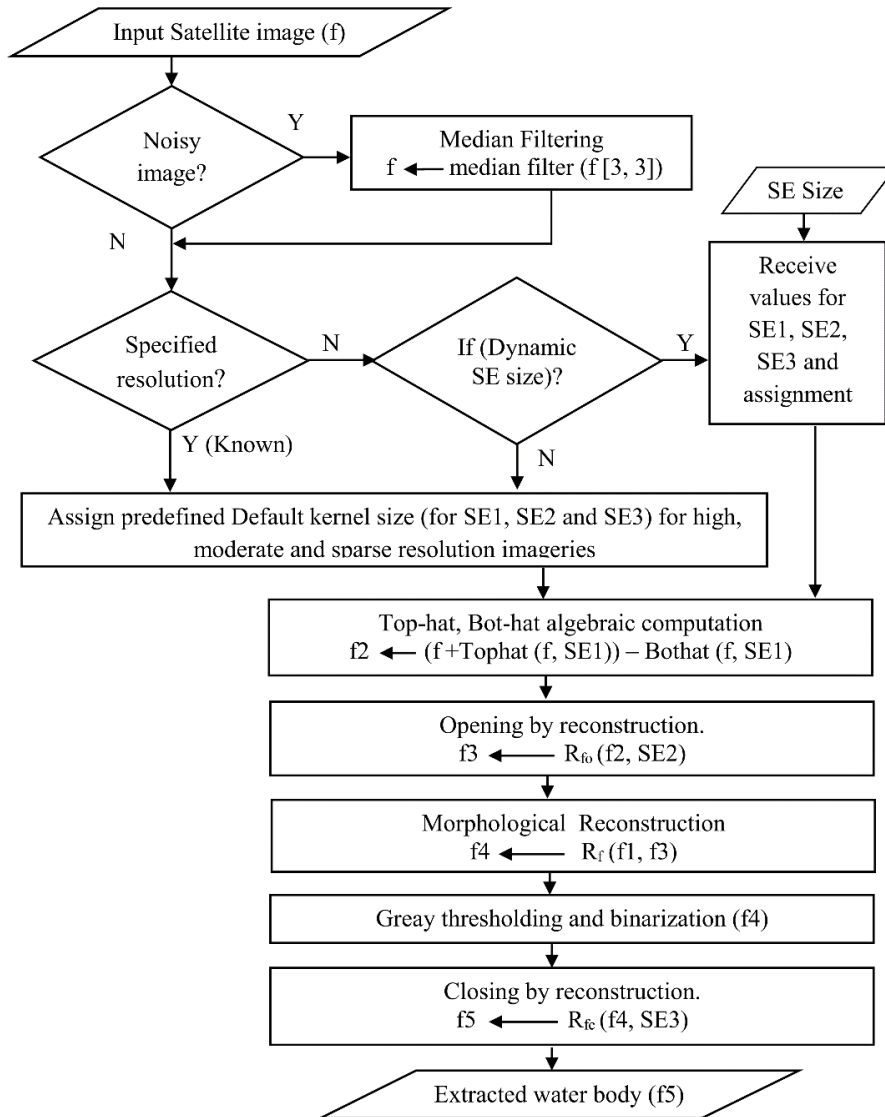
Figure 5.1. Flowchart of the proposed approach for water body extraction

The calibrated image is then fed to a median filter to smooth out and eliminate noises such as salt and pepper. Depending upon the spatial resolution of the input satellite imagery, the algorithm should receive either the appropriate SE kernel size denoted by

Feature Extraction Strategies Based on Mathematical Morphology for the Analysis of Remotely Sensed Imagery, PhD Thesis, 2019, NITK Surathkal, India.

56

SE1, SE2, and SE3 or the algorithm should rely on the default value fed by the programmer for low, medium and high-resolution images. Top-hat (white top-hat) and bot-hat (black top-hat) algebraic computations (addition of original image f to the top-hat filter result of image f and then subtraction of the bottom-hat result of the image f) were performed upon the image for easier identification of water body from the imagery followed by a set of powerful MM operations such as Closing to remove objects and noise smaller than the SE kernel size and reconstruction-driven Opening operations applied multiple times to delineate water bodies. Since the proposed MM algorithm uses morphological reconstruction-driven operations, the actual size and shape of the objects in the output are preserved. The theoretical and mathematical background of these MM operations is explained in detail in section 1.3 of chapter 1.

The MM approaches have a significant influence on the specification of the structuring element (SE), so one should take a little attention to it. Since the proposed algorithm provides a provision to feed the SE Kernel size dynamically, the highest possible accuracy for any resolution imagery can be obtained. To make use of it, the user should understand the correlation between the spatial resolution and SE size, i.e., images with higher resolution require SEs of larger size as compared to moderate and low-resolution imageries.

5.2.4.1 Algorithm development

The stepwise algorithm development of the flowchart shown in figure 5.1 is described in this section.

Input: An N x N matrix sized satellite input image (f1).

Output: An N x N matrix sized extracted output image (f5).

                    Nomenclatures for functions:

         Rf- Morphological Reconstruction;

         Rfo- Opening by reconstruction;

         Rfc- Closing by reconstruction;

                  Step-1: **Start**

                  Step-2: Procurement and registration of the satellite image.

Feature Extraction Strategies Based on Mathematical Morphology for the Analysis of Remotely Sensed Imagery, PhD Thesis, 2019, NITK Surathkal, India.

57

Step-3: **If** (image is noisy) then Pre-processing operations such as Median filtering (f1 = Mf (f, [3, 3])) to remove noises such as salt and pepper. **Else**, go to step 4.

Step-4: **If** (spatial resolution of input images were specified/ known), **then** Auto-assignment of best matching optimal SE kernel size for SE1, SE2 SE3 as per the spatial resolution specified, ranging from very high resolution to sparse resolution imageries (optimal values).

　　　　Else If (User opts for dynamic SE size for SE1 and SE3) **then**

　　　　for (i=1:3) Receive SEi at runtime from end user.

　　　　Else: proceed with default SE size and go to Step 5.

Step-5: Compute Top-hat, Bot-hat algebra;

　　　　(f2 = f1+ Tophat (f1, SE1)) - Bothat (f1, SE1)).

Step-6: Opening by reconstruction; (f3 = Rfo (f2, SE2)).

Step-7: Morphological Reconstruction; (f4 = Rf (f1, f3))

Step-8: Gray thresholding and binarization (f4).

Step-9: Closing by reconstruction; (f5 = Rfc (f4, SE3)).

Step-10: Display or write extracted resultant imagery (f5).

Step-11: **End**.

5.2.5　Results and discussion

The following section describes qualitative and quantitative assessment of the results drawn for different sets of the input imageries. The proposed MM approach is compared with the well-known approaches such as ML classifier, NDWI, and MNDWI. The ground truth data are prepared collectively combining the knowledge of the user via field visit with GPS at possible locations and digitized sketches. Also, manual examination was conducted using Google earth imagery for verification and correction at pixel and object level in an iterative fashion to obtain maximum possible accuracy.The metrics (F-score, Accuracy and MCC) used to evaluate the performance of the system are calculated based on the ground truths. The performance assessment comparison of proposed MM approach with ML classifier is shown in Table 5.2.

Table 5.2. Accuracy assessment comparison of proposed MM approach with ML classifier

Sensor and AOI chosen	Method	TP	FP	TN	FN	F-score	Accuracy	MCC
TM Lanier Lake	MLC	25643	4489	227721	3268	0.8686	0.9702	0.8521
	MM	24402	2907	229303	4509	0.8681	0.9715	0.8526
LISS-III Nethravathi River	MLC	82068	8836	383308	448	0.9464	0.9804	0.9361
	MM	78906	2999	389145	3610	0.9598	0.9861	0.9514
CARTOSAT1 Bhopal lake	MLC	3625025	321580	22712481	113406	0.9433	0.9837	0.9343
	MM	3666556	91948	22942113	71875	0.9782	0.9938	0.9746
CARTOSAT2 Nethravathi River	MLC	8468633	502308	16713176	445701	0.9469	0.9637	0.9194
	MM	8855827	65408	17150076	58507	0.9931	0.9953	0.9895
LISS - IV Bhopal lake	MLC	670180	31195	3924482	19348	0.9636	0.9891	0.9573
	MM	664743	24000	3931677	24785	0.9646	0.9895	0.9584

In general, the figures numbered 5.2 to 5.6 illustrates the different input data sets, ground truth images, MM algorithm processing stages, output drawn from the proposed MM approach and the results drawn from an ML classifier. Figure 5.2 (a)–(e) illustrates the results and ground truth data of Landsat (TM) Lanier lake imagery. Here, the algorithm can extract the entire Lanier Lake by avoiding minor independent lakes present in the nearby areas with 97.15 % accuracy as compared to the accuracy of 0.9702 % of ML classification results. The MCC (0.8526) and F-score (0.8681) values are also satisfactory as the ML classification approach.

(a)   (b)   (c)   (d)   (e)
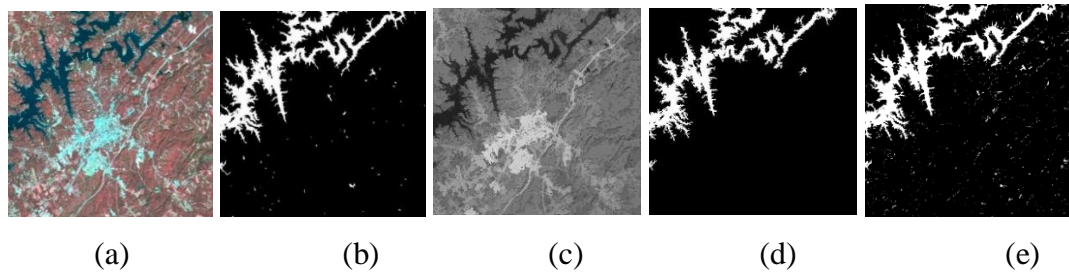
Figure 5.2 (a)–(e). Algorithm results with Landsat (TM) Lanier lake imagery (a) Original Image (b) Ground Truth (c) MM reconstruction stage (d) Proposed MM approach (e) ML classifier

Figure 5.3(a)–(e) shows the results of different algorithms (proposed MM and ML classifier) and ground truth data with IRS P6-LISS III Nethravathi river imagery. Here, the algorithm extracts 98.61 % of the river segment correctly by discarding very small ponds. The ML classifier also shows almost near values of the accuracy of 98.04%. But the MCC (0.9514) and F-score (0.9598) values are quite better than the traditional ML classification approach.

(a)   (b)   (c)

(d)   (e)
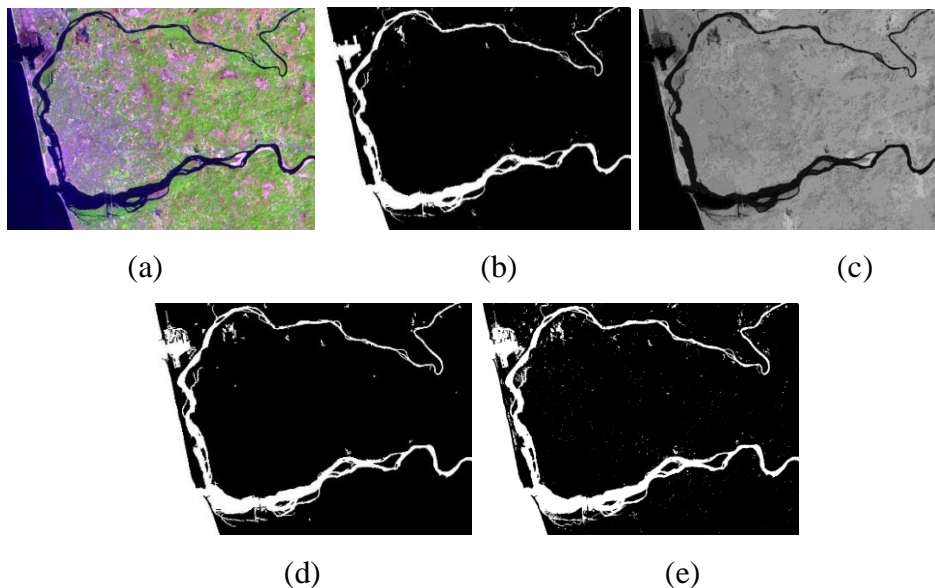
Figure 5.3 (a)–(e). Algorithm results with LISS III Nethravathi River imagery (a) Original Image (b) Ground Truth (c) MM reconstruction stage (d) Proposed MM approach (e) ML classifier

Figure 5.4 (a)–(e) shows the results of different algorithms (proposed MM and ML classifier) and ground truth data with CARTOSAT-1(PAN) image of Bhopal Lake

covering a broader area. In this case, the proposed algorithm is capable of extracting all big lakes and most minor lakes beyond a certain range of pixels. Here, 99.38% accuracy is achieved by the proposed MM algorithm and an accuracy of 98.37% by ML classifier. MCC and F-score values of 0.9746 and 0.9782 are observed for the proposed algorithm, and for the ML classifier, it is observed to be 0.9343 and 0.9433.

| (a) | (b) | (c) | (d) | (e) |
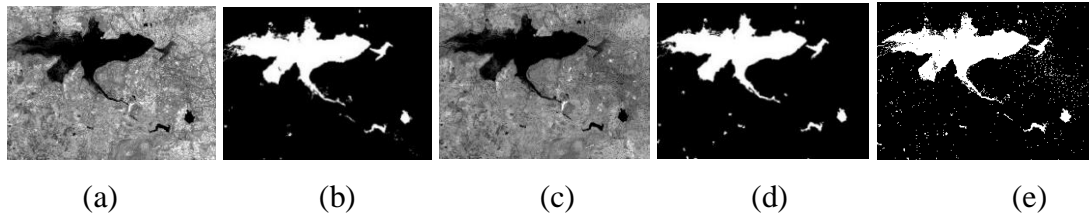
Figure 5.4 (a)–(e). Algorithm results with CARTOSAT 1 (PAN) Bhopal lake imagery (a) Original Image (b) Ground Truth (c) MM reconstruction stage (d) Proposed MM approach (e) ML classifier

Figure 5.5 (a)–(e) illustrates the results of different algorithms (proposed MM and ML classifier) and ground truth data using CARTOSAT-2 (PAN) image dataset of Nethravathi river subset. In this case, the algorithm can detect and extract all most all waterbodies including very small lakes. The performance of the proposed MM algorithm and ML classification method is shown in figure 5.5 (d) and 5.5 (e) respectively. In this case, the proposed algorithm extracts lakes with an accuracy of 99.53% compared to the highest accuracy of 96.37% using traditional ML classifier. Also, a better MCC (0.9895) and F-score (0.9931) are recorded for the proposed approach. The MCC and F-score values of 0.9194 and 0.9469 are recorded for the ML classifier method which is marginally less than the proposed method's performance. This high resolution CARTOSAT-2 dataset exhibited highest overall performance compared to all other datasets.

Figure 5.6 (a)–(e) illustrates the results of different algorithms (proposed MM and ML classifier) and ground truth data using LISS–IV dataset of Bhopal Lake. In this case, the proposed algorithm is capable of extracting all big lakes and most minor lakes beyond a certain range of pixels. The performance of the proposed MM algorithm and ML classification method is shown in figure 5.6(d) and 5.6(e) respectively. Here,

98.95% accuracy is achieved by the proposed MM algorithm compared to an accuracy of 98.91% by ML classifier. MCC and F-score values of 0.9584 and 0.9782is observed for the proposed algorithm, and the ML classifier has shown almost near values of MCC (0.9573) and F-score (0.9636).

(a) (b) (c) (d) (e)
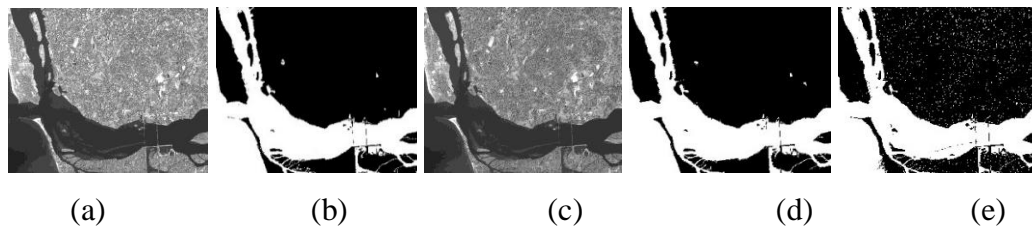
Figure 5.5 (a)–(e). Algorithm results with CARTOSAT-2 Nethravathi river subset (a) Original Image (b) Ground Truth (c) MM reconstruction stage (d) Proposed MM approach (e) ML classifier

(a) (b) (c) (d) (e)
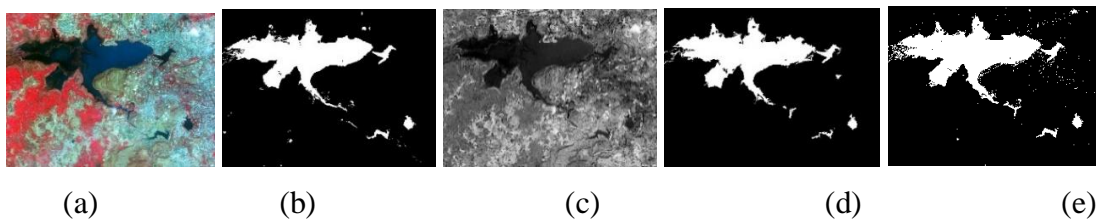
Figure 5.6 (a)–(e). Algorithm results with LISS IV Bhopal lake imagery (a) Original Image (b) Ground Truth (c) MM reconstruction stage (d) Proposed MM approach (e) ML classifier.

On comparison of CARTOSAT 1(PAN) (Figure 5.4) and LISS-IV dataset of Bhopal lake (Figure 5.6), the higher resolution CARTOSAT 1 (PAN) imagery exhibited better performance. In the case of all, MSS datasets tested the ML classification method has exhibited almost near performance with the proposed MM approach, but in the case of PAN imageries (CARTOSAT 1 and 2) the performance of the proposed MM approach was far better. Even though the result of ML classifier with MSS imagery is satisfactory, a large amount of labeled training data are required and hence is laborious.

Visually it is clear from the MM reconstruction stage of processing (Figure 5.2-5.6 (c)) that, the algorithm discriminates water bodies clearly and makes it ready to be extracted. The computational cost of the proposed MM method is influenced by the size of the

---

structuring element used and the total number of pixels present in the input imagery. That is, use of small structuring elements will considerably decrease the processing time. The maximum size (in default cases) of the structuring elements SE1, SE2 SE3 are found to be less than 20 pixels. It ensures that the processing time bound will be of few minutes or less. Methods such as MLC requires much time for training input imagery. Most algorithms in mathematical morphology show a pseudo-polynomial complexity (Géraud et al. 2013). For example, the trivial algorithm of dilation has a complexity of $O(N \times |B|)$ Where N and $|B|$ denote the number of points of the image and that of the structuring element, respectively.

5.2.5.1 Comparison with spectral indices methods

The results of MM approach is compared with results of the indices methods NDWI and modified NDWI. These methods require spectral bands green and NIR for NDWI and green and MIR for MNDWI respectively. So the single band imageries from CARTOSAT series cannot be tested with these approaches also the LISS-IV used in this study doesn't have MIR band. Figure 5.7 (a) and (c), 5.8 (a) and (c) are the illustration of band raster calculation based NDWI and binarized NDWI outcomes respectively. Similarly, Figure 5.7 (b) and (d), 5.8 (b) and (d) represents the band raster calculation based MNDWI and binarized MNDWI outcomes respectively. After calculation of this spectral index, it is binarized with respect to zero. All the values above zero are changed to 1 and below zero to zero. This binarization helps in two ways: first, all the water pixels become 1, and all the non-water pixel becomes zero. These well-known methods are compared with the ground truth map and assessment results recorded.

| (a) | (b) | (c) | (d) |
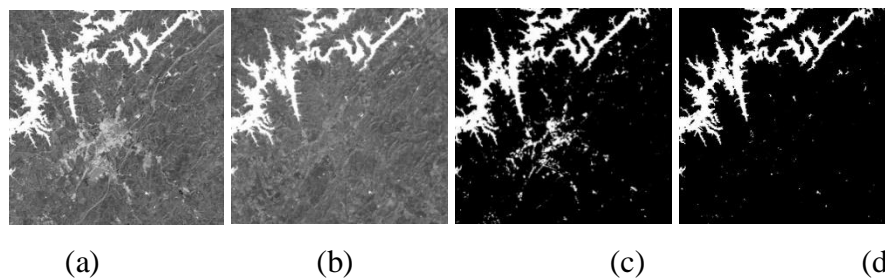
Figure 5.7 (a)–(d). Spectral indices algorithm results with Landsat (TM) Lanier lake imagery (a) NDWI (b) MNDWI   (c) Binarized NDWI (d) Binarized MNDWI

Feature Extraction Strategies Based on Mathematical Morphology for the Analysis of Remotely Sensed Imagery, PhD Thesis, 2019, NITK Surathkal, India.

63

| (a) | (b) | (c) | (d) |
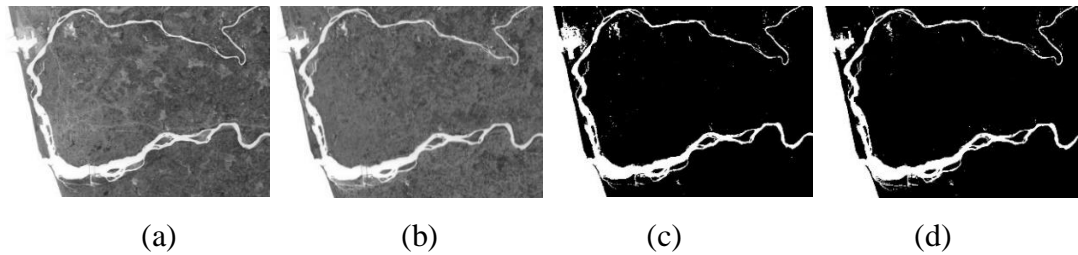
Figure 5.8 (a)–(d). Spectral indices algorithm results with LISS III Nethravathi River imagery (a) NDWI (b) MNDWI (c) Binarized NDWI (d) Binarized MNDWI

A comparison of results of the proposed MM approach with the results of MNDWI and NDWI methods is carried out. The performance of NDWI and MNDWI water body extraction approach is depicted in Table 5.3.

Table 5.3. Accuracy assessment of proposed MM approach with NDWI and MNDWI

Sensor and AOI chosen	Approach	TP	FP	TN	FN	F-score	Accuracy	MCC
TM, Lanier Lake	NDWI method	27593	37911	194299	1318	0.5845	0.8498	0.5727
	MNDWI method	27652	32089	200121	1259	0.6238	0.8723	0.6112
	Proposed MM Method	24402	2907	229303	4509	0.8681	0.9715	0.8526
LISS-III, Nethravathi River	NDWI method	82650	53127	340278	2	0.7568	0.8884	0.7255
	MNDWI method	82649	23461	369944	3	0.8757	0.9507	0.8558
	Proposed MM method	78906	2999	389145	3610	0.9598	0.9861	0.9514

The MNDWI method gives better performance than the NDWI method for all the performance metrics for both the multispectral images of sensor LISS III and TM. In case of Landsat TM imagery, the highest possible accuracy obtained with spectral indices method is 87.23% which is potentially lower than the proposed MM method

with 97.15% accuracy. Similarly, for the LISS-III imagery, the highest possible accuracy recorded with spectral indices method is 95.07% which is also lower than the proposed MM methodology with 98.61% accuracy. The Indices methods produced very less FN pixels but more number of FP pixels, thereby lowering its performance. In comparison with the ML Classifier, even though there are more misclassified pixels than that of the MNDWI, it has shown better results in all aspects than the spectral indices method. Similarly, a comparison of correlation coefficients of the spectral indices method and proposed MM approach is carried out. The highest MCC value of 0.8526, 0.9514 is recorded for the proposed MM method, followed by that of MNDWI, with MCC values of 0.6112 for TM Lanier lake and 0.8558 for LISS-III imagery. The above results emphasize the fact that the proposed MM approach is found efficient and performs better in water body extraction from different satellite images.

5.2.6   Conclusions

Detection and extraction of water bodies have been challenged by the spectral and spatial heterogeneity of the satellite imageries. This study proposes an MM driven approach which is very effective and useful for the extraction of water bodies from several sensors driven satellite imageries with different spatial resolutions. This study uses morphological reconstruction driven operations which preserves the actual size and shape of the objects in the outcome. Moreover, the availability of more than one spectral band details of satellite imagery is not compulsory for the proposed algorithm, and it provides a provision to feed the most sensitive SE kernel size at runtime. So the highest possible accuracy can be achieved for different high-resolution imagery ensuring this approach effective and adaptive than other common methods. The performance of well-known methods such as NDWI, MNDWI, and ML classifier is compared with the proposed MM approach. This study reveals the fact that the proposed MM approach is dominant regarding performance and hence MM based approaches can be used for practical applications.

Feature Extraction Strategies Based on Mathematical Morphology for the Analysis of Remotely Sensed Imagery, PhD Thesis, 2019, NITK Surathkal, India.

65

5.3 APPROACH FOR GLACIAL LAKE EXTRACTION

5.3.1   Introduction

With advances in remote sensing (RS) technology and platforms, very high quality and fine spatial resolution satellite images are available. Automated glacier lake extraction techniques can drastically minimize the time and cost of data acquisition and database updation. Thus automated and reliable technique plays a vital role in updating glacial lake database to evaluate the spatial and temporal evolution of glacial inventory especially for vastly developing regions. Methods like normalized difference water index (NDWI) can not be calculated in the absence of either green or near infrared (NIR) bands of the satellite imagery.

This section presents a mathematical morphology based approach which is effective and useful for the extraction of glacial lakes from satellite and aerial imageries with better accuracy and minimal turnaround time. Maintenance of actual size and shape of the glacial lakes, run-time control over structuring elements, automation, faster processing, and single band adaptability are predominant features of this work. The accuracy of developed methodology has been assessed with the ground truths of the study area in comparison with Otsu-threshold based methods.

5.3.2   Related works

Glacier Lake Outburst Floods (GLOFs) are progressively alarming the environment along with the comfort and security of humans downstream, and this has drawn excessive attention from researchers and scientists all over the world (Huggel et al. 2002; Dussaillant et al. 2009; Ives et al. 2010, Emmer and Vilímek., 2013). On the other hand, Huggel et al. (2002) assessed the hazards from glacier lake's outbursts using remote sensing. With the development of high spatial as well as temporal resolution satellite imageries for disaster monitoring, it is possible to utilise the remotely sensed data to monitor and predict the lake dynamics and outburst potential (Cenderelli and Wohl, 2001; Mergili et al. 2011; Song et al. 2014; Huang, et al. 2015).

Traditional spectral based methods of data extraction from remotely sensed images are not suitable for high spatial resolution imagery (Blaschke, 2010). McFeeters (1996) proposed an NDWI assisted approach for waterbody extraction using raw DN (Digital Number) values of satellite imagery. Later on, Xu (2006) revised this approach as modified NDWI by altering the spectral band employed in the NDWI method. Since these techniques cannot calculate using a single spectral band, making them unfit for worldview-1 or CARTOSAT series driven datasets. Spectrally based classification approaches are highly dependent on the spectral information and neglect some important information from high spatial resolution images, such as spatial features. Mathematical morphology is the fundamental theory for several image processing algorithms, which can extract image shape features by employing various shape-structuring elements (Shih et al. 1995, Kupidura 2013). This processing technique has prooved to be a powerful tool for several computer-vision tasks in binary and grey scale images, such as edge detection, skeletonization, noise suppression, image enhancement and pattern recognition (Ortiz, et al. 2002).

Mathematical morphology offers an approach to image processing based on geometrical shape. Depending on the type of the operation, specific characteristics of the objects in the image, like shape, size, neighborhood etc. can be taken into account. Morphology is commonly applied in remote sensing because of its ability to process image, de-noising, and segmentation of objects of different texture and completing edges, which is very promising and potentially helpful for extracting features in photogrammetry (Kowalczyk, 2008).The MM strategies consider shape, neighborhood, size and other features of the object besides DN values which is the only factor considered in the traditional pixel based approaches. This section describes an MM driven semi-automated approach which is effective and useful for the extraction of glacial lakes from remotely sensed imageries with better accuracy and minimal turnaround time.

5.3.3 Data and methods

This study uses multiple sets of satellite imageries to identify how well the proposed approach is performing with data sets. The important data sets used for this study is procured from various sources and agencies mentioned in Table 5.4.

Table 5.4 Specification of datasets details

Satellite Sensor	Spatial Resolution	Source / Agency	AOI (Area of Interest)	Date of pass
MODIS Aqua	250m	NASA https://visibleearth.nasa.gov/view.php?id=84585	Himalaya, Nepal	October 16, 2014
Landsat ETM+	30m	USGS https://earthexplorer.usgs.gov/	Ladakh, Jammu and Kashmir, India;	05th Mar 2017

The methodological flowchart of the present investigation is presented in figure 5.9. The acquired image which is cloud-free initially undergoes various pre-processing operations to rectify radiometric and geometric errors. The SE declaration (SE1 and SE4) and initialization which governs important processing activities are performed before the execution of the algorithm. The SE values initialized or fed at runtime to the algorithm have a greater significance, their slight variation changes the entire glacier lake extraction result and accuracy. Testing with multiple sets of the dataset identifies the optimum SE values. A set of MM operations were applied, starting with few fundamental MM opening, MM erosion operations. Morphological reconstruction is used to recover the actual size and shapes of objects which is affected during any MM operations. Top-hat and bot-hat algebraic computations (addition of original image f to the top-hat filter result of image f and then subtraction of the bottom-hat result of the image f) were performed upon the image for easier identification of glacier derived water-bodies from the imagery followed by a set of powerful MM operations such as closing to remove objects and noise smaller than the specified SE kernel size and MM intersection applied multiple times to identify glacier lakes. The theoretical and

mathematical background of these MM operations is explained in detail in section 1.3 of chapter 1. It is apparent from the MM closing operation (with SE4 values) that the algorithm discriminates glacier lakes, and is prepared for further extraction. Finally, the algorithm separates out the glacier lakes portions by imposing appropriate grey-thresholds to the imageries. The details of these operations are outlined in algorithm part of this section.
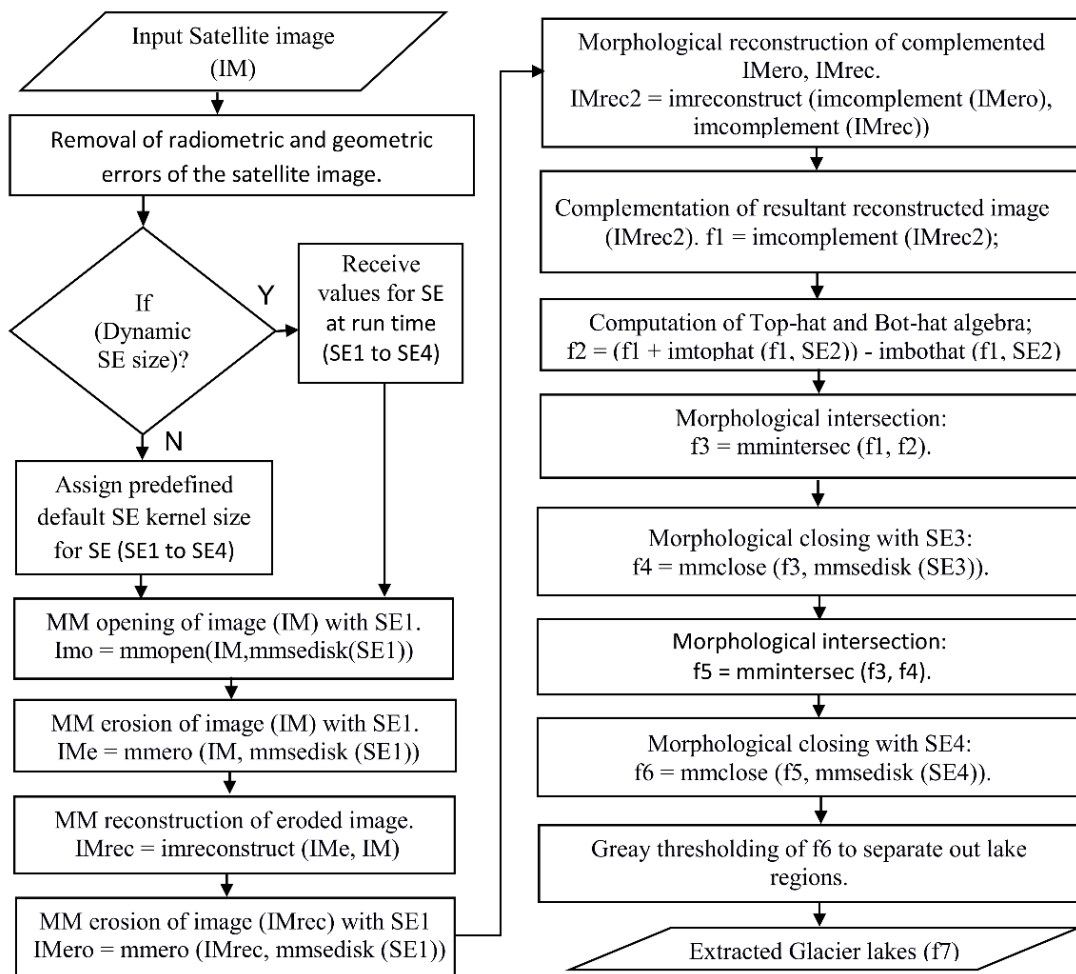
Figure 5.9 Flowchart of the proposed approach for glacier lake extraction.

5.3.3.1 Algorithm development

The stepwise algorithmic development of the flowchart shown in figure 5.9 is described in this section.

Input: An N x N matrix sized satellite input image (IM).

Output: An N x N matrix sized extracted output image (f7).

Waterbody Extraction

1-   Start

2-   Read the N x N matrix sized image (IM) in grey-level format.

3-   **If** (User opts for dynamic SE size for SE1 and SE4) **then**
             Receive SE1 & SE4 on runtime,

      Else
      Declaration & initialization of default structuring elements (SE1 to SE4).

4-   Morphological opening operation of image (IM) with SE1.

5-   Morphological erosion operation of image (IM) with SE1.

6-   Morphological reconstruction of eroded image. IMrec = imreconstruct (IMe, IM)

7-   Morphological erosion of image (IMrec) with SE1

8-   Morphological reconstruction using complemented eroded and reconstructed images.
      IMrec2 = imreconstruct (imcomplement (IMero), imcomplement (IMrec))

9-   Complementation of resultant reconstructed image (IMrec2) and assign to f1.

10-   Computation of Top-hat and Bot-hat algebra;
      f2 = (f1 + imtophat (f1, SE2)) - imbothat (f1, SE2)

11-   Morphological intersection: f3 = mmintersec (f1, f2).

12-   Morphological closing with SE3: f4 = mmclose (f3, mmsedisk (SE3)).

13-   Morphological intersection: f5 = mmintersec (f3, f4).

14-   Morphological closing with SE4: f6 = mmclose (f5, mmsedisk (se4)).

15-   Thresholding of f6 to separate out lake regions.

16-   End.

5.3.4   Results and discussion

This section describes the results drawn from different sets of the input imageries including visual, qualitative and quantitative assessments. The results obtained are compared with that of Otsu-threshold driven approach. The metrics (Precision, F-score, Accuracy and MCC values) used to assess the performance of the system are calculated based on the ground truths. The performance of the proposed MM based extraction approach and that of the Otsu-threshold driven extraction approach is depicted in the table 5.5 (pixel statistics comparison) and 5.6 (Performance comparison of proposed MM approach and Otsu-threshold driven approach). In general, the figures numbered 5.10 to 5.13 (a) – (e) illustrates the different input data sets, ground truth images, results drawn from an Otsu-threshold based approach based approach, MM algorithm

----
Feature Extraction Strategies Based on Mathematical Morphology for the Analysis of Remotely Sensed Imagery, PhD Thesis, 2019, NITK Surathkal, India.

70

intermediate processing stages and the output drawn from the proposed MM approach.

Table 5.5. Pixel statistics comparison of proposed MM approach and Otsu-threshold driven approach

Sensor and AOI	Method	TP	FP	TN	FN	Total (TN+TP+FN+FP)
MODIS Nepal, Subset 1	MM	14535	80	362539	2511	379665
	Otsu	13164	23	362596	3882	379665
MODIS Nepal, Subset 2	MM	6803	820	990923	2563	1001109
	Otsu	6867	24983	966760	2499	1001109
MODIS Nepal, Subset 3	MM	12295	358	313138	938	326729
	Otsu	12601	695	312801	632	326729
Landsat 8 ETM+, Ladakh	MM	436145	41742	12971815	45973	13495675
	Otsu	399583	246627	12766930	82535	13495675

Table 5.6. Performance comparison of proposed MM and Otsu-threshold based approach.

Sensor and AOI	Method	Precision	F-score	Accuracy	MCC
MODIS Nepal, Subset 1	MM	0.99452	0.91816	0.99317	0.91757
	Otsu	0.99825	0.87083	0.98971	0.87331
MODIS Nepal, Subset 2	MM	0.89243	0.80087	0.99662	0.80349
	Otsu	0.21560	0.33322	0.97254	0.38835
MODIS Nepal, Subset 3	MM	0.97170	0.94993	0.99603	0.94812
	Otsu	0.94772	0.94997	0.99593	0.94786
Landsat 8 ETM+, Ladakh	MM	0.912652	0.90863	0.99350	0.90527
	Otsu	0.61834	0.70827	0.97560	0.70396

Figure 5.10, which represents the illustration of algorithm results with MODIS Aqua imagery of subset-1. The performance of an Otsu-threshold based method (Fig. 5.10 c)

and the proposed MM algorithm (Figure 5.10 e) is shown. Here, the proposed algorithm extracts glacier lakes with ann accuracy of 99.31% as compared to the accuracy of 98.97% for the traditional Otsu-threshold based approach. Also, a better MCC (0.91757), F-score (0.91816) are recorded for the proposed approach, but the precision (0.99452) was slightly lower than Otsu-threshold based method.

| (a) | (b) | (c) | (d) | (e) |
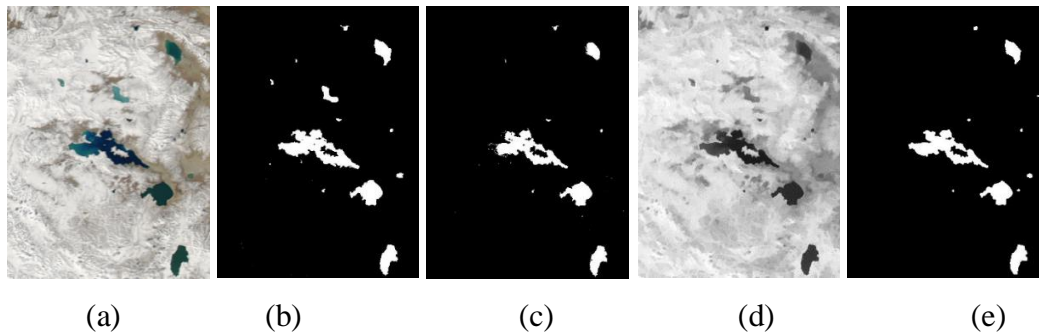
Figure 5.10 (a) – (e). Illustration of algorithm results with MODIS Aqua imagery of subset-1. (a) Original image (b) Ground truth (c) Otsu-threshold based approach   (d) MM processed image (intermediate stage) (e) Proposed MM algorithm outcome.

Figure 5.11 illustrates the algorithm performance with MODIS Aqua imagery of subset-2. Here, the proposed MM algorithm can extract glacier lakes with 99.66% accuracy and satisfactory MCC (0.80349), F-score (0.80087) and precision (0.89243) values. The presence of deep mountains and other shadow regions resembling glacier lakes had attributed to lower MCC value. Even though traditional Otsu-threshold based method has an accuracy of 97.25%, its MCC (0.38835), F-score (0.80087) and precision (0.21560) values are marginally lower than that of proposed MM based approach. Due to hill shadows, numerous misclassification causes an abrupt increase of false positive pixels for traditional threshold based method leading to this undesirable performance.

Figure 5.12 illustrates the performance of the algorithm with MODIS Aqua imagery of subset-3. Here, an accuracy of 99.60% and 99.59% is achieved by the proposed algorithm and the Otsu-threshold based method respectively. MCC, F-score and Precision values of 0.94812, 0.94993 and 0.97170 is observed for the proposed MM algorithm while for the Otsu-threshold based approach it is observed to be 0.94786,

----
Feature Extraction Strategies Based on Mathematical Morphology for the Analysis of Remotely Sensed Imagery, PhD Thesis, 2019, NITK Surathkal, India.

72

0.94997 and 0.94772. Also, this imagery datasets yields highest overall performance (highest accuracy, F-score, MCC) and precision for proposed MM as well as Otsu-threshold approaches.

(a)　　　　　(b)　　　　　(c)　　　　　(d)　　　　　(e)
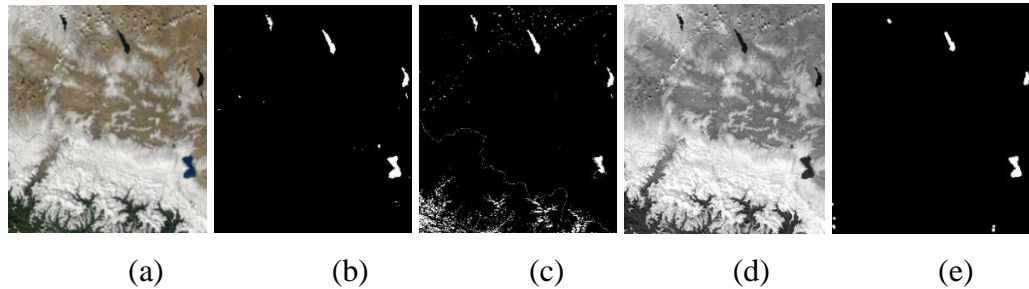
Figure 5.11 (a) – (e). Illustration of algorithm results with MODIS Aqua imagery of subset-2.　(a) Original image (b) Ground truth (c) Otsu-threshold based approach (d) MM processed image (intermediate stage) (e) Proposed MM algorithm outcome.

(a)　　　　　　　　(b)　　　　　　　　(c)

(d)　　　　　　　　(e)
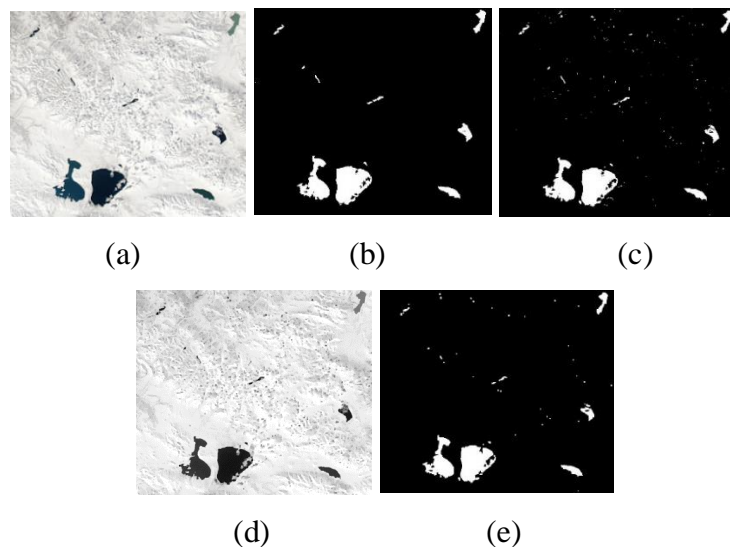
Figure 5.12 (a) – (e). Illustration of algorithm results with MODIS Aqua imagery of subset-3.　(a) Original image (b) Ground truth (c) Otsu-threshold based approach (d) MM processed image (intermediate stage) (e) Proposed MM algorithm outcome.

Figure 5.13 illustrates the performance of the algorithm with Landsat ETM+ sensor imagery of Ladakh region. The proposed MM algorithm extracts glacier lakes with an

----

Feature Extraction Strategies Based on Mathematical Morphology for the Analysis of Remotely Sensed Imagery, PhD Thesis, 2019, NITK Surathkal, India.

73

accuracy of 99.35% as compared to the accuracy of 97.56% for the Otsu-threshold driven approach. MCC, F-score and Precision values of 0.90527, 0.90863 and 0.912652 is recorded for the proposed MM algorithm whereas for the Otsu-threshold based approach it is observed to be 0.70396, 0.70827 and 0.61834 which is far lesser than the proposed one. Despite the large areal coverage and mountain shadows, the algorithm offers satisfactory performance.

(a)   (b)   (c)

(d)   (e)
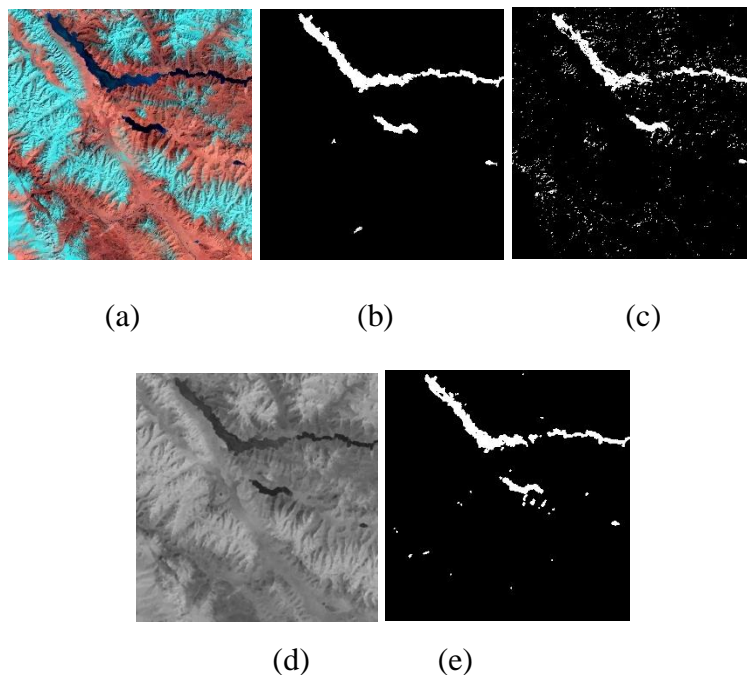
Figure 5.13 (a) – (e). Illustration of algorithm results with Landsat ETM+ sensor imagery of Ladakh region. (a) Original image (b) Ground truth (c) Otsu-threshold based approach (d) MM processed image (intermediate stage) (e) Proposed MM algorithm outcome.

5.3.5   Conclusions

Detection and tracking spatial and temporal changes of glacier lake from remotely sensed imagery is very important and useful for many GIS activities. Glacial lake outburst floods (GLOFs) are among the most critical natural hazards in high mountain regions. Thus automated and reliable techniques play a vital role in updating glacier lake inventories to evaluate the spatial and temporal changes in glacial lakes in the view of disaster prediction, critical zone identification, impact assessment, etc. In this

section, the application and effectiveness of mathematical morphology assisted approach for the extraction of glacier lakes are elucidated. The Otsu-threshold based methods do not make any structural changes to the features present in the imagery. It does not guarantee good accuracy in many cases as it is prone to noises and loss of feature details if the calculated or obtained threshold is not the desired value. The proposed MM algorithm facilitates a provision to feed the SE Kernel size SE1 and SE4 values dynamically, the highest possible accuracy from different sets of inputs (with varying spatial resolution and swath distance) can be obtained. Since the pixel flow characteristics and shape of water body should have definite signatures, this research provides the significance of how MM assisted approach works well in such situations. The band details of satellite imagery (like NIR or green) is not mandatory since the algorithm works with a single spectral band making this approach effective over commonly used methods. The accuracy of the developed methodology has been evaluated with manually prepared ground truths, revealing better performance with different datasets compared to Otsu-threshold based method.

5.4. ANN SUPPORTED ALGORITHM FOR LAKE EXTRACTION

Automated and reliable technique plays a significant role in updating lake database to evaluate the spatial and temporal variation of lakes and ponds, especially for vastly growing urban areas. This research work presents an artificial neural network (ANN) computed threshold value based mathematical morphology driven approach for extraction of lakes from satellite imageries with better accuracy. The accuracy of developed methodology has been assessed with the ground truths of the study area revealing better performance with different datasets compared to ML classifier and Otsu-threshold based methods.

5.4.1. Introduction and related works

Precise extraction and automatic identification of water bodies are of great significance in the present times. Remote sensing, as a suitable, fast, efficient, and timely earth observation practice, can provide the increasing potential for information extraction

Feature Extraction Strategies Based on Mathematical Morphology for the Analysis of Remotely Sensed Imagery, PhD Thesis, 2019, NITK Surathkal, India.

75

such as water bodies (Huang, et al. 2015). A brief review on remote sensing methods used for Lake feature extraction has been given by Jawak et al. (2015), and they also pointed out that misclassification of dark pixels in feature extraction accounts for inaccuracies in lake extraction. It is observed particularly in rough terrains such as mountain shadows that act as dark pixels. Similarly, Song et al. (2014) discussed the factors leading to inaccuracy of detecting lake area and water-level variations from multisource satellite imageries and studied the current uncertainties in mapping characteristics of glacial lakes using remote sensing strategies. A texture analysis based water extraction method without using spectral characteristics of water was proposed by Wang et al. (2008). This algorithm works well for high-resolution panchromatic imagery and the changes in the spatial resolution which affects its performance.

McFeeters (1996) suggested an NDWI assisted approach for surface water extraction using raw DN (Digital Number) of Landsat imagery by imposing a threshold value of zero, where all negative NDWI values were categorized as non-water and positive values as water. Recently, Feyisa, et al. (2014) proposed a novel Automated Water Extraction Index (AWEI) to refine the accuracy of classification containing dark and shadow regions in the imagery in which state-of-the-art classification strategies fail to classify acceptably. Performance of the classifier was matched with that of the MNDWI and Maximum Likelihood (ML) classifiers.

Mathematical morphology is a theory and technique used to process and analyze images (Mukhopadhyay and Chanda, 2002). It provides an alternative move towards image processing based on shape concept rooted from set theory (Naegel, 2007) rather than traditional mathematical modeling and analysis. Gonzales and Woods (2002) described how the techniques of mathematical morphology would be useful in automating feature extraction task. Kupidura (2013) in his study proved that mathematical morphology operations far exceeded in accuracy. However, this algorithm lacked provision to feed the most sensitive SE kernel size at runtime which could affect the results from an input with substantially varying spatial resolution.

This study presents a novel semi-automated lake and pond extraction method using ANN and MM from satellite imageries with higher accuracy and minimal turnaround time. The ANN is employed as an aid for determining exact threshold value during extraction of lake features. Very few researchers have investigated the use of ANN in image thresholding along with MM techniques. Preservation of actual size and shape of the lake/pond boundary, dynamic control, semi-automation, faster processing and single band adaptability are the significant features of this work. The accuracy of developed methodology has been assessed with ground truths of the study area.

5.4.2. Dataset used for the study

The important datasets used for this investigation are obtained from various sources and agencies mentioned in Table 5.7. This study uses a different set of satellite imageries including high resolution Panchromatic data of 2.5m and low resolution 30m data of Landsat-8.

Table 5.7 Specification of datasets details

Sl. No	Satellite and Sensor	Spatial Resolution	Source / Agency	AOI	Date of procurement
1.	CARTOSAT 1, PAN	2.5	NRSC	Bhopal, India.	06-APR-2006
2.	LISS IV	5.8	NRSC	Ramagundam, Telangana, India	21-FEB-2015
3.	LISS IV	5.8	NRSC	Bhopal, India	29-JAN-2010
4.	Sentinel-2 dataset	10	USGS (ESA)	Ramagundam, Telangana, India	25-DEC-2017
5.	Sentinel-2 dataset	10	USGS (ESA)	Palghat, Kerala, India	03-FEB-2017
6.	Landsat-8 ETM+	30	USGS	Ladakh (Tibet), India.	05-MAR-2017

5.4.3. Methodology

The methodological flowchart of the present investigation is presented in figure 5.14. The cloud-free image is first corrected for radiometric and geometric errors if required.

Median filtering is executed if the image comes with noises such as salt and pepper, etc. The SE (SE1 to SE4), pixel limit (P) declaration and initialization which govern important processing activities are performed before the execution of the algorithm. Moreover, the initialized SEs and P values have a greater significance. Their slight variation can change the entire lake extraction result and accuracy. A series of MM operations is applied, starting with powerful MM reconstruction driven Opening, and then Closing, computation of Top-hat and Bot-hat algebra and so on, supported by an ANN assisted thresholding and binarization (neural network based automatic threshold selection). Then the algorithm aims to isolate unwanted objects through 'Binary area opening' with P pixel range. Complementation of image is carried out since 'area opening' operation considers a group of white pixels as objects. Depending on the noise level, the end user can set the range of P dynamically offering further refined results. The details of these operations are outlined in the flowchart (Figure 5.14) of the present section. The theoretical and mathematical background of these MM operations is explained in detail in section 1.3 of chapter 1.

The neural network is designed to obtain the threshold value automatically by using the frequency components of the histogram curve for every digital number or gray level value. Threshold values are effectively obtained for each image in diverse situations. Thresholding operation involves selecting a particular value Tr and assigning zero (0) to the pixels with values smaller than or equal to Tr and one (1) to the remaining pixels. For a dark object on a light background, the parameter Tr, termed the brightness threshold, is chosen and applied to the image f (x, y) as follows (eq. 5.1):

$$f(x,y) = \begin{Bmatrix} 0 & if \geq Tr \\ 1 & if < Tr \end{Bmatrix} \qquad\qquad (5.1)$$

The ANN is manually trained with several threshold values obtained for different images. For every sample, the frequencies for each grey level or digital number are taped in a file to form the input data to ANN and for each input data vector set the threshold value is matched. These values so obtained are normalized between zero to one for the feature of sigmoid function activation. In normalization, same maximum

----

Feature Extraction Strategies Based on Mathematical Morphology for the Analysis of Remotely Sensed Imagery, PhD Thesis, 2019, NITK Surathkal, India.

78

and minimum values are employed. A neural network is designed using the attained weights derived from off-line training. The number and statistics of neurons employed in the hidden layer are determined experimentally.
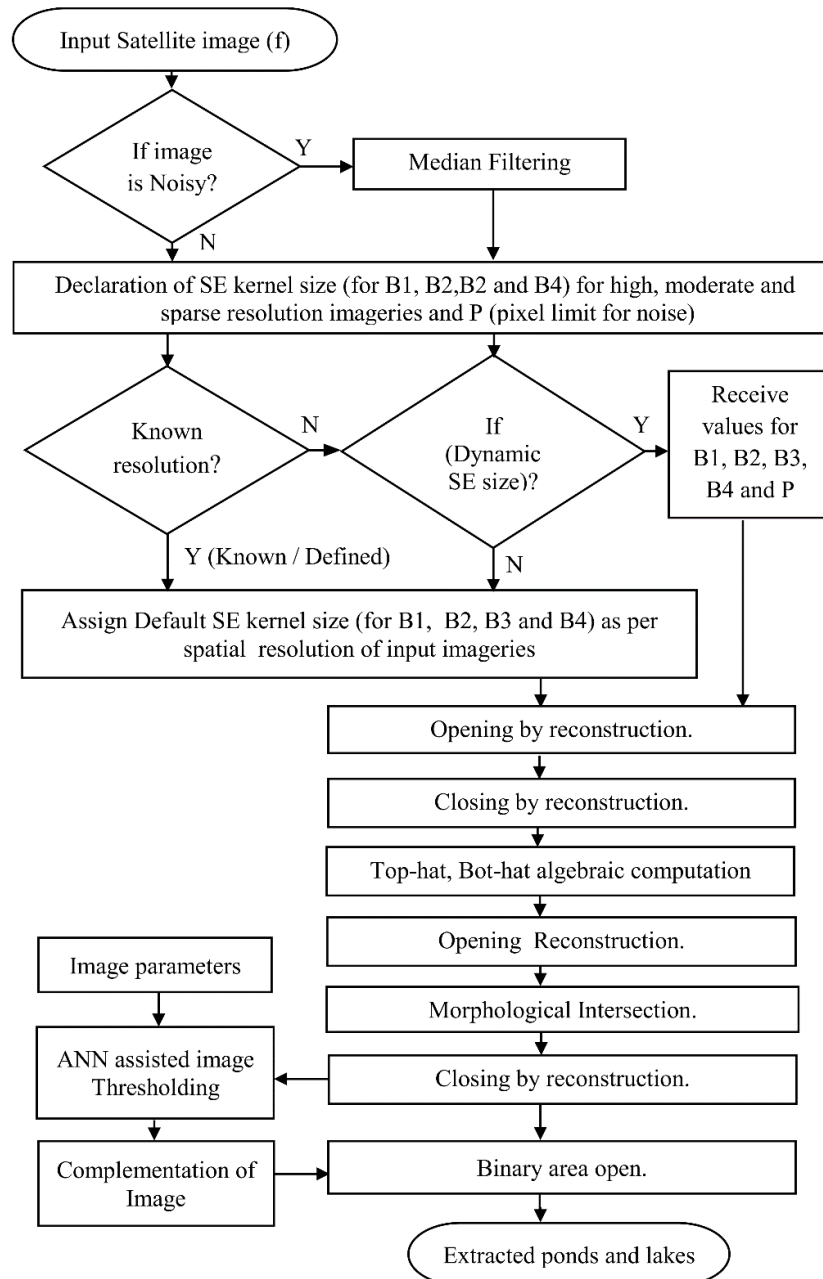
Figure 5.14. Flowchart of the proposed lake extraction approach.

The performance of the proposed MM approach is evaluated with the performance of ML classifier and Otsu-threshold based methods. The traditional supervised

Feature Extraction Strategies Based on Mathematical Morphology for the Analysis of Remotely Sensed Imagery, PhD Thesis, 2019, NITK Surathkal, India.

79

classification is performed for water and non-water separation. This classification is carried out in such a way that it ensures maximum accuracy and least misclassifications. The class signatures merged all non-water regions for the assessment, thus only water and non-water regions will remain. In the threshold driven method, a threshold is applied to each input imagery to separate water and non-water regions. Thereafter, sufficient range of noise removal strategies is applied to demarcate all unnecessary object noises.

5.4.4. Results and discussion

This section describes the results drawn from visual, qualitative and quantitative assessments of different sets of the input imageries and its comparison with other traditional methods. In general, the figures numbered 5.12 to 5.17 (a) – (f) illustrates the different input data sets, ground truth images, MM algorithm intermediate processing stages, result drawn from the proposed MM approach, Otsu-threshold based method and an ML classifier. The critical comparison has been carried out between proposed MM approach results and the best results of the traditional methods.

Figure 5.15 illustrates the results of different algorithms (proposed MM, ML classifier and Otsu-threshold based) and ground truth data using LISS IV dataset of Ramagundam region of Telangana state. The performance of the proposed MM algorithm, ML classification method and threshold based method and is shown in Figures 5.15 d, 5.15 e and 5.15 f respectively. In this case, the proposed algorithm extracts lake with an accuracy of 99.673% compared to the highest accuracy of 99.664% for the traditional threshold based approach. In addition, a better MCC (0.96149), F-score (0.96283) and precision (0.98871) are found for the proposed approach. The thresholding assisted method has shown good results among the existing methods with almost nearer values of MCC (0.96037), F-score (0.96171) and precision (0.98944).

The performance of the proposed MM approach, traditional Otsu-threshold based and ML classifer approaches are depicted in table 5.8 (pixel statistics comparison) and 5.9 respectievely (Performance comparison of proposed MM and existing approaches).

Feature Extraction Strategies Based on Mathematical Morphology for the Analysis of Remotely Sensed Imagery, PhD Thesis, 2019, NITK Surathkal, India.

80

Table 5.8. Pixel statistics comparison of proposed MM approach, traditional Otsu-threshold based and ML classifer approaches.

Sensor and AOI	Method	TP	TN	FP	FN	Total pixels
LISS IV, Ramagundam	Classification	460645	10282483	16043	25025	10784196
	Threshold Based	454337	10293681	4845	31333	10784196
	Proposed MM	455693	10293326	5200	29977	10784196
Sentinel-2, Ramagundam ROI	Classification	24610	646252	185	5465	676512
	Threshold Based	27655	644760	1677	2420	676512
	Proposed MM	27175	646268	169	2900	676512
LISS IV Bhopal	Classification	670180	3924482	31195	19348	4645205
	Threshold Based	648526	3944889	10788	41002	4645205
	Proposed MM	663853	3936987	18690	25675	4645205
CARTOSAT 1-PAN Bhopal lake	Classification	3623492	22707657	317499	113373	26762021
	Threshold Based	3550365	22971097	54059	186500	26762021
	Proposed MM	3549946	22986999	38157	186919	26762021
Landsat-8, ETM+	Classification	475003	12609208	404349	7115	13495675
	Threshold Based	430036	12938092	75465	52082	13495675
	Proposed MM	436145	12971815	41742	45973	13495675
Sentinel-2 dataset	Classification	6958	2291435	936	825	2300154
	Threshold Based	5756	2291044	1327	2027	2300154
	Proposed MM	6770	2291365	1006	1013	2300154

Feature Extraction Strategies Based on Mathematical Morphology for the Analysis of Remotely Sensed Imagery, PhD Thesis, 2019, NITK Surathkal, India.

81

Table 5.9. Accuracy assessment comparison of proposed MM approach, traditional Otsu-threshold based and ML classifer approaches

Sensor and AOI chosen	Method	Precision	F-score	Accuracy	MCC
LISS IV, Ramagundam ROI	Classification	0.96634	0.95732	0.99619	0.95537
	Threshold Based	0.98944	0.96171	0.99664	0.96037
	proposed	0.98871	0.96283	0.99673	0.96149
Sentinel-2, Ramagundam ROI	Classification	0.99253	0.89702	0.99164	0.89723
	Threshold Based	0.94282	0.93103	0.99394	0.92794
	Proposed MM	0.99381	0.94655	0.99546	0.94535
LISS IV Bhopal dataset	Classification	0.95552	0.96366	0.98911	0.95731
	Threshold Based	0.98363	0.96160	0.98885	0.95541
	proposed	0.97261	0.96766	0.99044	0.96208
CARTOSAT 1-PAN Bhopal lake	Classification	0.91943	0.94388	0.98389	0.93494
	Threshold Based	0.98500	0.96723	0.99101	0.96223
	proposed	0.98936	0.96927	0.99158	0.96467
Landsat-8, ETM+	Classification	0.54017	0.69777	0.96951	0.71755
	Threshold Based	0.85071	0.87085	0.99054	0.86621
	proposed	0.93882	0.94152	0.99581	0.93935
Sentinel-2 dataset	Classification	0.88142	0.88766	0.99923	0.88730
	Threshold Based	0.81265	0.77438	0.99854	0.77451
	proposed	0.87062	0.87023	0.99912	0.86979

Figure 5.16 illustrates the performance of the the algorithm with Ramagundam AoI of Sentinel-2 imagery. The proposed MM algorithm extracts lake regions with an accuracy of 99.54% compared to the accuracy of 99.39% for the Otsu-threshold driven approach. The statistics of MCC, F-score, and Precision are 0.94535, 0.94655 and 0.99381 respectively formed for the proposed MM algorithm whereas for the Otsu-threshold based approach it is observed to be 0.92794, 0.93103 and 0.94282, which is lesser than

----

Feature Extraction Strategies Based on Mathematical Morphology for the Analysis of Remotely Sensed Imagery, PhD Thesis, 2019, NITK Surathkal, India.

82

the proposed method. The performance of LISS IV imagery of the same region is better as compared to this Sentinel data set. It is mainly because of its higher spatial resolution, sensor capabilities and temporal changes such as acquisition date and time, season, etc.

(a)   (b)   (c)

(d)   (e)   (f)
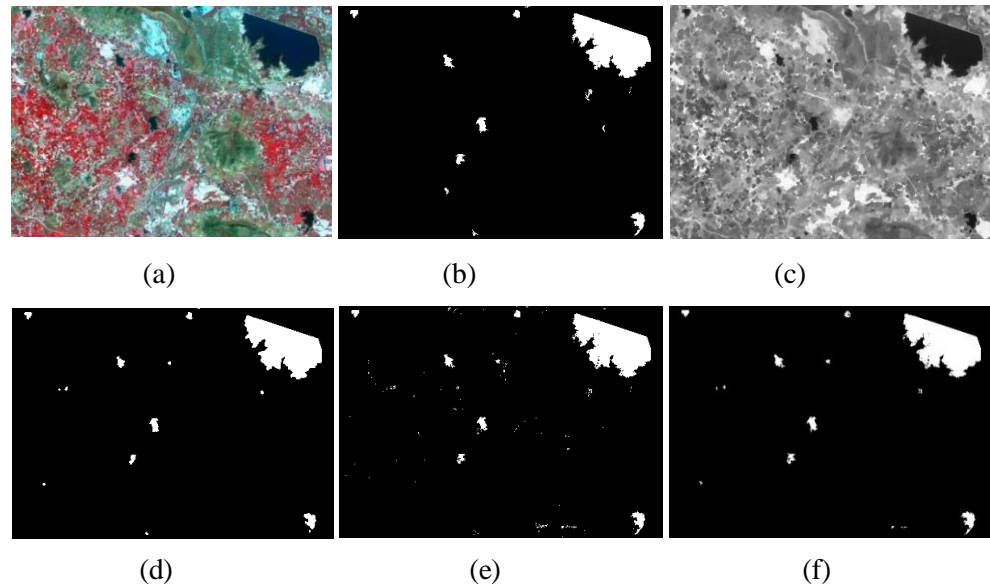
Figure 5.15. (a) – (f). Illustration of results with LISS IV data set of Ramagundam region of Telangana state (a) Original image (b) Ground truth (c) MM processed image (intermediate stage) (d) Proposed MM algorithm outcome (e) ML classification (f) Otsu-threshold based method.

Figure 5.17 illustrates the results of different algorithms (proposed MM and existing) and ground truth data using Landsat-8 imagery. Here, the proposed MM algorithm can extract lakes with 99.58% accuracy and better MCC (0.93935), F-score (0.94152) and precision (0.93882) values. Even though traditional threshold based method has an accuracy of 99.05%, its MCC (0.86621), F-score (0.87085) and precision (0.85071) values are recorded lower than that of proposed MM based approach. The undesirable performance of traditional classification method can be attributed to the increased false positive due to the presence of hill shadows. The presence of deep mountains and other shadow regions with and without glaciers had attributed to lower MCC and other performance metrics values.

(a)   (b)   (c)

(d)   (e)   (f)
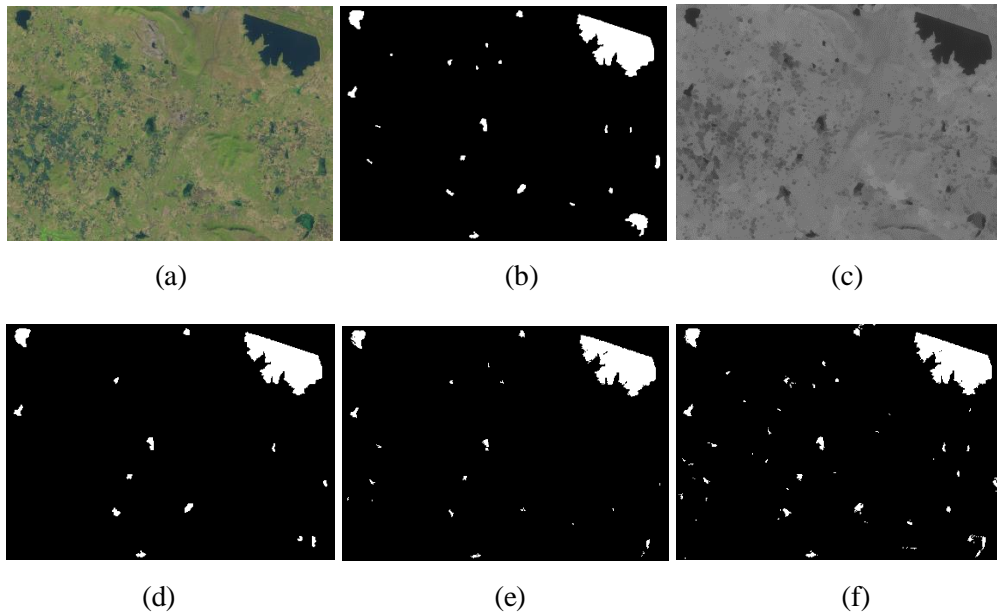
Figure 5.16. (a) – (f). Illustration of results with Ramagundam AOI of Sentinel-2 imagery (a) Original image (b) Ground truth (c) MM processed image (intermediate stage) (d) Proposed MM algorithm outcome (e) ML classification (f) Otsu-threshold based method.

(a)   (b)   (c)

(d)   (e)   (f)
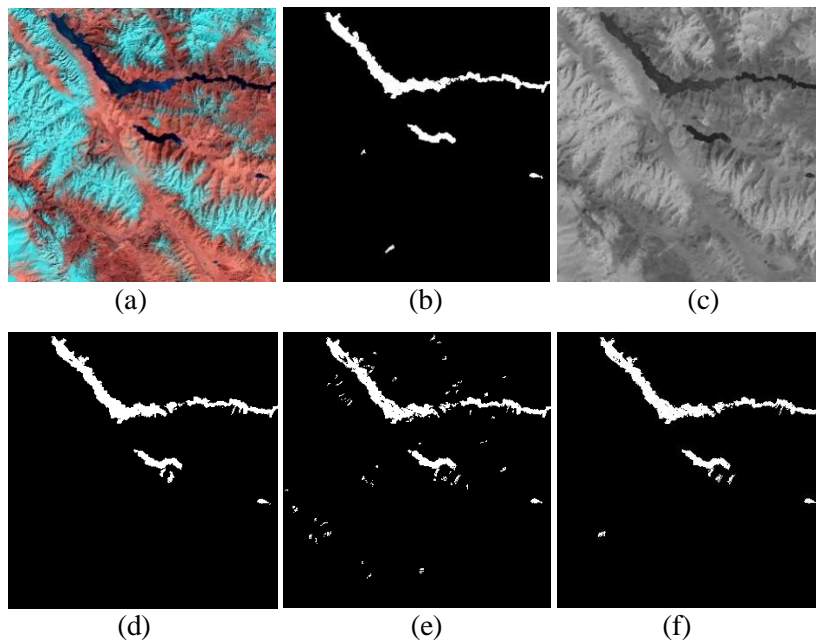
Figure 5.17. (a) – (f). Illustration of results with Landsat-8 imagery (a) Original image (b) Ground truth (c) MM processed image (intermediate stage) (d) Proposed MM algorithm outcome (e) ML classification (f) Otsu-threshold based method.

Figure 5.18 illustrates the results of different algorithms (proposed MM, ML classifier and Otsu-threshold based) and ground truth data using Sentinel-2 imagery. Here, an accuracy of 99.91% and 99.92% is achieved by the proposed algorithm and the existing classification based method respectively. MCC, F-score and Precision values of 0.86979, 0.87023and 0.87062 respectively are observed for the proposed MM algorithm while for the ML classifier method it is observed to be 0.88730, 0.88766 and 0.88142 respectively. It is the only dataset which has shown a slightly improved performance compared to the proposed approach. Since the geographical extent is small, the classification approach was able to perfectly identify water signatures and classify water and non-water regions precisely.

(a)   (b)   (c)   (d)

(e)   (f)
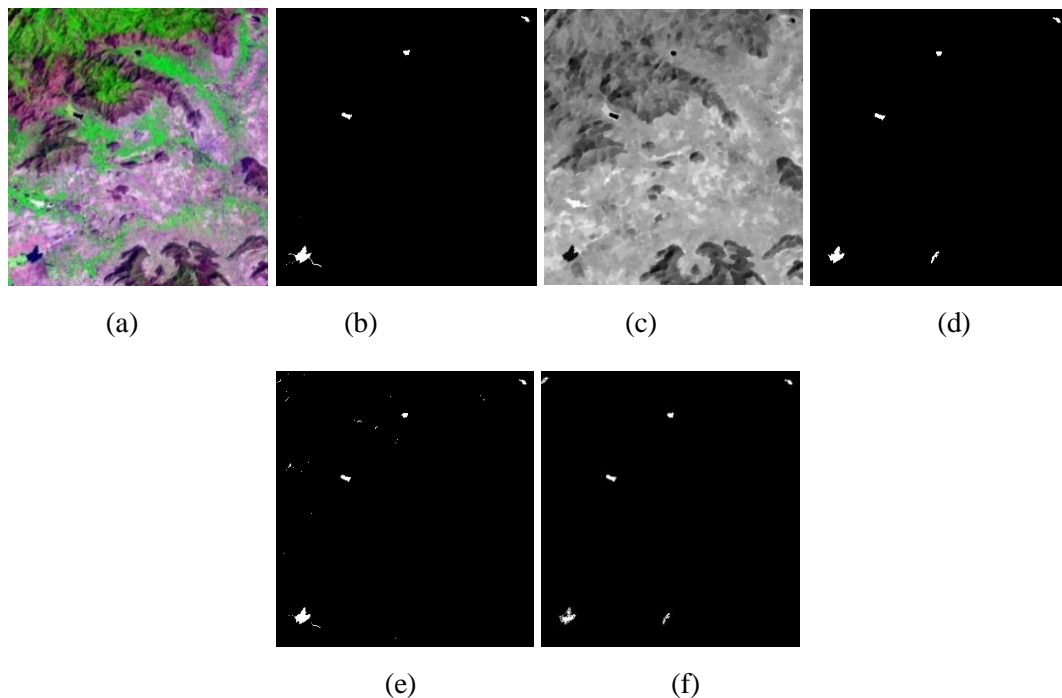
Figure 5.18. (a) – (f). Illustration of results with Sentinel-2 imagery Kerala AoI (a) Original image (b) Ground truth (c) MM processed image (intermediate stage) (d) Proposed MM algorithm outcome (e) ML classification (f) Otsu-threshold based method.

Figure 5.19 illustrates the performance with Cartosat-1 (PAN) imagery of Bhopal region. The proposed algorithm extracts lake regions with an accuracy of 99.158% compared to the accuracy of 99.10% for the Otsu-threshold driven approach. MCC, F-

Feature Extraction Strategies Based on Mathematical Morphology for the Analysis of Remotely Sensed Imagery, PhD Thesis, 2019, NITK Surathkal, India.

85

----

score and Precision values of 0.96467, 0.96927 and 0.98936 is recorded for the proposed MM algorithm whereas for the Otsu-threshold based approach it is observed to be 0.96223, 0.96723 and 0.9850, which is lesser than the proposed method's performance. The algorithm offers satisfactory performance despite the large areal coverage including urban settlements, agricultural lands, and few mountain shadows.

| (a) | (b) | (c) |

| (d) | (e) | (f) |
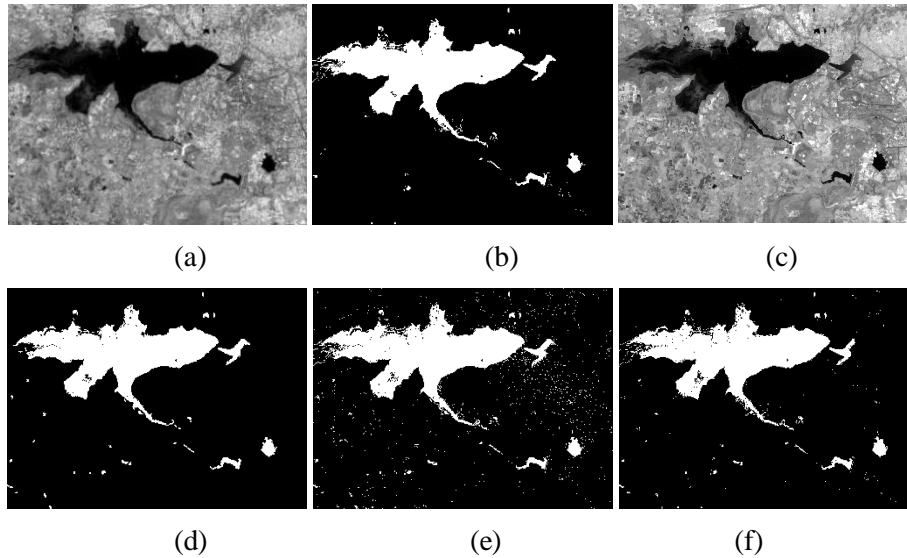
Figure 5.19. (a) – (f). Illustration of results with Cartosat-1 (PAN) imagery of Bhopal region (a) Original image (b) Ground truth (c) MM processed image (intermediate stage) (d) Proposed MM algorithm outcome (e) ML Classifier (f) Otsu-threshold based method.

Figure 5.20 shows the algorithm performance with LISS IV dataset of Bhopal region. Here, the proposed MM algorithm can extract lakes with 99.04% accuracy and better MCC (0.96208), F-score (0.96766) and precision (0.97261) values. The traditional classification assisted method has performed with an accuracy of 98.911%, its MCC (0.95731), F-score (0.96366) and precision (0.95552) values are found lower than that of proposed MM based approach. The traditional classification method has failed to discriminate water signatures from this dataset due to the presence of hill shadows and urban features. Similarly, among LISS IV and Cartosat datasets of the same region, Cartosat performed better. It is mainly because of its advanced sensor capabilities and higher pixel density (resolution).

Feature Extraction Strategies Based on Mathematical Morphology for the Analysis of Remotely Sensed Imagery, PhD Thesis, 2019, NITK Surathkal, India.

86

(a) (b) (c)

(d) (e) (f)
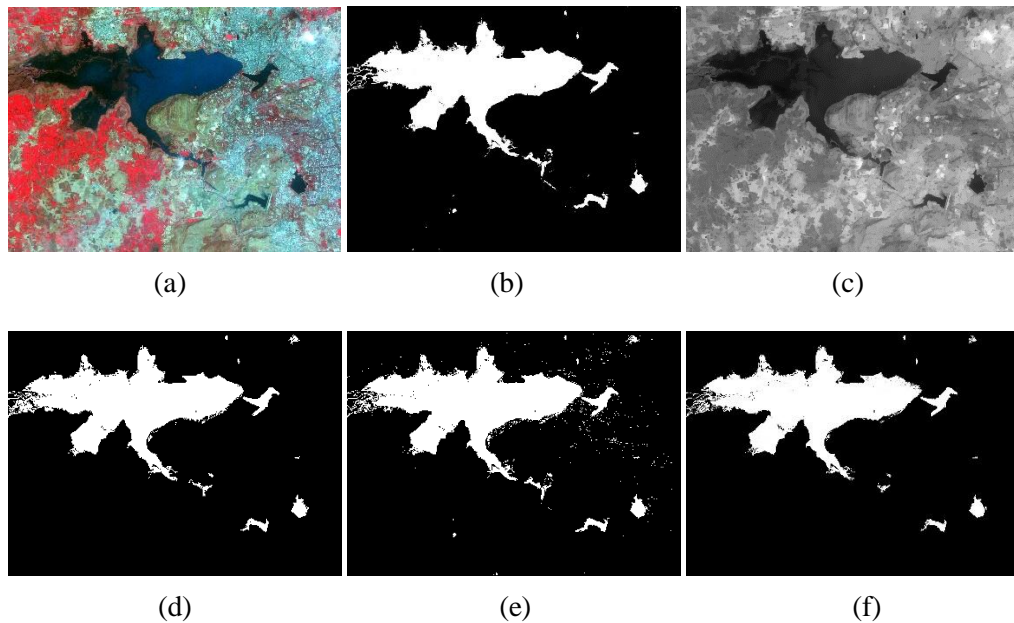
Figure 5.20. (a) – (f). Illustration of results with LISS IV Data set of Bhopal region(a) Original image (b) Ground truth (c) MM processed image (intermediate stage) (d) Proposed MM algorithm outcome (e) ML Classifier (f) Otsu-threshold based method.

5.4.5. Conclusions

Monitoring and tracking of lake mobility are critical to support sustainable management of water resources. The application and effectiveness of mathematical morphology assisted approach for the extraction of ponds and lakes from several varieties of satellite images have been studied. The proposed MM algorithm extracted lakes with an average accuracy of 99.47% and MCC of 0.9397 for all the datasets used. Similarly, the ML classifier and Otsu-threshold driven method exhibited an accuracy of 98.75% and 99.31% respectively. A correlation coefficient of 0.89049 and 0.90374 were obtained for the MLC and Otsu-threshold methods used. Through the use morphological reconstruction driven operations, the actual size and shape of the objects in the output are preserved in the result as compared to other basic MM assisted approaches. The proposed algorithm provides a provision to feed the most sensitive SE kernel size and P value at runtime. Features or objects may have diverse responses for a set of SE sizes, depending on the interactions between the SE size and the size of the features and

Feature Extraction Strategies Based on Mathematical Morphology for the Analysis of Remotely Sensed Imagery, PhD Thesis, 2019, NITK Surathkal, India.

87

----

spatial resolution of imagery. If the user recognizes this correlation, highest possible accuracy from any resolution imagery can be obtained with a certain level of experience. For feature extraction, it is a good idea to generate multidimensional morphological profiles and use a multiscale approach based on a series of different SE sizes.

The threshold-based methods do not make any physical changes to the features present in the imagery. However, it is susceptible to noises and loss of information if the obtained threshold is not the desired value. Therefore, it does not guarantee good accuracy in certain cases. Classification methods are heavily depended on training pixels and manually assigning the training pixels is a tedious task. Similarly in unsupervised method specification of number of classes needed for an accurate lake classification is a laborious task.

Feature Extraction Strategies Based on Mathematical Morphology for the Analysis of Remotely Sensed Imagery, PhD Thesis, 2019, NITK Surathkal, India.

88

CROP FIELD BOUNDARY EXTRACTION

6.1 GENERAL

Accurate and precise information on agricultural field boundaries has considerable significance in precision agriculture and greatly contributes to land information and administration systems. The information obtained from remotely sensed imageries can provide valuable input for agricultural applications such as cultivation, crop monitoring, yield predictions and so on. Wide varieties of morphological transformations exist for structural information extraction from spatial data. MM techniques focus on the analysis of the spatial connections and associations between groups of pixels, provided with image processing technique complementary to those based on the analysis of spectral signature of pixels. In this chapter, the applications and effectiveness of MM assisted approach for the extraction of crop field boundaries from multiple satellite imageries have been presented. The accuracy of the developed methodology has been assessed from ground truths, revealing that the developed MM algorithm has the edge over the existing approaches such as Canny and Sobel.

6.2 BACKGROUND AND RELATED WORKS

The domain of remote sensing and image processing has witnessed dramatic changes in the past few decades. Cutting edge technologies, like remote sensing and geo-information systems, are revolutionizing agriculture. Remote sensing techniques, different from the exhaustive and expensive field evaluations (Addo et al. 2011), have prominent advantages being macroscopic, comprehensive, high-frequency, dynamic, and low-cost. Spatial and spectral resolution capabilities of image acquisition sensors have increased significantly. The proportion of image acquisition has been escalating day by day, thus leading to the formation of huge remotely sensed data warehouses in private and public establishments. These changes have had a tremendous impact on

processing and analyzing satellite images (Aptoula, 2014). With the rapid increase of remote sensing data on a gigabytes scale at daily basis, the need for robust and automated tools for retrieval, management, and processing the data for effective exploitation has also increased. Numerous researchers (Armenakis and Savopol, 2004; Quackenbush, 2004; Momm and Easson, 2010; Tian 2013; Ghanea et al. 2014) have stressed the significance of designing and implementing flexible automated feature extraction tools to advance the information extraction procedures.

An automated computational methodology was proposed to extract agricultural crop fields from 30 m Web Enabled Landsat (WELD) time series data (Yan and Roy, 2014). Coherent fields that are visually apparent were extracted by object-based approach and watershed algorithm yielding relatively limited apparent errors. Sebari and Dong-Chen (2013) presented an automated method for object extraction from high-resolution satellite imageries using both segmentation primitives and fuzzy rule sets for image interpretation. They used IKNOS imagery for the study and obtained an overall extraction accuracy of 80%. Sharma, et al. (2008) automated the process of extracting feature boundary from satellite imagery intending to eventually replace manual digitization. They used the Delaunay graph and Voronoi tessellation to extract boundary along with skeletonization using a color-image segmentation algorithm. A line driven feature extraction and demonstration strategy and captured the spatial and structural patterns in the scene (Harini and Anil, 2013). A tiered analysis scheme was used to address the computational challenges involved in the representation of large-scale image analysis.

The shape-oriented processing capability of the mathematical morphology toolbox has rendered it popular with remote sensing images (Stankov and He, 2013; Soille and Pesaresi, 2002). It provides an alternate approach to image processing based on shape concept stemmed from set theory rather than traditional mathematical modeling and analysis (Naegel, 2007). MM assisted image processing techniques provide an efficient means for decreasing the effect of noise such as in edge detection and filling in broken edges. As the performance of classic edge detectors degrades with noise, morphological

Crop Field Boundary Extraction

----

edge detector has been studied (Mukhopadhyay and Chanda, 2002). The mathematical morphology assisted remote sensing application range includes texture analysis (Huang et al. 2009) simplification (Soille, 2008) and segmentation (Tarabalka et al. 2010). In addition, morphological approaches have been used broadly for spatial structure extraction problems, e.g., building detection and extraction (Ouzounis et al. 2011), road network delineation (Valero et al. 2007), rubble detection (Ouzounis et al. 2011), target detection (Velasco-Forero and Angulo 2010), etc. These MM based image processing operations have been broadly reviewed and discussed in (Gonzalez and Woods, 2002; Parker, J., 1997; Seul et al. 2001; Soille, 1999).

It is imperative to find efficient and affordable methods that assist in decision-making and aid the effective use of land resources. Thus, research based agricultural developments, high precise and low cost technologies are appropriate for information extraction practice. The present chapter proposes a novel MM driven approach which is very effective and useful for the extraction of crop field boundaries from satellite and aerial imageries with higher accuracy and minimal turnaround time. We are looking for objects defined as a specific spatial arrangement of image pixels rather than single pixels with a specific spectral signature. Preservation of actual size and shape of the crop field boundary, runtime SE definition if required, automation, faster processing, and single band adaptability are salient features of this work. The accuracy of developed methodology has been assessed with ground truths of the study area. The proposed approach has a good potential in extracting crop rows, patterns, and their dominant orientations.

6.3 DATA AND METHODS

This investigation uses multiple sets of cloud free satellite imageries to identify how well the proposed approach executes. The important data sets used for the present investigation are procured from various sources and agencies with different spatial resolutions as mentioned in Table 6.1.

Feature Extraction Strategies Based on Mathematical Morphology for the Analysis of Remotely Sensed Imagery, PhD Thesis, 2019, NITK Surathkal, India.

91

Table 6.1 Datasets employed for the present study

Satellite & Sensor	Spatial Resolution (Meters)	Source	RoI	Date of Pass
Cartosat 2, PAN	0.8	NRSC	Mangalore, India	12 NOV 2008
Cartosat 1, PAN	2.5	NRSC	Bhopal, India	06 APR 2006

6.3.1 Methodology

The methodological flowchart of the present investigation is presented in Figure 6.1. If there exist any radiometric or geometric errors with the procured cloud free imagery, various preprocessing operations should be performed. Before the execution of the algorithm commences, the threshold, SE declaration (SE1 and SE2) and initialization, which governs important processing activities such as detection and extraction of boundaries, noise reduction, etc., is carried out. If the end user opts for dynamic SE sizes and threshold, then these values can be recorded from the user. The threshold values and SE sizes are essential for the execution of the algorithm, and the algorithm is already coded with default values to choose. Initially, an MM Erosion operation is followed by a subtraction operation to identify all important edges. This operation depends on the size of the initialized value of structuring element SE1. To enhance all the detected edges, image sharpening and intensity value adjustment operation of the imagery has been carried out. Morphological top-hat and bot-hat algebraic computations are essential in enhancing and highlighting all boundary features present in the imagery. Usually, the top-hat transform is an operation that extracts small elements and details from a given image. White top-hat transform extracts feature that is smaller than SE and are brighter than their surroundings. However, the black top-hat yields the features that are darker than their surroundings. Then the algorithm isolates unwanted objects that are irrelevant in crop boundary delineation through thresholding by Opening top-hat operation followed by a very lighter thinning operation. Further details and sequence of these MM operations are outlined in algorithm section A of data and methods.

```
┌─────────────────────────────┐                    ┌─────────────────────────────┐
│  Input satellite image (X)  │          ┌────────→ │ Line structuring element    │
└─────────────────────────────┘          │         │ definition using SE2 size.  │
              │                           │         └─────────────────────────────┘
              ▼                           │                        │
┌─────────────────────────────┐          │                        ▼
│ Declaration and             │          │         ┌─────────────────────────────┐
│ initialization of SE size   │          │         │ MM Top-hat operation.       │
│ (SE1 and SE2) and threshold │          │         │ (white top-hat transform)   │
│ values                      │          │         └─────────────────────────────┘
└─────────────────────────────┘          │                        │
              │                           │                        ▼
              ▼                           │         ┌─────────────────────────────┐
┌──────────┐    ◇                         │         │ MM Bot-hat operation.       │
│ Receive  │ Y ◇ If (dynamic              │         │ (black top-hat transform)   │
│ SE1, SE2 │←──◇ SE size and              │         └─────────────────────────────┘
│ & thresh │   ◇ threshold)               │                        │
│ values on│    ◇                         │                        ▼
│ runtime  │      │ N                      │         ┌─────────────────────────────┐
└──────────┘      ▼                        │         │ Algebraic computation using │
     │   ┌─────────────────────────────┐  │         │ MM Bot-hat and MM top-hat   │
     │   │ MM Erosion operation by     │  │         │ results with processed      │
     └──→│ structuring element SE1.    │  │         │ imagery (P5).               │
         └─────────────────────────────┘  │         └─────────────────────────────┘
                      │                    │                        │
                      ▼                    │                        ▼
         ┌─────────────────────────────┐  │         ┌─────────────────────────────┐
         │ Subtraction of MM eroded    │  │         │ MM Opening Top Hat          │
         │ image from original image.  │  │         │ operation.                  │
         └─────────────────────────────┘  │         └─────────────────────────────┘
                      │                    │                        │
                      ▼                    │                        ▼
         ┌─────────────────────────────┐  │         ┌─────────────────────────────┐
         │ Adjust image intensity      │  │         │ Image thresholding (thresh) │
         │ values                      │  │         │ & Morphological thinning    │
         └─────────────────────────────┘  │         └─────────────────────────────┘
                      │                    │                        │
                      ▼                    │                        ▼
         ┌─────────────────────────────┐  │         ┌─────────────────────────────┐
         │ Image Sharpening            │──┘         │ Display and record results. │
         └─────────────────────────────┘            │ (overlay original image     │
                                                     │ with result: optional)      │
                                                     └─────────────────────────────┘
                                                                    │
                                                                    ▼
                                                     ┌─────────────────────────────┐
                                                     │    Extracted results        │
                                                     └─────────────────────────────┘
```

Figure 6.1. Flowchart of the proposed approach for crop field boundary extraction.

The ground truths are prepared collectively by combining the knowledge of the user via field visit with GPS instruments and sketches obtained from manual digitization operations. Feature wise and object wise corrections are employed in multiple stretches with the aid of Google earth imagery to achieve maximum possible correctness and accuracy. Well-known existing methods such as Canny and Sobel is selected for comparison with the proposed approach. Canny is a Laplacian based method; it searches zero crossings in the second derivative of the image to find edges. While Sobel is a Gradient based technique and it detects edges by looking for maximum and minimum of the first derivative

Feature Extraction Strategies Based on Mathematical Morphology for the Analysis of Remotely Sensed Imagery, PhD Thesis, 2019, NITK Surathkal, India.

93

6.3.2 Algorithm development

This section describes the stepwise algorithmic development of the flowchart shown in figure 6.1.

Input: An NxN sized satellite input image (X).

Output: An NxN sized extracted output image (P7).

1:	**Start**
2:	Procurement, registration and preprocessing of the satellite image.
3:	Declaration and initialization of SEs (SE1 & SE2), parameters (e.g., threshold) for processing activities such as detection and extraction of crop edges, noise reduction, boundary enhancements, etc.

If (End user opts for dynamic SE sizes and threshold') **then**

> Receive SE1, SE2 and Thresh values on runtime,

Else go to Step 5

5:	MM Erosion operation by structuring element SE1. [P1= imerode (X, SE1)]
6:	Subtraction of MM eroded image from original image: [P3=X-P2]
8:	Adjust image intensity values:

> [P4 = imadjust (P3, stretchlim (P3))]
>
> [P5 = imadjust (P4, stretchlim (P4))]

9:	Image Sharpening. [P5 = imsharpen (P5,'Radius', rad,'Amount', amt)]
10:	Line SE definition using SE2 size. [SE4 = strel ('line', SE2, deg)]
11:	MM Top-hat operation. [TH = imtophat (P5, SE4)]
12:	MM Bot-hat operation. [BH = imbothat (P5, SE4)]
13:	Algebraic computation using MM Bot-hat and MM top-hat results with processed (P5) imagery. [AC = ((P5 + TH) - BH)]
14:	MM Opening Top-hat operation. [P6 =mmopenth (AC, mmseline (Thresh)]
15:	Morphological thinning of thresholded image.

> [P7=mmthin (P6, mmendpoints)]

16:	Print or display results.

Overlay of result with original image (optional). [mmshow (X, P7)]

17:	**End.**

6.4 RESULTS AND DISCUSSION

This section describes the results drawn from different sets of the input imageries including visual, qualitative and quantitative assessments. The results of this investigation are also compared with the results of the established methods such as Canny and Sobel approach. Pixel statistics comparison of proposed MM approach with Canny and Sobel is shown in Table 6.2.

Table 6.2 Pixel statistics comparison of proposed MM approach with Canny and Sobel.

Sensor and AOI	Approach	TP	TN	FP	FN	Total
Cartosat 1, PAN, Bhopal #CP1	Canny	9570	207310	15137	23172	255189
	Sobel	12727	213005	9442	20015	255189
	Proposed MM	23891	212390	10057	8851	255189
Cartosat 1, PAN, Bhopal #CP2	Canny	10029	271956	9515	24900	316400
	Sobel	12730	276330	5141	22199	316400
	Proposed MM	28816	266705	14766	6113	316400
Cartosat 1, Bhopal #CP3	Canny	17094	338480	15131	31595	402300
	Sobel	19092	348061	5550	29597	402300
	Proposed MM	33469	335002	18609	15220	402300
Cartosat 2, PAN, Mangalore CP	Canny	22164	575793	11572	71312	680841
	Sobel	25411	578251	9114	68065	680841
	Proposed MM	64283	553434	33931	29193	680841

In general, the figures numbered 6.2 to 6.5 (a) – (e) illustrates the different input data sets, ground truth images, results drawn from Canny and Sobel methods and the output drawn from the proposed MM approach. Figure 6.2 represents the crop parcel, CP#1 of Cartosat 1, PAN imagery of Bhopal AOI. The performance of existing methods Canny, Sobel and the proposed MM algorithm is shown in figures 6.2c, 6.2d and 6.2e respectively. Here, the proposed algorithm extracts crop field boundaries with an

accuracy of 92.59% as compared to 88.45% accuracy obtained from traditional approach (highest from Sobel). In addition, a better MCC (0.6740), F-score (0.7164) and Precision (0.7037) are recorded for the proposed MM approach.

(a)   Original image   (b) Ground truth   (c) Canny

(d) Sobel   (e) MM approach
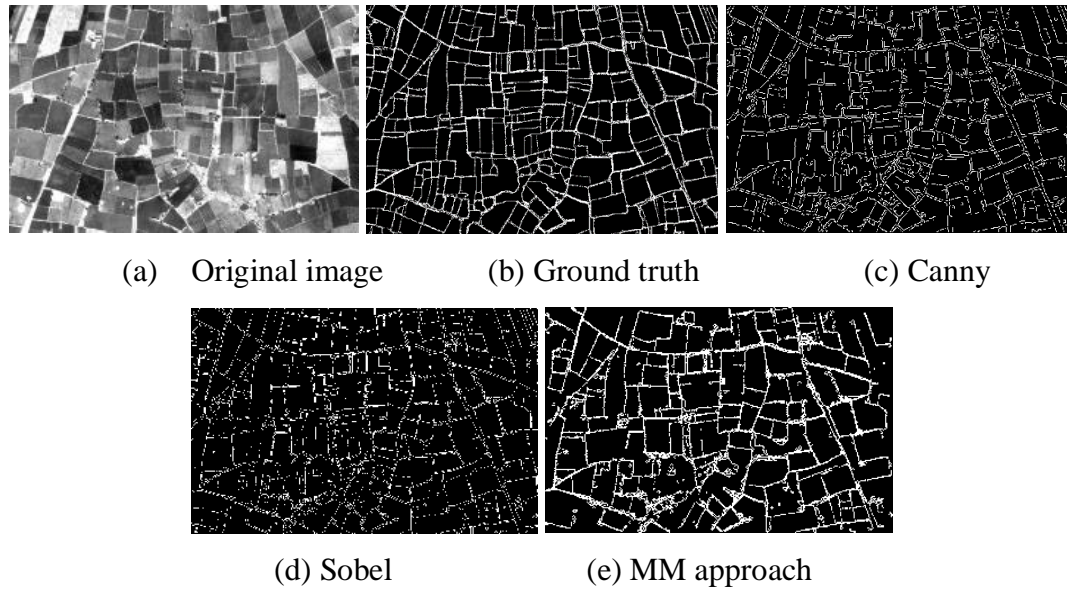
Figure 6.2. Cartosat 1, PAN imagery of Bhopal region subset-1, CP#1

Figure 6.3 illustrates the crop parcel subset, CP#2 of Cartosat 1, PAN imagery of Bhopal region. Here, the proposed MM algorithm can extract crop field boundaries with better accuracy of 93.40 % and satisfactory MCC (0.70247), F-score (0.73406) and precision (0.66119) values. Even though traditional edge detection based methods has an accuracy of 91.35%, its precision (0.71232), F-score (0.48219) and MCC (0.46995) values are marginally lower than that of proposed MM based approach. The proposed algorithm and traditional approaches can detect most crop parcels with an accuracy of more than 90% even when the crop parcels are very irregular. This dataset exhibits highest overall performance (highest accuracy and MCC) for proposed as well as Canny and Sobel approaches compared to other datasets employed.

Feature Extraction Strategies Based on Mathematical Morphology for the Analysis of Remotely Sensed Imagery, PhD Thesis, 2019, NITK Surathkal, India.

96

(a)Original image (b) Ground truth (c) Canny (d) Sobel   (e) MM approach

Figure 6.3. Cartosat 1, PAN imagery of Bhopal region subset, CP#2

Figure 6.4 illustrates the crop parcel subset, CP#3 of Cartosat 1, PAN imagery of Bhopal region with larger areal coverage than #CP2 and CP and almost equal to #CP1.The proposed MM algorithm extracts crop field boundaries with an accuracy of 91.59% compared to the highest accuracy of 91.26% for the existing approaches. MCC, F-score and Precision values of 0.61673, 0.66428 and 0.64267 are recorded for the proposed MM algorithm whereas for the existing approach it is observed to be 0.51200, 0.52070and 0.77477 which is marginally less than the proposed one.
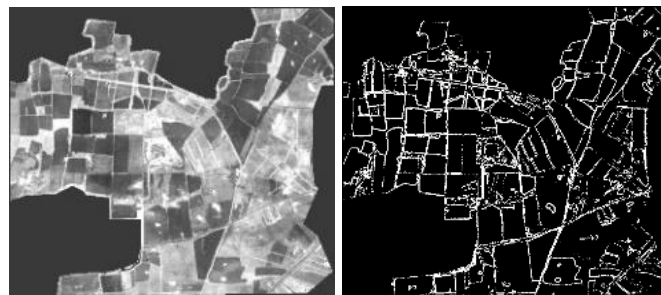
(a)   Original image   (b) Ground truth

(c) Canny   (d) Sobel   (e) MM approach

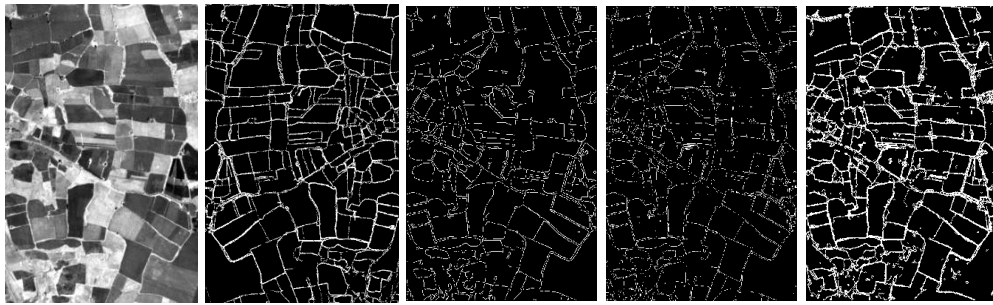**Figure 6.4. Cartosat 1, PAN imagery of Bhopal region subset-3, CP#3**

Figure 6.5 illustrates the crop parcel (CP) subset of Cartosat-2 imagery near to Mangalore International airport and Nethravathi riverbank. In this case, the proposed algorithm extracts crop field boundaries with an accuracy of 90.72% in comparison to the highest accuracy of 88.66% for the existing edge detection based methods. MCC, F-score and Precision values of 0.61703, 0.67069and 0.65451 is recorded for the proposed MM approach whereas for the existing approaches it is observed to be 0.40207, 0.39704 and 0.73601 which is significantly lesser than the proposed one. It is evident that in existing approaches, MCC and F-score values recorded are very less while a satisfactory value was obtained for precision.

(a) Original image   (b) Ground truth   (c) Canny

(d) Sobel   (e) MM approach
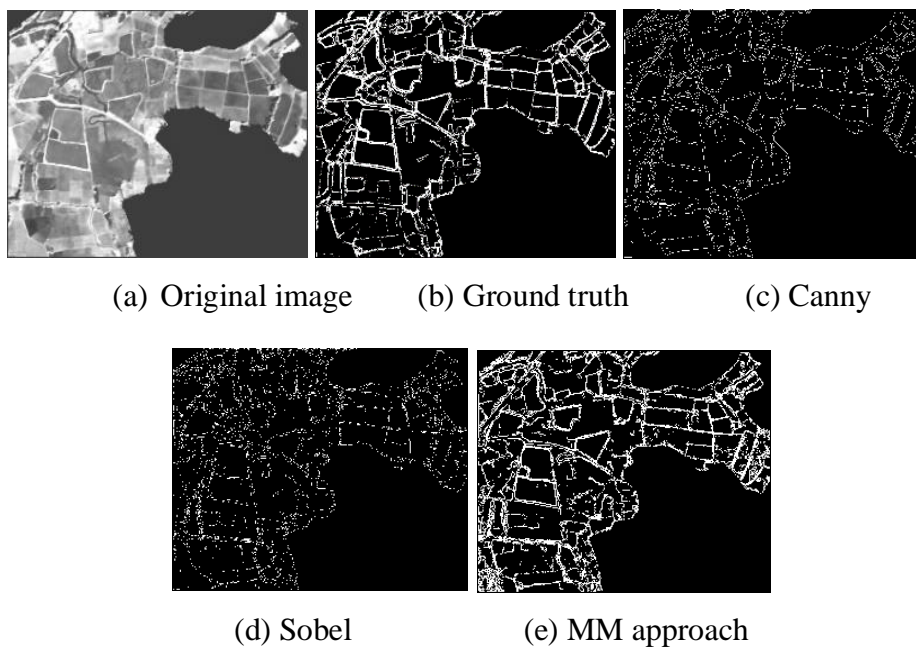
Figure 6.5. Cartosat 2, PAN imagery of crop parcel (CP) of Mangalore region.

The performance of the proposed MM extraction approach and that of the existing approaches such as Canny and Sobel is depicted in Table 6.3. As per the result obtained in this study Sobel slightly outperformed Canny because more number of FP pixels were recorded in Canny compared to Sobel approach. The Canny edge detection algorithm extracts most of the feature edges present in the imagery that is not relevant in this study since the feature of interest is only crop boundaries.

Table 6.3. Performance comparison of proposed MM approach with Canny and Sobel.

Sensor and AOI	Approach	Precision	F-score	MCC	Accuracy
Cartosat 1, PAN, Bhopal #CP1	Canny	0.38733	0.33316	0.25359	0.84987
	Sobel	0.57408	0.46355	0.41114	0.88456
	Proposed MM	0.70375	0.71647	0.67402	0.92590
Cartosat 1, PAN, Bhopal #CP2	Canny	0.51314	0.36821	0.32976	0.89122
	Sobel	0.71232	0.48219	0.46995	0.91359
	Proposed MM	0.66119	0.73406	0.70247	0.93401
Cartosat 1, Bhopal #CP3	Canny	0.53045	0.42252	0.37042	0.88385
	Sobel	0.77477	0.52070	0.51200	0.91263
	Proposed MM	0.64267	0.66428	0.61673	0.91591
Cartosat 2, PAN, Mangalore CP	Canny	0.65698	0.34845	0.34478	0.87826
	Sobel	0.73601	0.39704	0.40207	0.88664
	Proposed MM	0.65451	0.67069	0.61703	0.90728

6.5 CONCLUSION

In this chapter, the applications and effectiveness of MM assisted approach for the extraction of crop field boundaries from different set of satellite imageries have been presented. The proposed MM driven approach is effective and useful for the extraction of crop field boundaries for medium to high-resolution satellite imageries. Since the proposed algorithm uses single band for its computation, it is convenient to apply in single band imagery obtained from satellites such as Cartosat. Also, the proposed MM approach provides a provision to input the important result governing SE size and threshold values at runtime, thereby highest possible accuracy can be tuned for different high-resolution imagery. Therefore, this approach is more effective and flexible than other commonly used methods. The proposed algorithm is fast compared to manual digitization procedure that is for processing, turnaround time is only a few minutes, and for very small crop parcels it hardly takes few seconds.

URBAN FEATURE EXTRACTION FROM UAV AND SATELLITE DATASETS

This chapter presents the effectiveness and usefulness of MM driven approach for the extraction of urban features including urban settlements, important road networks, etc. from different sets of satellite and aerial imageries with high spatial resolution. Section 7.1 specifically discusses an MM algorithm and its performance for UAV data sets. Section 7.2 discusses about a slightly modified MM algorithm capable to process both UAV and satellite imageries. The performance of both the algorithms are assessed in comparison with the results of Otsu-threshold based approach and an ML classifier respectively.

7.1 APPROACH FOR UAV DATASETS

7.1.1　Introduction

Remote sensing image processing domains have witnessed the application of many intelligent methodologies for feature extraction over the past few decades; however, the effective use of mathematical morphology (MM) driven computing techniques for feature detection for aerial imageries has been less explored. This study presents an effective MM driven approach for urban feature extraction from Unmanned Aerial Vehicle (UAV) driven imageries. The morphological reconstruction assisted operations, helps to preserves the actual size and shape of the objects in the input imagery. In addition to that, faster processing, semi-automation and no particular spectral band requirement are the key features of this approach. State-of-art MM based approaches do not give an option to feed result-governing variables dynamically. However, proposed approach provides a provision to feed the important result governing SE Kernel size and pixel limit at run time, hence highest possible accuracy

can be tuned for different spatial resolution, topography and geographic coverage. Accuracy of the developed methodology has been assessed with manually prepared ground truths of the study area and compared with Otsu's threshold driven approach.

7.1.2 Background and related work

Data extraction from remotely sensed imageries is the focus of research issues in photogrammetry, remote sensing and GIS communities. Satellite and aerial images inherently tend to be a little noisy, complex and ambiguous. Scientists and researchers have identified the significance of designing and implementing more flexible automated feature extraction practices to advance the information extraction procedures (Momm and Easson, 2010). The need for using remote sensing data to accomplish the complex task of automated extraction of natural, manmade and cartographic features has significantly increased in the past few decades.

"Let them fly and they will create a new market" (MarketsandMarkets, 2013). Certainly, it is referring to Unmanned Aerial Systems (UAS) and UAS-based aerial remote sensing and mapping. Over the time, UAVs have developed as a fast, efficient, low-cost and suitable data acquisition system for remote sensing applications (Colomina, 2014). The acquired data can be of high accuracy and resolution, for a precision varying from a sub-meter to a few centimetres (Gerke, et al. 2016). Crommelinck et al. (2016) in their review states that UAVs have advanced as a flexible acquisition system that acts as a feasible tool in cadastral mapping. A workflow that automatically extracts boundary features from UAV data could increase the pace of current mapping procedures. Aerial remote sensing and its mapping, for some years now, has been delivering the necessities of large-scale, low-altitude imaging for geospatial data users and has led to the crafting of an industry of its own (Cho et al. 2013; Mayr, 2013; Petrie, 2013).

MM-assisted image processing techniques provide an efficient means for reducing the effect of noise such as edge detection and filling broken edges. By choosing the size and shape of the neighbourhood, one can make a morphological operation that is sensitive to definite shapes in the input image (Castro and Centeno 2010). Morphological

Feature Extraction Strategies Based on Mathematical Morphology for the Analysis of Remotely Sensed Imagery, PhD Thesis, 2019, NITK Surathkal, India.

101

reconstruction is useful, but is a less explored technique for extracting significant information about shapes in an image (Gonzalez and Woods, 2002). Kupidura (2013) in his study reveals that the accuracy of mathematical morphology operations far exceeded that of traditional techniques. Bellens, et al. (2008) proposed the usage of operators based on "partial reconstruction" in place of the conventional geodesic reconstruction to minimize the "leakage effect." It can be seen that the addition of the line-based MP provides a considerable enhancement of the classification result. A second improvement is achieved by using "partial morphological reconstruction" instead of the normal morphological reconstruction. Morphological reconstruction is commonly used to better preserve the shape of objects.

The concept of attribute profile (AP), proposed by Mura, et al. (2010) was used for modelling the structural information of the scene to enhance the effectiveness of classification and building extraction. According to the attribute and criterion considered, different information can be extracted from the structures in the scene leading to different multilevel characterizations of the image. Ghamisi, et al. (2015) discussed about the morphological profile, which is a powerful tool to model spatial information (e.g., contextual relations) of the image. APs can be considered as a generalization of the morphological profile, the concept of AP and its extensions EAP (Extended Attribute Profile) and EMAP (Extended Multi-Attribute Profile) have proven to be effective in the analysis of remote sensing images.

Benediktsson et al. (2005) introduced a method based on MM techniques and principal component analysis for pre-processing of hyperspectral data. A morphological profile is constructed based on the repetitive use of opening and closing operation with a structuring element of increasing size, beginning with one original image. Similarly, Plaza, et al. (2005) explained series of extended morphological transformations for filtering and classification of high-dimensional hyperspectral datasets. Experimental results shows that, by designing MM filtering methods that take into consideration the complementary nature of spatial and spectral information in a simultaneous manner, it is possible to lighten the problems related to each of them when taken independently. A

drawback in their proposed approach is the heavy computational burden when processing high-dimensional data.

This study propose an MM based efficient approach for the detection and extraction of urban settlements from aerial imageries. By picking the shape and size of the neighbourhood, one can make a morphology assisted operation that is useful to particular shapes (such as urban settlements) in a given image. Preservation of actual size and shape of the urban features, semi-automation, and minimal turnaround time are focused in this work. The accuracy of the developed methodology has been assessed with manually prepared ground truths of the study area and a comparison is performed with Otsu thresholding approach.

7.1.3   Aerial datasets

The important data sets used for the present study are procured from various sources and agencies mentioned in Table 7.1.

Table 7.1. Specification of datasets for the present study

Satellite and Sensor	Spatial Resolution	Source / Agency	RoI	Date of procurement
NITK, Aerial Dataset-1	High (>1m)	UAV Lab, Applied Mechanics Dept., NITK.	NITK campus, Mangalore, India	12 JAN 2014
NITK, Aerial Dataset-2	High (>1m)	UAV Lab, Applied Mechanics Dept. NITK.	NITK campus, Mangalore, India	24 NOV 2013
Color- infrared aerial photograph	High (>2m)	Intergraph Corp. (ERDAS IMAGINE)	Eastern Illinois, USA	Not Available

7.1.4   Methodology

The methodological flowchart of the present investigation is presented in figure 1. Primarily, the PL (pixel limit), structuring element (SE1 to SE3) declaration and initialization is carried out. This governs important processing activities such as detection and extraction of boundaries, noise reduction, etc. Moreover, the SE1, SE3

Feature Extraction Strategies Based on Mathematical Morphology for the Analysis of Remotely Sensed Imagery, PhD Thesis, 2019, NITK Surathkal, India.

103

and PL values employed are sensitive and their slight variation changes the entire extraction result and accuracy. Since this study is programmed with default SE kernel size for high resolution aerial imageries, if the user works with images of higher swath or lower resolutions, then the user has to feed appropriate SE kernel size at run time for maintaining better performance. Top-hat and bot-hat algebraic computations (the top-hat transformation is used to exclude the disturbances of the bright spots and the bot-hat transformation is employed to enhance the dark details in the grey image) were performed on the image to enhance urban features for easier identification. This process is followed by a set of powerful MM operations such as reconstruction-driven opening, area-closing operations applied along with conventional thresholding and binarization to delineate the desired urban features. The details of these operations are outlined in the algorithm section 7.1.4.1 and flowchart is illustrated in Figure 7.1. The theoretical and mathematical background of these MM operations are explained in detail in section 1.3 of the chapter 1.

Top-Hat and Bottom-Hat transforms are commonly known as Open Top-Hat (White Top-Hat) and Close Top-Hat (Black Top-Hat) respectively. These Top-Hat and Bottom-Hat transforms are used to improve the contrast of images through morphological methods (Serra, 1982). One major application of these transforms is in eliminating the objects that does not fit in from an image by making use of an SE in the opening and closing (Li, et al. 2014). The top-hat is used for light objects on a dark background and the bottom-hat – for dark objects on a light background (Dougherty and Lotufo, 2003). An important application of top-hat transformation is in correcting the effects of non-uniform illumination (Wang et al. 2017).
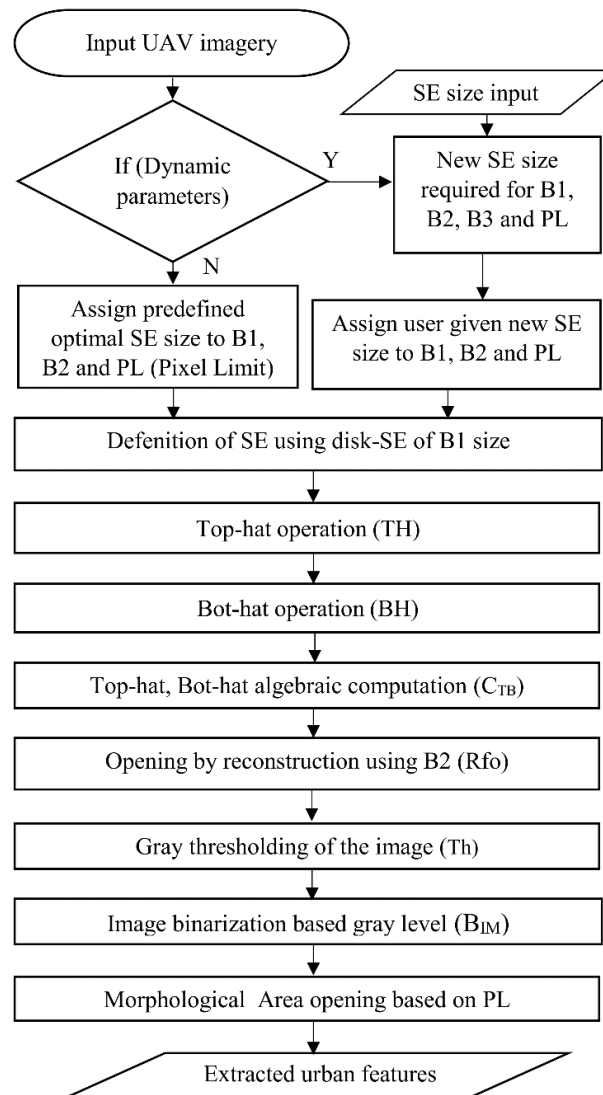
Figure 7.1 Flowchart of the proposed approach for urban feature extraction.

If the user identifies the correlation between the spatial resolution of imagery and SE size, the highest possible accuracy from any resolution imagery can be achieved with certain level experience. Some objects or features may have varied reactions for a set of SE sizes, depending on the interactions between the SE size and the size of the features. Intermittently, we know correctly the SE size for the feature that we want to detect (Pesaresi and Benediktsson, 2001). Nevertheless, that is commonly not possible, and then a particular SE-size approach looks more simplified. Due to these motives, in urban regions, it is a worthy idea to generate multi-dimensional MM profiles and use a

multiscale method based on a sequence of different SE sizes (Dell'Acqua et al. 2004). This permits us to explore a sequence of dissimilar hypothetical spatial domains and to use the best results of the feature/object in the image for the extraction process.

7.1.4.1 Algorithm development

Input: An NxN sized UAV input image (I).

Output: An NxN sized extracted output image (final).

1:     **Start**

2:     Acquisition, registration and optional pre-processing of the UAV imageries.

3:     **If** (End user opts for dynamic SE sizes and Pixel Limit') **then**

Receive values of SE1 to B1, SE2 to B2 and PL on runtime.

Else, go to Step 4

4:     Assign predefined optimal SE size to B1, B2 and PL (Pixel Limit)

5:     Definition of SE using disk-SE of B1 size. [SE1 = strel ('disk', B1)].

6:     MM Top-hat operation. [TH = imtophat (I, SE1)].

7:     MM Bot-hat operation. [BH = imbothat (I, SE1)].

8:     Algebra computations using MM Bot-hat and MM Top-hat results with original imagery. [C_{TB}= ((I + TH) - BH)]

9:     MM Opening by reconstruction [I2 = Rfo (C_{TB}, B2)].

10:    Calculation gray-threshold (Th) of processed image (I2)

11:    Binarization of image using threshold (Th).

[B_{IM} = im2bw (I2, Th)]

12:    Morphological Area opening using PL value

[final = mmareaopen (B_{IM}, PL)]

14:    Print or display results (final).

15:    **End.**

An Otsu's threshold based method is implemented for comparison with the proposed approach. This traditional method utilizes well-known Otsu thresholding for urban and non-urban feature separation. It automatically determines exact threshold values for binarization of images and is being used for different applications. The ground truths are prepared collectively combining the knowledge of the user via field visit with GPS instruments and sketches combined from manual digitization operation. Feature wise

and object wise corrections are employed in multiple stretches with the aid of Google earth imagery to achieve maximum possible correctness and accuracy.

7.1.5 Results and discussion

This section describes the results drawn from different sets of input imageries for visual, qualitative and quantitative assessments. The results of this analysis are also compared with the results of the Otsu thresholding based approach. Figure 7.2, which represents the illustration of algorithm results with Color- IR aerial images of ERDAS Imagine sample dataset-I (eastern Illinois) shows the performance of an Otsu's threshold based method (Fig. 7.2 d) and the proposed MM algorithm with Color-IR aerial images of ERDAS Imagine sample dataset-I (Fig. 7.2 e). Here, the proposed algorithm extracts urban features with a better accuracy of 95.80% as compared to the accuracy of 94.91% for the traditional thresholding approach. Also, a better MCC (0.8904) is recorded for the proposed approach, but the precision (0.9602) was slightly lower than thresholding based method.
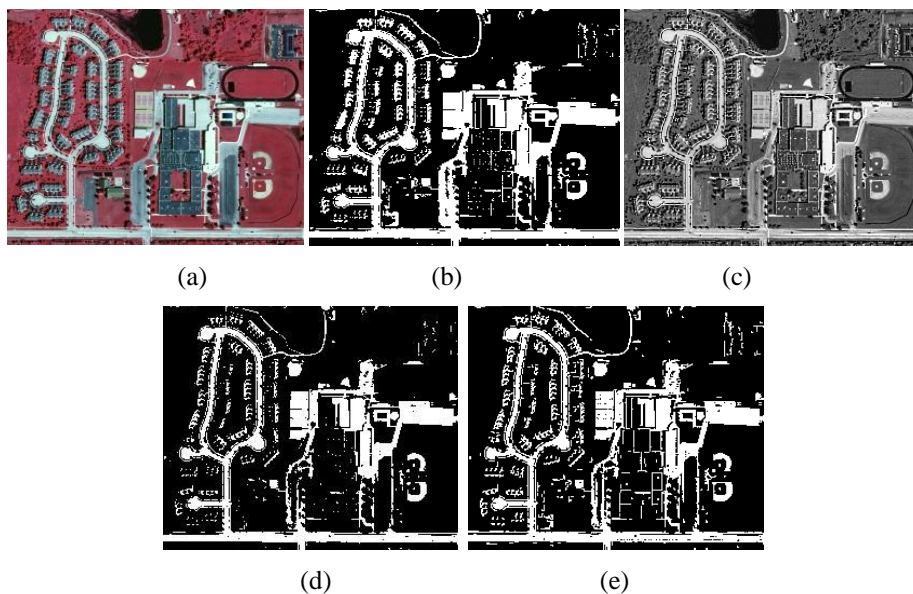

(a)　　　　　　(b)　　　　　　(c)

(d)　　　　　　(e)

Figure 7.2 (a)–(e). Illustration of algorithm results with Color- IR aerial images of ERDAS Imagine sample dataset-I of eastern Illinois (a) Original image (b) Ground truth (c) MM processed image (intermediate stage) (d) Otsu thresholding approach (e) Proposed MM algorithm outcome.

Figure 7.3 illustrates the algorithm performance with NITK, Aerial dataset-I. Here, the proposed algorithm is able to extract urban features with 92.87% accuracy and satisfactory MCC (0.8218) and precision (0.8604) values. Even though traditional thresholding based method has a precision of 0.9680, its accuracy 90.96% and MCC (0.76781) values are marginally lower than that of proposed MM based approach. The threshold-based methods does not perform any structural or physical changes to objects/features present in the imagery. Therefore, the objects size and location will be exactly as it is, since there is no processing operations to change its position or size. However, it is susceptible to noises and loss of information (feature details) if the threshold is not the desired value. Therefore, these factors ensures better precision but does not guarantee good accuracy and other measures in most of the cases.

(a) (b) (c)

(d) (e)
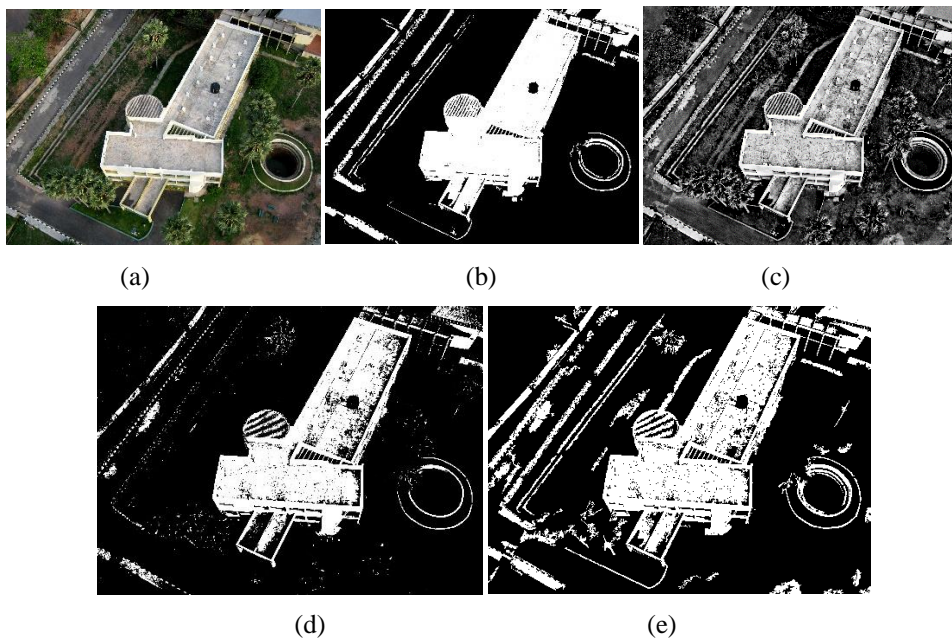
Figure 7.3. (a)– (d). Illustration of algorithm results with NITK, Aerial dataset-1. (a) Original image (b) Ground truth (c) MM processed image (intermediate stage) (d) Otsu thresholding approach (e) Proposed MM algorithm outcome.

Figure 7.4 illustrates the performance of the algorithm with NITK, Aerial dataset-2. Here, an accuracy of 94.39% and 91.73% is achieved by the proposed algorithm and the Otsu thresholding based method respectively. MCC and Precision values of 0.8859 and 0.9825 is observed for the proposed MM algorithm; and for the Otsu-thresholding

based approach it is observed to be 0.83530 and 0.99080.

(a) (b) (c)

(d) (e)
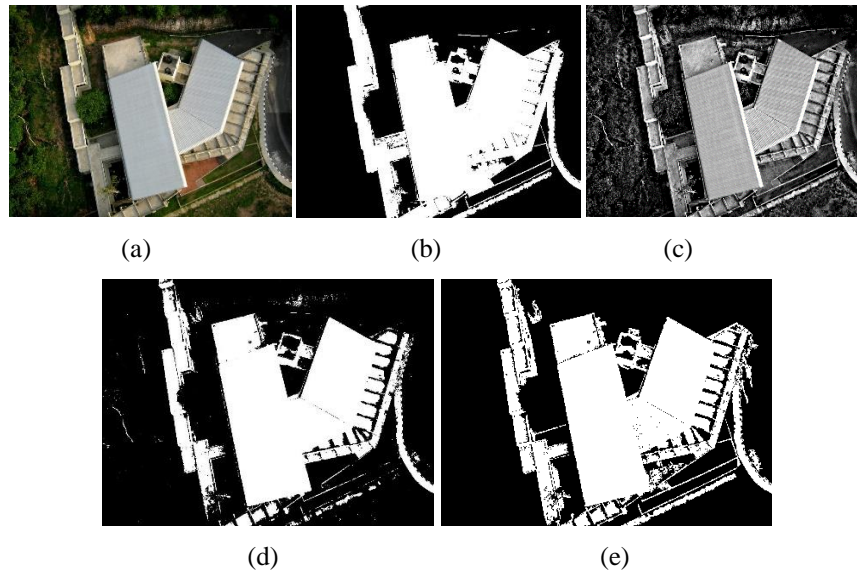
Figure 7.4. (a)– (e). Illustration of algorithm results with NITK, Aerial dataset-2. (a) Original image (b) Ground truth (c) MM processed image (intermediate stage) (d) Otsu thresholding approach (e) Proposed MM algorithm outcome.

Figure 7.5 illustrates the performance of the algorithm with Color-IR aerial images of ERDAS Imagine sample datasets II of eastern Illinois. The proposed algorithm extracts urban features with an accuracy of 98.36% as compared to the accuracy of 94.41% for the Otsu's threshold driven method. MCC and Precision values of 0.9653 and 0.9562 is observed for the proposed MM algorithm; and for the Otsu's threshold based approach it is observed to be 0.88345 and 0.88662. In this case the proposed algorithm has shown overall better performance than the Otsu's threshold based method. The Color-IR aerial dataset-II imagery provides the highest overall performance with highest accuracy, MCC and precision among all data sets.

(a) (b) (c)

(d)   (e)
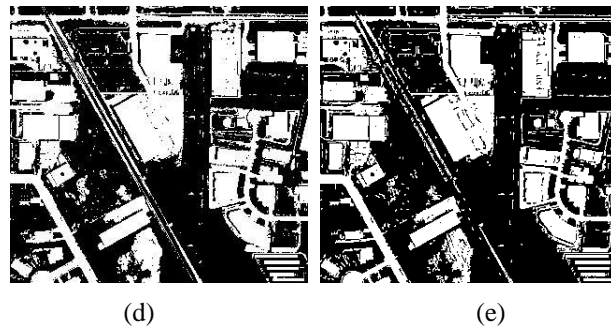
Figure 7.5. (a) – (e). Illustration of algorithm results with Color-IR aerial images of ERDAS Imagine sample dataset-II of eastern Illinois. (a) Original image (b) Ground truth (c) MM processed image (intermediate stage) (d) Otsu thresholding approach (e) Proposed MM algorithm outcome.
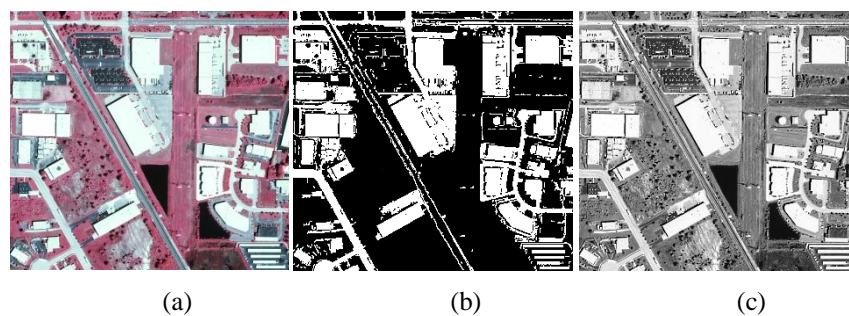
Accuracy assessment was performed based on the ground truth maps shown in figures 7.2(b), 7.3(b), 7.4(b) and 7.5(b) by pixel-by-pixel comparison of manually delineated and extracted urban features. Ground truths are prepared for all images to evaluate the algorithm performance. The metrics (Precision, Accuracy and MCC values) used to evaluate the performance of the system are calculated based on the ground truths. The performance of the proposed extraction approach and that of the Otsu's threshold based extraction approach is depicted in the table 7.2 and 7.3 respectively. In general, the figures numbered 7.2 to 7.5 (a) – (e) illustrates the different input data sets, ground truth images, MM algorithm processing stages, results drawn from an Otsu's threshold based approach and the output drawn from the proposed MM approach.

Table 7.2. Accuracy assessment of proposed MM approach

Sensor and AoI chosen	Precision	Accuracy	MCC
Color-IR aerial DS-I of Eastern Illinois	0.9602	0.9580	0.8904
Color-IR aerial DS-II of Eastern Illinois	0.9562	0.9836	0.9653
NITK, Aerial Dataset-1	0.8604	0.9287	0.8218
NITK, Aerial Dataset-2	0.9825	0.9439	0.8859

Table 7.3. Accuracy assessment of Otsu's threshold based method.

Sensor and AoI Description	Precision	Accuracy	MCC
Color-IR aerial DS-I of Eastern Illinois	0.99954	0.94911	0.86814
Color-IR aerial DS-II of Eastern Illinois	0.88662	0.94417	0.88345
NITK, Aerial Dataset-1	0.96808	0.90960	0.76781
NITK, Aerial Dataset-2	0.99080	0.91730	0.83530

7.1.6 Conclusion

Automated feature extraction approaches can significantly shrink the time and cost of data acquisition and can update database effectively with minimal turnaround time. In this research, the application and effectiveness of mathematical morphology assisted approach for the extraction of urban features is clearly brought out. Since we utilize morphological reconstruction based operations, the actual size and shape of the objects in the outcome is preserved. The MM approaches have a significant influence in the specification of the structuring element. Since the proposed algorithm provides a provision to feed the SE Kernel size and PL values dynamically, the highest possible accuracy from different sets of inputs (with varying resolution and swath) can be obtained with certain level of training or experience. As compared to the manual digitization, the proposed MM algorithm takes very less time for processing, i.e., the turnaround time is only few minutes. The accuracy of the developed methodology has been assessed with manually prepared ground truths which reveals that proposed MM algorithm performs better with different input aerial datasets in comparison with Otsu threshold based method.

7.2 APPROACH FOR UAV AND SATELLITE DATASETS

This section describes a different MM driven approach (utilizing image parameter statistics and different thresholding schemes) which is very effective and useful for the extraction of urban features including urban settlements, important road networks, etc. from different sets of high resolution satellite and aerial imageries. The proposed approach is tested with various UAV and satellite acquired images with high resolution.

Accuracy of the developed methodology has been assessed with manually prepared ground truths of the study area and compared with supervised classification (ML) method. This approach is found successful in urban feature extraction based on the results drawn from visual and quantitative assessments.

7.2.1 Background and related works

The need for using remote sensing data to accomplish the complex task of automated extraction of natural, manmade and cartographic features has significantly increased. Satellite and aerial images inherently tend to be a little noisy, complex and ambiguous. Scientists and researchers have identified the significance of designing and implementing more sophisticated and flexible automated feature extraction practices to advance the information extraction procedures (Momm and Easson, 2010).

MM assisted image processing techniques provide an efficient means for reducing the effect of noise such as in edge detection and filling in broken edges. By choosing the size and shape of the neighborhood, one can make a morphological operation that is sensitive to definite shapes in the input image (Castro and Centeno, 2010). The shape-oriented processing capability of the mathematical morphology toolbox has rendered it popular with remote sensing images (Stankov and He, 2013; Soille and Pesaresi, 2002). A method for building detection in very high spatial resolution MSS images is presented using spectral similarity and hit-or-miss transform (HMT) from MM (Stankov and He, 2013). Spectral similarity is used for building location enhancement and hit-or-miss transform for assigning pixels to Buildings. Even though the suggested method is with promising results, but the level of computational complexity and the user intervention required to define classes is higher. In addition, morphological approaches have been also used broadly for spatial structure extraction problems, e.g., building detection and extraction (Ouzounis, et al. 2011), road network delineation (Valero, et al. 2007). This study presents an MM driven approach, which is very effective and useful for the extraction of urban features including urban settlements, important road networks, etc. from different satellite and aerial imageries with high resolution.

Feature Extraction Strategies Based on Mathematical Morphology for the Analysis of Remotely Sensed Imagery, PhD Thesis, 2019, NITK Surathkal, India.

112

7.2.2 Data

The important data sets used for this investigation is procured from various sources and agencies mentioned in Table 7.4.This research utilizes very high spatial resolution satellite imageries to moderate spatial resolution.

Table 7.4. Specification of datasets for the present study

Satellite / Sensor	Spatial Resolution	Source / Agency	Region of Interest	Date of Pass
CARTOSAT 2, PAN	0.8m	NRSC	Mangalore, India	12 NOV 2008
NITK, Aerial Dataset	Very high (> 0.5m)	UAV Lab, Applied Mechanics Dept. NITK, India	NITK campus, Mangalore, India	24 NOV 2013
Color- IR aerial images (titled as 4-3 imagery)	High (> 2m)	ERDAS IMAGINE Remote Sensing sample data sets	Eastern Illinois, USA	Not Available
Resourcesat-2, LISS IV	5.8m	NRSC	Mangalore. India	01 DEC 2012
UC Merced Land Use Dataset	High (> 5m)	http://vision.ucmerced.edu/ datasets/landuse.html (Yang et al. 2010)	Not Available	Not Available

7.2.3 Methodology and algorithm design

The acquired satellite images initially may undergo various pre-processing operations to rectify noises, radiometric and geometric errors if any. The methodological flowchart of the present investigation is shown in figure 7.6.

Feature Extraction Strategies Based on Mathematical Morphology for the Analysis of Remotely Sensed Imagery, PhD Thesis, 2019, NITK Surathkal, India.

113
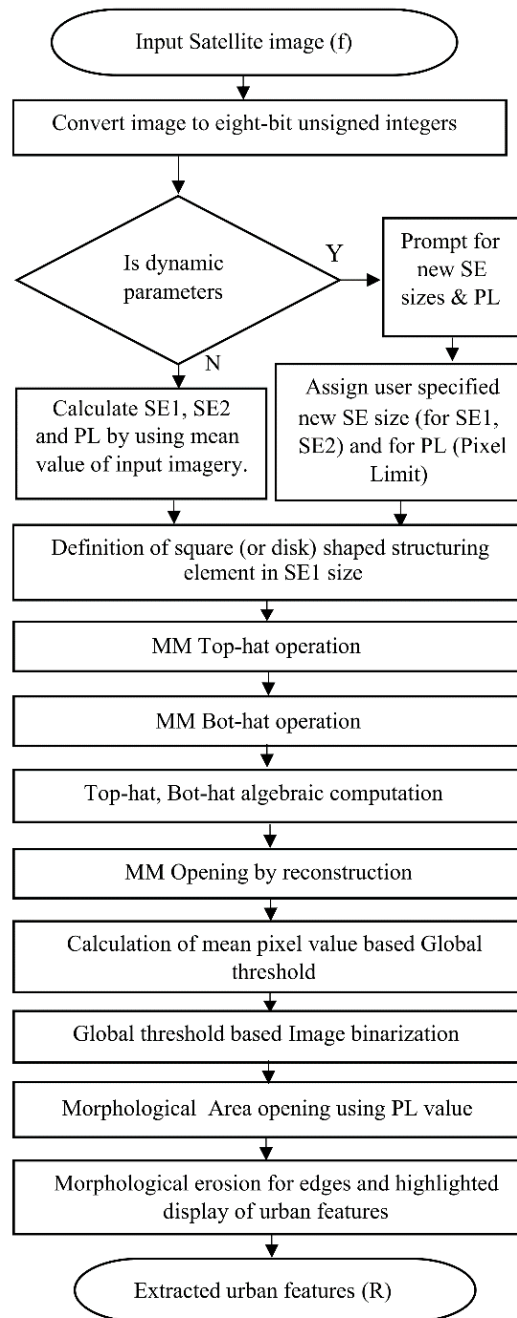
Figure 7.6. Flowchart of the proposed MM extraction approach

The algorithm will compute values for SEs and PL by using calculated mean value of the input imagery and formulas programmed. In addition to this, if the user wanted to work with coarse and medium resolution imagery then the user can feed appropriate SE kernel size (recommended range) at run time for more fine results rather than depending on image mean based SE and PL values. Top-hat and bot-hat algebraic computations

(the bot-hat transformation is employed to enhance the dark details in the grey image and the top-hat transformation is used to exclude the disturbances of the bright spots) were performed on the image to enhance urban features for easier identification. This process is followed by a set of powerful MM operations such as reconstruction-driven Opening, Area closing operations applied along with Global thresholding and binarization to delineate the desired urban features. The Area Opening (bwareaopen) removes small objects from binary image, which resembles noise. The pixel range is defined by the variable PL. The highlighted urban features is displayed by overlaying the obtained resultant imagery with its slightly eroded imagery.

The MM approaches have a major influence on the specification of the structuring element, so one should take it into consideration. The proposed algorithm provides a provision to feed the pixel range (PL) to eliminate unwanted objects and SE Kernel size dynamically, if the user recognizes the correlation between the spatial resolution of imagery and SE size. So, the highest possible accuracy from any resolution imagery can be obtained with certain level training or experience.

Some features may have diverse responses for a set of SE sizes, depending on the interactions between the SE size and the size of the features. Occasionally, we know correctly the size of the feature that we want to detect. Nevertheless, that is often not possible, and then a single-SE-size approach appears to be over simplified. Due to these reasons, in urban areas, it is a good idea to generate multidimensional morphological profiles and use a multiscale approach based on a series of different SE sizes. This permits us to discover a variety of different hypothetical spatial domains and to use the best response of the feature in the image.

The following section describes the algorithemic step involved in implementing the proposed approach.

7.2.3.1 Algorithm development

   Input: An NxN sized satellite input image (f).

   Output: An NxN sized output image (R).

1-	**Start**
2-	Procurement /Acquirement, registration and Pre-processing of the RS imageries.
3-	Convert imagery to 8-bit unsigned integers.
4-	**If** (End user opts for dynamic SE sizes and PL') **then** Receive SE1, SE2 and PL values on runtime,
5-	**Else** go to Step 5
6-	Calculate SE1, SE2 and PL by based on mean value of input imagery.

$$T = mean2\ (f);$$
$$SE1 = round\ (0.10 * T);$$
$$SE2 = round\ (0.01 * T);$$
$$PL = T/B2;$$

7-	Square shaped structuring element definition using SE1. [se1 = strel ('square', SE1)]
8-	MM Top-hat operation. [TH = imtophat (f, SE1)]
9-	MM Bot-hat operation. [BH = imbothat (P5, SE4)]
10-	Computations using MM Bot-hat and MM top-hat results with original imagery. [CF = ((f + TH) - BH)]
11-	MM Opening by reconstruction [OR = mmopenrec (CF, mmsedisk (B2))]
12-	Calculation of mean pixel value of OR and Calculation of Global threshold (Th) of processed image. [Mn = mean2 (OR)]
13-	Binarization of image using threshold (Th). [G = im2bw (OR, Th/255]
14-	Area Opening [R = mmareaopen (G, PL)]
15-	Morphological erosion for edges. [GE = mmero(GE, mmsedisk(1))]
16-	Print or display results (R).
17-	Highlighted result [Rh = mmshow (R, GE)]
18-	End.

7.2.4   Results and discussion

This sections describes the results drawn from different sets of the input imageries including visual, qualitative and quantitative assessments. The ground truths are prepared collectively combining the knowledge of the user via field visit with GPS at possible locations and digitized sketches. Also manual visual examination using Google earth imagery for verification and correction at pixel and object level in an iterative fashion to obtain maximum possible accuracy have been carried out.

The performance of the proposed MM based extraction approach and that of the ML classifier approach is depicted in the table 7.5 (pixel statistics comparison) and 7.6 (Performance comparison of proposed MM and ML Classifier approaches).

Feature Extraction Strategies Based on Mathematical Morphology for the Analysis of Remotely Sensed Imagery, PhD Thesis, 2019, NITK Surathkal, India.
116

Table 7.5. Pixel statistics comparison of proposed MM approach and ML Classifier.

Sensor /AoI chosen	Method	TP	TN	FP	FN	Total Pixels
Illinois Color-IR (infrared) aerial image	MM	33147	56322	4478	796	94743
	MLC	28362	50767	9885	5729	94743
NITK Arial Dataset	MM	249160	415239	18255	8546	691200
	MLC	224464	405676	1866	59194	691200
CARTOSAT 2 (PAN), MRPL	MM	84418	328643	21702	7217	441980
	MLC	89964	300947	49279	1790	441980
LISS IV, MRPL	MM	14459	30402	5348	1091	51300
	MLC	14082	26258	9492	1468	51300
UC Merced, Dense residential-31	MM	37236	21101	4637	2562	65536
	MLC	29126	24556	1182	10672	65536

Table 7.6. Accuracy assessment comparison of proposed MM approach and ML Classifier.

Sensor /AoI chosen	Method	F-score	Precision	Accuracy	MCC
Illinois Color-IR (infrared) aerial image	MM	0.92630	0.88098	0.94433	0.88479
	MLC	0.78415	0.74154	0.83519	0.65439
NITK Arial Dataset	MM	0.94896	0.93173	0.96122	0.91812
	MLC	0.88027	0.99175	0.91166	0.82466
CARTOSAT 2 (PAN), MRPL	MM	0.85376	0.79549	0.93456	0.81553
	MLC	0.77891	0.64609	0.88445	0.73322
LISS IV, MRPL	MM	0.81788	0.72999	0.87448	0.60458
	MLC	0.71986	0.59735	0.78635	0.59031
UC Merced, Dense residential-31	MM	0.91185	0.88926	0.89015	0.76812
	MLC	0.83091	0.96100	0.81912	0.67184

In general, the figures numbered 7.7 to 7.11 (a) – (e) illustrates the different input datasets, reference images, results drawn from ML classifiers, MM algorithm intermediate processing stages and the output drawn from the proposed MM approach.

Feature Extraction Strategies Based on Mathematical Morphology for the Analysis of Remotely Sensed Imagery, PhD Thesis, 2019, NITK Surathkal, India.

117

Figure 7.7(a)–(e) illustrates the performance of the algorithm with Color-IR (infrared) aerial image of eastern Illinois. In this case, the proposed MM algorithm is able to extract urban features with 94.433% accuracy and better MCC (0.88479), F-score (0.92630) and precision (0.88098) values. Even though traditional thresholding based method has an accuracy of 83.519%, its MCC (0.65439), F-score (0.78415) and precision (0.74154) values are marginally lower than that of proposed MM based approach.

(a)　　　　　　　　(b)　　　　　　　　(c)

(d)　　　　　　　　(e)
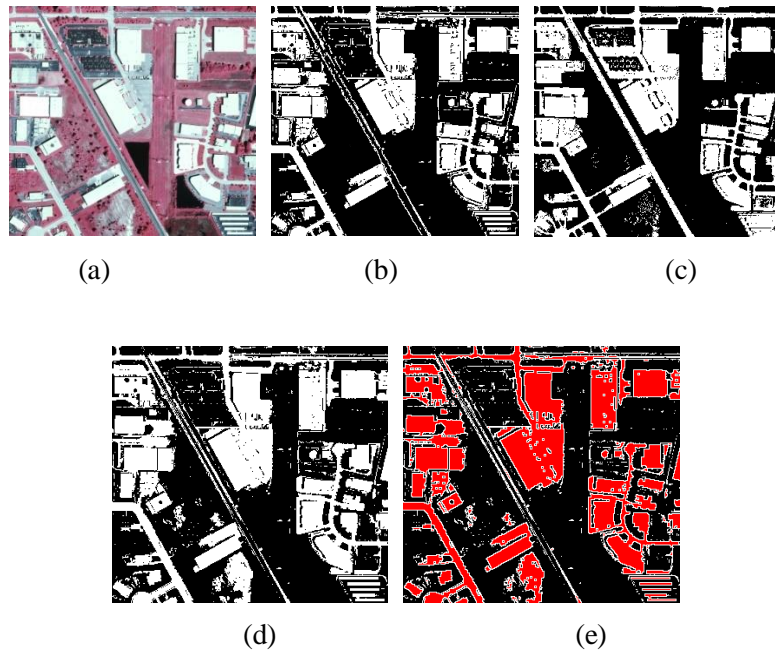
Fig. 7.7. (a)–(e). Illustration of algorithm results with Color-IR aerial images of ERDAS Imagine sample dataset. (a) Original image (b) Ground truth (c) ML classifier (d) Proposed MM approach (e) MM approach highlighted result

Figure 7.8(a)–(e) Illustrates the algorithm performance with NITK Arial Dataset. In this case, the algorithm is able to extract all the urban features more accurately since this imagery has very high spatial resolution. Here, an accuracy of 96.122% and 91.166% is achieved by the proposed MM algorithm and the ML classifier method respectively. MCC, F-score and Precision values of 0.91812, 0.94896and 0.93173 is observed for the proposed MM algorithm while for the ML classifier it is observed to be 0.82466, 0.88027and 0.99175. Also this dataset exhibits highest overall performance (highest accuracy, F-score, MCC) and precision for proposed as well as Otsu's threshold based

---

approaches.

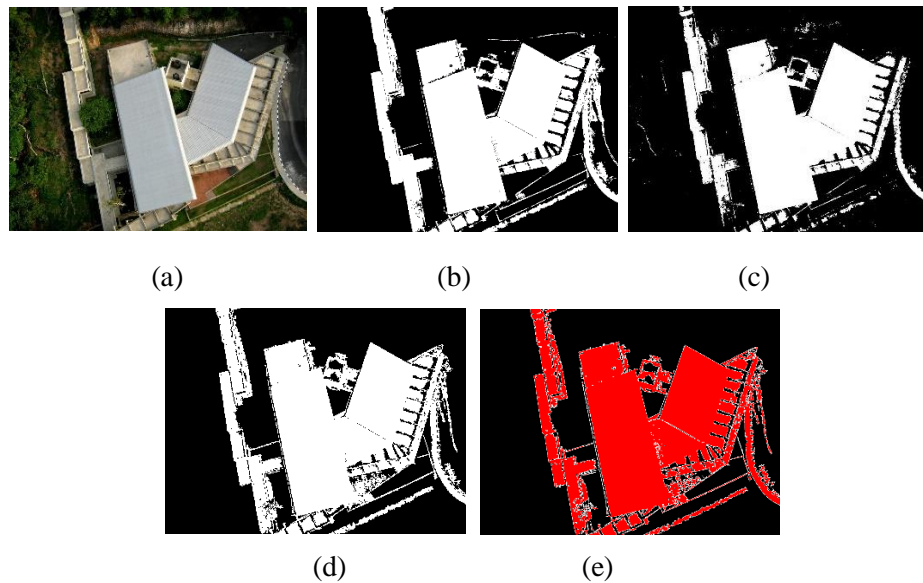**Fig. 7.8. (a)–(e). Illustration of algorithm results with NITK, Aerial dataset. (a) Original image (b) Ground truth (c) ML classifier (d) Proposed MM approach (e) MM approach highlighted result**

Figure 7.9(a)–(e) illustrates the performance of the algorithm with CARTOSAT-2 (PAN), imagery covering Mangalore Refinery and Petrochemicals Limited (MRPL) area. The proposed algorithm extracts glacier lakes with an accuracy of 93.456% as compared to the accuracy of 88.445% for the MLC approach. MCC, F-score and Precision values of 0.81553, 0.85376and 0.79549 is recorded for the proposed MM algorithm whereas for the ML classifier approach it is observed to be 0.73322, 0.77891and 0.64609 which is lesser than the proposed one. In addition, few minor misclassification has been observed for proposed MM and MLC method. This may be due to the presence of dark pixels and barrels.

Figure 7.10 illustrates the algorithm results with LISS IV (Mangalore refinery) dataset. The performance of an ML classifier (Fig. 7.10 c) and the proposed MM algorithm (Figure 7.10 d) is shown. The proposed MM algorithm extracts urban areas with an accuracy of 87.448% compared to the accuracy of 78.635% for the ML classifier approach. MCC, F-score and Precision values of 0.60458, 0.81788and 0.72999 is

recorded for the proposed MM algorithm whereas for the ML classifier it is observed to be 0.59031, 0.71986 and 0.59735, which is lesser than the proposed MM method's performance. The poor performance of the algorithms can be attributed to the presence of diverse objects in the area of interest including barrels, water body, vegetation and urban settlements.

(a)   (b)   (c)

(d)   (e)
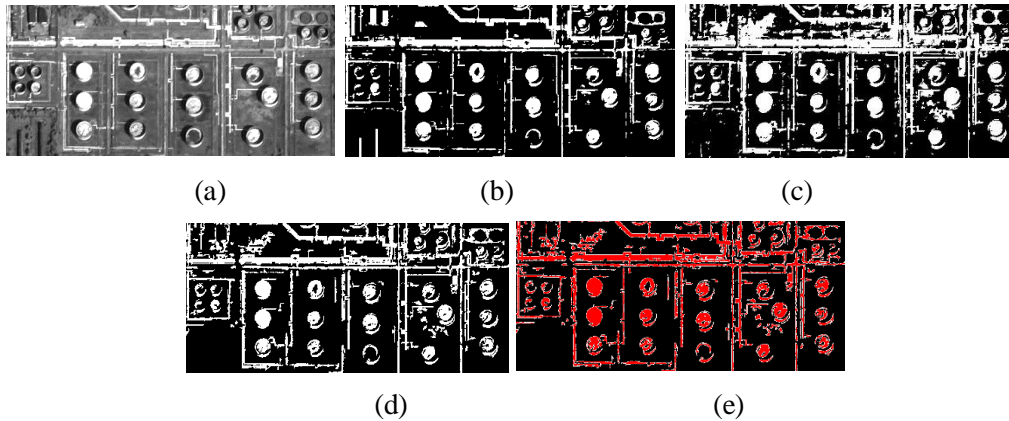
Fig. 7.9. (a)–(e). Illustration of algorithm results with CARTOSAT 2 (PAN), MRPL dataset. (a) Original image (b) Ground truth (c) ML classifier (d) Proposed MM approach (e) MM approach highlighted result.

(a)   (b)   (c)

(d)   (e)

Fig. 7.10. (a)–(e). Illustration of algorithm results with LISS IV (mangalore refinary) dataset. (a) Original image (b) Ground truth (c) ML classifier (d) Proposed MM approach (e) MM approach highlighted result

Feature Extraction Strategies Based on Mathematical Morphology for the Analysis of Remotely Sensed Imagery, PhD Thesis, 2019, NITK Surathkal, India.

120

Figure 7.11 (a)–(e) shows the algorithm performance with UC Merced dataset, dense residential-31. Here the proposed MM algorithm is able to extract urban features with 89.015% accuracy and satisfactory MCC (0.76812), precision (0.88926) and better F-score (0.91185) values. The traditional ML classifier method obtained lesser accuracy of 81.912%, MCC (0.67184), F-score (0.83091). While a better precision of 0.96100 was obtained for the same.
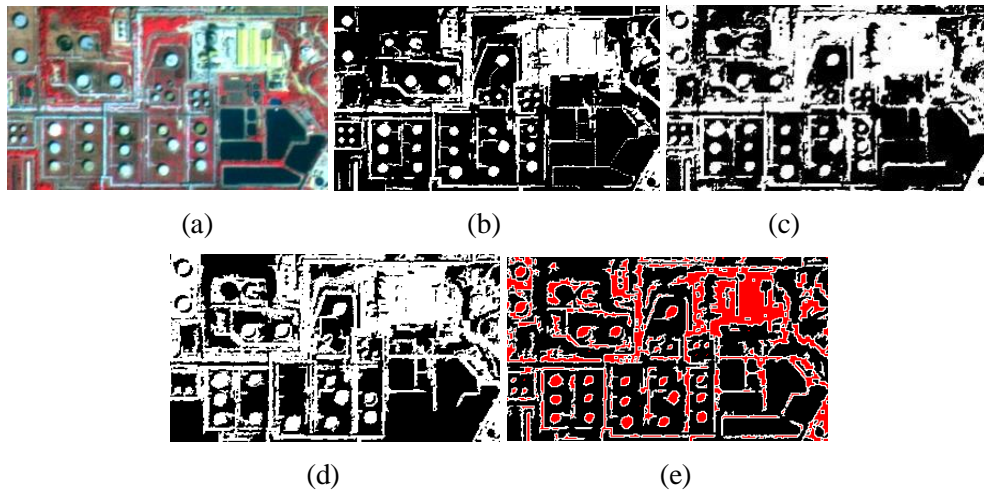

(a)　　　　　　　(b)　　　　　　　(c)

(d)　　　　　　　(e)
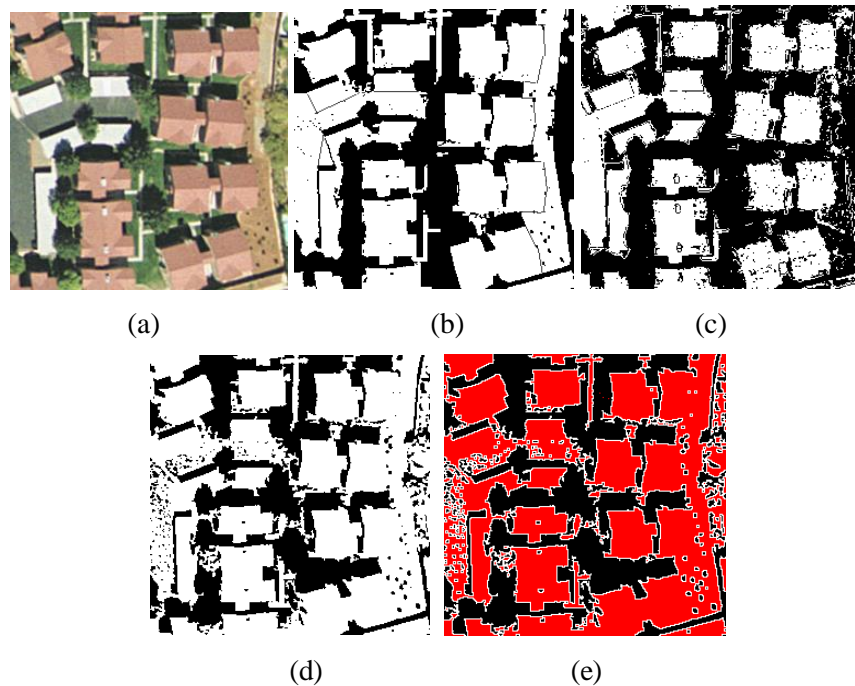
Fig. 7.11. (a)–(e). Illustration of algorithm results with UC Merced dataset, dense residential-31. (a) Original image (b) Ground truth (c) ML classifier (d) Proposed MM approach (e) MM approach highlighted result

The NITK Arial imagery exhibits the highest overall performance with accuracy (0.96122), precision (0.93173), F-score (0.94896) and MCC (0.91812) followed by the Cartosat-2 PAN imagery with almost near values of accuracy (0.93456) MCC (0.81553), F-score (0.85376) and satisfactory precision of (0.79549). The LISS IV imagery exhibits lowest accuracy (0.87448) and MCC (0.60458), precision (0.72999)

Feature Extraction Strategies Based on Mathematical Morphology for the Analysis of Remotely Sensed Imagery, PhD Thesis, 2019, NITK Surathkal, India.

121

and F-score (0.81788) values since the data has the lowest spatial resolution compared to other datasets employed.

7.2.5 Conclusions

Automated feature extraction approaches can significantly shrink the time and cost of data acquisition and can update database effectively with minimal turnaround time. This study presents a flexible MM driven approach for urban feature extraction, which is capable of preserving the actual size and shape of the objects. The proposed MM driven approach is an adaptive and useful technique for the extraction of urban features from satellite and aerial imageries. The availability of more than one spectral band of satellite imagery is not necessary for the proposed algorithm, as it utilizes only a single band for its computation. This makes it convenient to apply in single band imageries obtained from satellites such as Cartosat. The algorithm will compute values for SEs and PL by using calculated mean value of the input imagery thereby making it convenient to apply with different resolution imagery. The accuracy of the developed methodology has been evaluated with manually prepared ground truths, revealing better performance with different satellite and aerial datasets compared to the ML classifier result. The proposed algorithm is less time consuming compared to manual digitization that is for processing, turnaround time is only few minutes and for very small stretch of AoI parcels it hardly takes few seconds.

CONCLUSIONS AND FUTURE PERSPECTIVES

This chapter presents a general summary of the work described in the research reviewing the main contributions. Specific concluding remarks on the research topics treated in the thesis are also presented. Finally, perspectives on possible future developments of the work are discussed.

8.1 GENERAL CONCLUSIONS

The contributions provided in this thesis have been focused on the development of novel feature extraction methods for remotely sensed images improving the robustness and the generalization properties of the feature extraction system with respect to the standard techniques. The proposed methodologies contribute to a more effective use of last generation of remote sensing data in many real world applications related to the monitoring and management of environmental resources. The proposed algorithms are effective for the extraction of different features like shoreline, water bodies, crop parcel boundaries and urban features. The final results are in general promising, encourage the development of future improvements and could open the ways to new trends.

The salient features of the present study include the following:

- The proposed algorithms preserve the actual size and shape of the objects in the outcome by exploring morphological reconstruction centered operations.

- The availability of more than one spectral band of satellite imagery is not necessary for the proposed algorithm as it utilizes only a single band for its computation (such as red or NIR or PAN). This makes it convenient to apply in single band imageries obtained from satellites such as Cartosat thereby making the proposed approaches effective over commonly used methods.

- The state-of-the-art MM based approaches do not focused to feed result-governing variables dynamically. However, most of the proposed approaches in this study provide a provision to feed the important result governing parameters such as programmable SE size (some cases threshold values and PL value for noise reduction) at run time, hence the highest possible accuracy can be achieved for different spatial resolution, topography and geographic coverage.

The computational cost of the proposed MM method is influenced by the size of the SEs used and the total number of pixels present in the input imagery. That is, the use of small structuring elements will considerably decrease the processing time. The specific conclusions on computational cost are as follows:

- The processing time is linear with respect to the image size.

- The latency is mostly equal to the operator latency inferred by the size of the SE used. The memory requirements are small and proportional to the size of the SE used.

- The operation-specific parameters, i.e., image size, SE size, erosion/dilation select, are run-time programmable up to some specified upper bound at the beginning of processing of each image.

Methods such as MLC requires much time for training input imagery. Most algorithms in mathematical morphology show a pseudo-polynomial complexity. For example, the trivial algorithm of dilation has a complexity of $O(N \times |B|)$ Where N and $|B|$ denote the number of points of the image and of the structuring element, respectively.

- **Shoreline Extraction**

In chapter 4 a novel shoreline extraction approach for the remotely sensed images were presented. Shoreline extraction is inevitable for several studies such as coastal zone management, coastline erosion monitoring, GIS database updating, watershed definition, flood prediction, the evaluation of water resources, etc. For simple stretches of coast, it is easy to trace the coastline regions manually, whereas, it is practically difficult when the coastline becomes very wide, long and complex. So automated and

replicable techniques play a vital role in updating coastline maps, to evaluate the spatial and temporal evolution of alterations due to natural and anthropogenic events, especially for large areas. The accuracy of the developed methodology has been assessed with reference maps, which concluded that the proposed MM algorithm performs better with different imagery datasets in comparison with ML classifier.

- **Waterbody extraction**

In Chapter 5, multiple approaches for extraction of different types of waterbodies (such as lakes, rivers and glacier lakes) were discussed. Firstly, this study proposes an MM driven approach which is very effective and useful for the extraction of water bodies from several satellite imager with different spatial resolutions. The proposed approach has been compared against well-known methods such as NDWI, MNDWI and ML classifier. This study concludes that the proposed MM approach is dominant in terms of performance and hence MM based approaches can be used for practical applications.

Secondly, the application and effectiveness of mathematical morphology assisted approach for the extraction of glacier lakes is elucidated. Detection and tracking glacier lake dynamics from remotely sensed imagery is very important and useful for many GIS activities. GLOFs are among the most critical natural hazards in high mountain regions in the past few decades. Thus, automated and replicable techniques play a vital role in updating glacier lake inventories to evaluate the spatial and temporal changes in glacial lakes in view of disaster prediction, critical zone identification, impact assessment, etc. The accuracy of the developed methodology has been evaluated with reference maps, revealing better performance with different imagery datasets compared to Otsu's threshold based method.

Finally, the efficiency of MM assisted approach for the extraction of ponds and lakes from different satellite images have been presented. Monitoring and tracking lake dynamics is critical to support sustainable management of water resources on this terrestrial earth. Unlike the above two which adopted grey thresholding scheme, the present case uses ANN based threshold values. Considerably good results obtained in

----

this study, makes this approach promising for the lake extraction task from remote sensing images.

- **Crop field extraction**

In chapter 6 the performance of MM has been exploited for the extraction of crop field boundaries from multiple satellite imageries. The proposed MM driven approach is effective and useful for the extraction of crop field boundaries for medium and high-resolution satellite imageries. The proposed algorithm is less time consuming compared to manual digitization that is for processing, turnaround time is only few minutes and for very small crop parcels it hardly takes few seconds.

- **Urban feature extraction**

At last, Chapter 7 introduces two innovative feature extraction methods for UAV and satellite images. As described in the previous chapters, the use of UAV for civilian applications is continuously on the rise. UAV driven images may be of great advantage as they would allow a detailed description of the scenes, but, at the same time, they would need appropriate image analysis techniques to exploit and adapt all the potential to these aims. In this context, it would be particularly interesting to develop techniques for the extraction of urban features including urban settlements, important road networks, etc. The timely and extremely detailed capacity of acquiring information of UAV is suitable for these purposes. Manual digitization, segmentation and classification approaches may be extremely time consuming and may produce inaccurate result for the UAV images.

In the first algorithm, the application and usefulness of mathematical morphology assisted approach for the extraction of urban features is clearly brought out. As compared to the manual digitization, the proposed algorithm takes very less time for processing, i.e., the turnaround time is less (in minutes). The accuracy of the developed methodology has been assessed with ground truths which reveals that this algorithm performs better with different input aerial datasets in comparison with Otsu-threshold based method. In second approach, an adaptive and useful technique for the extraction

----

of urban features from satellite and aerial imageries were analysed. The algorithm could compute values for SEs and PL by using calculated mean value of the input imagery thereby making it convenient to apply with different resolution imagery. The accuracy of the developed methodology has been evaluated with manually prepared reference maps, revealing better performance with different satellite and aerial datasets compared to the ML classifier result. As compared to the manual digitization, the proposed algorithm takes less time compared to the manual digitization that is for processing, turnaround time is only few minutes.

8.2. FUTURE PERSPECTIVES

Based on the analysis and the experiments carried out in the framework of this thesis, following are some of the identified and interesting avenues of research as future developments to this work.

- Further investigations aiming at exploiting higher spectral resolution imageries including hyperspectral images, Landsat thermal band capabilities, etc. can be carried out. In particular, it is believed that these could be better utilized for performing a region-based analysis of the image. Moreover, the combination of different bands could also be used for gathering information on the composition of the scene according to the relations that exist between the region/objects of the image.

- The extension and investigation of the proposed techniques on data acquired by other optical and microwave sensors (e.g., LIDAR and SAR images) should also be of interest. Indeed, very few applications of mathematical morphology techniques on other data than optical images exist.

- Another interesting direction would be to extend the presented techniques by considering the capabilities of different Indices (such as LAI, NDWI, and NDWI) along with MM (hybrid approach). Similarly different soft computing techniques such as SVM, genetic algorithms and machine learning techniques can be combined with MM technique for various image processing applications.

REFERENCES

Aboras, M., Amasha, H., & Ibraheem, I. (2015). Early detection of melanoma using multispectral imaging and artificial intelligence techniques. American Journal of Biomedical and Life Sciences, 3(2-3), 29-33.

Addink, E. A., De Jong, S. M., & Pebesma, E. J., (2007). "The importance of scale in object-based mapping of vegetation parameters with hyperspectral imagery". *Photogrammetric Engineering & Remote Sensing*, 73(8), 905-912.

Addo, K. A., Jayson-Quashigah, P. N., and Kufogbe, K. S., (2011). "Quantitative Analysis of Shoreline Change Using Medium Resolution Satellite Imagery in Keta, Ghana", *Mar Sci* 11-9.

Aptoula, E., (2014). "Remote Sensing Image Retrieval with Global Morphological Texture Descriptors", *IEEE Transactions on Geoscience and Remote Sensing*, Vol. 52, No. 5, pp-3023-3034.

Armenakis, C., & Savopol, F. (2004). "Image processing and GIS tools for feature and change extraction". *International Archives of Photogrammetry", Remote Sensing & Spatial Information Sciences*, 35, 611-616.

Athira K & Sreekumar K., (2014). "A Survey on Image Segmentation and Feature Extraction Methods for Acute Myelogenous Leukemia Detection in Blood Microscopic Images". *International Journal of Computer Science and Information Technologies*, 5(6), 7877-7879.

Azayev, T. (2016). "Object detection in high resolution satellite images", project report, Czech Technical University in Prague.

Baatz, M. (2000). Multi resolution Segmentation: an optimum approach for high quality multi scale image segmentation. In Beutrage zum AGIT-Symposium. Salzburg, Heidelberg, 2000(pp. 12-23).

Baatz, M., Benz, U., Dehghani, S., Heynen, M., Höltje, A., Hofmann, P., Lingenfelder, I., Mimler, M., Sohlbach, M., Weber, M. and & Willhauck, G. (2004). "eCognition professional user guide 4". Definiens Imaging, Munich.

Babar, M. A., Reynolds, M. P., Van Ginkel, M., Klatt, A. R., Raun, W. R., & Stone, M. L. (2006). "Spectral reflectance indices as a potential indirect selection criteria for wheat yield under irrigation". *Crop Science*, 46(2), 578-588.

Bagli, S., and Soille, P., (2003). "Morphological automatic extraction of coastline from PAN-European Landsat TM images" In: Proceedings of the Fifth International Symposium on GIS and Computer Cartography for Coastal Zone Management, Vol. 3, Genova, pp. 58–59.

Bayram, B., Acar, U., & Ari, A., (2008). "A novel algorithm for coastline fitting through a case study over the Bosphorus", *Journal of Coastal Research,* 24(4), 938–991.

Bellens, R., Gautama, S., Martinez-Fonte, L., Philips, W., Chan, J.C.W. and Canters, F., (2008). "Improved classification of VHR images of urban areas using directional morphological profiles". *IEEE Transactions on Geoscience and Remote Sensing*, 46(10), pp.2803-2813.

Benediktsson, J. A., Pesaresi, M., & Amason, K. (2003). Classification and feature extraction for remote sensing images from urban areas based on morphological transformations. IEEE Transactions on Geoscience and Remote Sensing, 41(9), 1940-1949.

Benediktsson, J.A., Palmason, J.A. and Sveinsson, J.R., (2005). "Classification of hyperspectral data from urban areas based on extended morphological profiles". *IEEE Transactions on Geoscience and Remote Sensing*, 43(3), pp.480-491.

Benz, U. C., Hofmann, P., Willhauck, G., Lingenfelder, I., & Heynen, M. (2004). "Multi-resolution, object-oriented fuzzy analysis of remote sensing data for GIS-ready information". *ISPRS Journal of photogrammetry and remote sensing*, 58(3-4), 239-258.

Beucher, S. (1992). The watershed transformation applied to image segmentation. SCANNING MICROSCOPY-SUPPLEMENT-, 299-299.

Beveridge J. R., Griffith J. Kohler R. R., Hanson A. R., and Riseman E. M., (1989). "Segmenting images using localized histograms and region merging," *International Journal of Computer Vision,* vol. 2, no. 3, pp. 311-347, 1989.

Bhadauria, A., Bhadauria, H., & Kumar, A. (2013). "Building extraction from satellite images. IOSR Journal of Computer Engineering, 12(2), 76-81.

Bin, L. Mehdi Samiei yeganeh, (2012). Comparison for Image Edge Detection Algorithms". *IOSR Journal of Computer Engineering (IOSRJCE)*, 2(6), 01-04.

Blaschke, T., (2010). "Object Based Image Analysis for Remote Sensing," *Journal of Photogrammetry and Remote Sensing (ISPRS)*, vol. 65, no. 1, pp. 2-16.

Blumberg, D., & Jacobson, D. (1997). "New frontiers: remote sensing in social science research". *The American Sociologist*, 28(3), 62-68.

Bo, G., Delleplane, S. and Laurentiis, R. D., (2001). "Coastline extraction in remotely sensed images by means of texture features analysis". In: Geoscience and Remote Sensing Symposium, IGARSS '01, Vol. 3, Sydney, NSW, Australia, pp. 1493–1495.

Bosilj, P., Aptoula, E., Lefèvre, S., & Kijak, E. (2016). "Retrieval of remote sensing images with pattern spectra descriptors". *ISPRS International Journal of Geo-Information*, 5(12), 228.

Boughorbel, S., Jarray, F., & El-Anbari, M. (2017). Optimal classifier for imbalanced data using Matthews Correlation Coefficient metric. PloS one, 12(6), e0177678.

Braga, F., Luigi Tosi, Claudio Prati and Luigi Alberotanza, (2013). "Shoreline detection: capability of COSMO-SkyMed and high-resolution multispectral images", *European Journal of Remote Sensing,* 46: 837-853.

Brito, P. L., & Quintanilha, J. A. (2012). "A literature review, 2001-2008, of classification methods and inner urban characteristics identified in multispectral remote sensing images". Proceedings of the 4th GEOBIA, 586-591.

Brydegaard, M., Guan, Z., & Svanberg, S. (2009). "Broad-band multispectral microscope for imaging transmission spectroscopy employing an array of light-emitting diodes". *American Journal of Physics*, 77(2), 104-110.

Buddhiraju, K. M., & Rizvi, I. A. (2010). "Comparison of CBF, ANN and SVM classifiers for object based classification of high resolution satellite images". In Geoscience and Remote Sensing Symposium (IGARSS), IEEE International (pp. 40-43). IEEE.

Caixia, D., Chen Yu, Bi Hui and Han Yao (2014). "The Improved Algorithm of Edge Detection Based on Mathematics Morphology", *International Journal of Signal Processing, Image Processing and Pattern Recognition*, Vol.7, No.5 (2014), pp.309-322

Canny J., (1986) "A Computational Approach to Edge Detection," *IEEE transactions on pattern analysis and machine intelligence*, vol. 8, no. 6, pp. 679-698.

Carleer, A. P., Debeir, O., & Wolff, E. (2005). 'Assessment of very high spatial resolution satellite image segmentations". Photogrammetric Engineering & Remote Sensing, 71(11), 1285-1294.

Cavallaro, G. (2016). "Spectral-Spatial Classification of Remote Sensing Optical Data with Morphological Attribute Profiles using Parallel and Scalable Methods" (Doctoral dissertation).

Cenderelli, D.A., Wohl, E.E., (2001). "Peak discharge estimates of glacial lake outburst floods and "normal" climatic floods in the Mount Everest region Nepal", *Geomorphology*, 40, 57–90.

Kuldeep C., & Garg, P. K. (2013). A Brief Review on Texture Analysis Methods. Studies in Surveying and Mapping Science, 1(2), 1-9.

Chen, X., Xiang, S., Liu, C. L., & Pan, C. H. (2014). "Vehicle detection in satellite images by hybrid deep convolutional neural networks". *IEEE Geoscience and remote sensing letters*, 11(10), 1797-1801.

Cho, G., Hildebrand, A., Claussen, J., Cosyn, P., Morris, S., (2013). "Pilotless aerial vehicle systems: size, scale and functions", *Coordinates* 9, 8–16.

Colomina, I., Molina, P., (2014). "Unmanned aerial systems for photogrammetry and remote sensing: A review", *ISPRS J. Photogramm. Remote Sens.*, 92, 79–97.

Comaniciu, D. and Meer, P., (2002). "Mean shift: A robust approach toward feature space analysis". *IEEE Transactions on Pattern Analysis Machine Intelligence* 24(5), pp. 603–619.

Crommelinck, S., Bennett, R., Gerke, M., Nex, F., Yang, M.Y., and Vosselman, G., (2016). "Review of Automatic Feature Extraction from High-Resolution Optical Sensor Data for UAV-Based Cadastral Mapping", *Remote Sens.*, 8, 689, pp: 2-28.

Dalla Mura, M. (2011). Advanced techniques based on mathematical morphology for the analysis of remote sensing images (Doctoral dissertation, University of Trento).

Daryal, M. N., & Kumar, V. (2010). "Linear Extraction of Satellite Imageries using Mathematical Morphology". *International Journal of Computer Applications*, 3(3).

de Castro, F. S. P, Centeno, J. A. S., (2010), "Road extraction from ALOS images using mathematical morphology", *IAPRS journal*, Vol. XXXVIII, Part 7B, pp.457-462.

Dell'Acqua, F., Gamba, P., Ferrari, A., Palmason, J.A., Benediktsson, J.A. and Árnason, K., (2004). "Exploiting spectral and spatial information in hyperspectral urban data with high resolution". *IEEE Geoscience and Remote Sensing Letters*, 1(4), pp.322-326.

Dey, V., Zhang, Y., and Zhong, M., (2010). "A Review on Image Segmentation Techniques with Remote Sensing Perspective," *International Society for Photogrammetry and Remote Sensing (ISPRS) Technical Commission VII Symposium*, vol. XXXVIII, pp. 31-42, 2010.

Di, K., Wang, J., Ma, R. and Li, R., (2003). "Automatic shoreline extraction from high-resolution IKONOS satellite imagery", In: Proceeding of ASPRS 2003 Annual Conference, Vol. 3, Anchorage, Alaska.

Dougherty, E.R. and Lotufo, R.A., (2003). "Hands-on morphological image processing" (Vol. 59). SPIE press.

Duong N. D., (2012). "Water body extraction from multispectral image by spectral pattern analysis", *International Archives of the Photogrammetry, Remote Sensing and Spatial Information Sciences*, Vol.XXXIX-B8, 181-186.

Dussaillant, A., Benito, G., Buytaert, W., Carling, P., Meier, C., Espinoza, F., (2009). "Repeated glacial-lake outburst floods in Patagonia: an increasing hazard?" *Natural Hazards*. http://dx.doi.org/10.1007/s11069-009-9479-8

Ekercin, S. (2007). "Coastline change assessment at the Aegean Sea Coasts in Turkey using multi-temporal Landsat imagery", *Journal of Coastal Research*, 23(3), 691–698.

Emmer, A and Vilímek, V (2013). "Review Article: Lake and breach hazard assessment for moraine-dammed lakes: an example from the Cordillera Blanca (Peru)", *Nat. Hazards Earth Syst. Sci.*, 13, 1551–1565.

ERDAS IMAGINE 8.4 Field Guide: ERDAS Inc.

Ershad, S. F. (2012). "Texture classification approach based on combination of edge & co-occurrence and local binary pattern". arXiv preprint arXiv:1203.4855.

Fan, L., Poh, K. L., & Zhou, P. (2009). "A sequential feature extraction approach for naïve bayes classification of microarray data". *Expert Systems with Applications*, 36(6), 9919-9923.

Feyisa G. L., Meilby, H., Fensholt, R., Proud S. R., (2014). "Automated Water Extraction Index: A new technique for surface water mapping using Landsat imagery", *Remote Sensing of Environment*, 140, 23–35.

Fisher, J. R., Acosta, E. A., Dennedy-Frank, P. J., Kroeger, T., & Boucher, T. M. (2017). "Impact of satellite imagery spatial resolution on land use classification accuracy and modeled water quality". *Remote Sensing in Ecology and Conservation*.

Fonseca, L. M. G., Namikawa, L. M., & Castejon, E. F. (2009). "Digital image processing in remote sensing". In Computer Graphics and Image Processing (SIBGRAPI TUTORIALS), 2009 Tutorials of the XXII Brazilian Symposium on (pp. 59-71). IEEE.

Forestier, G., Derivaux, S., Wemmert, C., & Gançarski, P. (2008). "An evolutionary approach for ontology driven image interpretation". In Workshops on Applications of Evolutionary Computation pp. 295-304 Springer, Berlin, Heidelberg.

Frigato, R., & Silva, E. (2008). Mathematical morphology application to features extraction in digital images. ASPRS, Pecora, 17.

Fugate, D., Tarnavsky, E., & Stow, D. (2010). "A survey of the evolution of remote sensing imaging systems and urban remote sensing applications". In Remote sensing of urban and suburban areas pp. 119-139. Springer, Dordrecht.

Gairns, J. (1993). "Feature Extraction Comparison of Image Analysis Systems and Geographic Information Systems". *International archives of photogrammetry and remote sensing*, 29, 365-365.

Gaurav, R. (2009). "A Mathematical Morphological Perspective in World of images". In Seminar on spatial Information Retrieval Analysis, Reasoning and Modelling 18th–20th March.

Geiß, C., Klotz, M., Schmitt, A., & Taubenböck, H. (2016). "Object-based morphological profiles for classification of remote sensing imagery". *IEEE Transactions on Geoscience and Remote Sensing*, 54(10), 5952-5963.

Geman, S., & Geman, D. (1987). "Stochastic relaxation, Gibbs distributions, and the Bayesian restoration of images". In Readings in Computer Vision (pp. 564-584).

Gens, R., & Rosselló, J. C. (2015). Remote sensing data normalization. In Remotely Sensed Data Characterization, Classification, and Accuracies (pp. 167-176). CRC Press.

Gens, R., (2015). "Remote sensing of coastlines: detection, extraction and monitoring", *International Journal of Remote Sensing,* 31:7, 1819-1836, DOI: 10.1080/01431160902926673.

Géraud, T., Talbot, H., & Van Droogenbroeck, M., (2013). "Algorithms for mathematical morphology". *Mathematical morphology: from theory to applications*, 323-353.

Gerke, M., Przybilla, H.J., (2016). "Accuracy analysis of photogrammetric UAV image blocks: Influence of onboard RTK-GNSS and cross flight patterns", *Photogramm. Fernerkund. Geoinf.*, 14, 17–30.

Ghamisi, P., & Benediktsson, J. A. (2015). "Feature selection based on hybridization of genetic algorithm and particle swarm optimization". *IEEE Geoscience and Remote Sensing Letters*, 12(2), 309-313.

Ghamisi, P., Dalla Mura, M. and Benediktsson, J.A., (2015). "A survey on spectral–spatial classification techniques based on attribute profiles". *IEEE Transactions on Geoscience and Remote Sensing*, 53(5), pp.2335-2353.

Ghanea, M., Moallem, P., & Momeni, M. (2014). "Automatic building extraction in dense urban areas through GeoEye multispectral imagery". *International journal of remote sensing*, 35(13), 5094-5119.

Giada, S.,DeGroove, T., Ehrlich D., Soille P., (2003), "Information extraction from very high resolution satellite imagery over Lukole refugee camp, Tanzania" *Int.J.Remote Sensing*, Vol. 24, No. 22, 4251–4266.

Giannini M. B., Parente, C., (2015). "An object based approach for coastline extraction from Quickbird multispectral images", *International Journal of Engineering and Technology (IJET),* Vol. 6, ISSN: 0975-4024.

Goel, A., & Vishwakarma, V. P. (2016). "Efficient feature extraction using DCT for gender classification". In Recent Trends in Electronics, Information & Communication Technology (RTEICT), IEEE International Conference on (pp. 1925-1928). IEEE.

Goetz, A. F., Vane, G., Solomon, J. E., & Rock, B. N. (1985). "Imaging spectrometry for earth remote sensing". *Science*, 228(4704), 1147-1153.

Gonzalez, R. C., Woods, R. E., & Eddins, S. L. (2010). Morphological reconstruction. Digital image processing using MATLAB, MathWorks.

Gonzalez, R., and Woods, R., (2002). *Digital image processing*, second edition: Addison-Wesley.

Govender, M., Chetty, K., Naiken, V., & Bulcock, H. (2008). "A comparison of satellite hyperspectral and multispectral remote sensing imagery for improved classification and mapping of vegetation". *Water SA*, 34(2), 147-154.

Guariglia, A., Buonamassa, A., Losurdo, A., Saladino, R., Trivigno, M. L., Zaccagnino, A., & Colangelo, A. (2006). "A multisource approach for coastline mapping and identification of shoreline changes'. *Annals of geophysics*, 49(1).

Gulch, E. (2000). "Digital systems for automated cartographic feature extraction". *International Archives of Photogrammetry and Remote Sensing*, 33(B2; PART 2), 241-256.

Hahn U., Vedel Jensen E. B., Van Lieshout M. C., and Nielsen L. S., (2003). "Inhomogeneous Spatial Point Processes by Location-Dependent Scaling," *Advances in Applied Probability*, vol. 35, no. 2, pp. 319-336, 2003.

Haralick, R. M., & Shanmugam, K., (1973). "Textural features for image classification". *IEEE Transactions on systems, man, and cybernetics*, (6), 610-621.

Haralick, R. M., Sternberg, S. R., & Zhuang, X. (1987). "Image analysis using mathematical morphology". *IEEE transactions on pattern analysis and machine intelligence*, (4), 532-550.

Harini, S., and Anil, C., (2013). "Multi-level feature analysis for semantic category recognition", IEEE International Geoscience and Remote Sensing Symposium – IGARSS, Melbourne, VIC, 4371 – 4374.

Hay, G. J., & Castilla, G. (2008). "Geographic Object-Based Image Analysis (GEOBIA): A new name for a new discipline". In Object-based image analysis (pp. 75-89). Springer, Berlin, Heidelberg.

Hecher, J., Filippi, A., Guneralp, I., & Paulus G., (2013). "Extracting river features from remotely sensed data: An evaluation of thematic correctness".

Heijmans, H. J., (1994). "Mathematical morphology as a tool for shape description". In Shape in Picture (pp. 147-176). Springer, Berlin, Heidelberg.

Hoeke, R. K., Zarrillo, G. A., & Synder, M., (2001). "A GIS based tool for extracting shorelines positions from aerial imagery (BEACHTOOLS) Coastal Engineering Technical Note IV". Washington DC: US Army Corps of Engineers (12 pp.)

Hoonhout, B., M., Radermacher, M., Baart, F., LJP Van der Maaten, (2015). "An automated method for semantic classification of regions in coastal images", *Coastal Engineering 105*, pp. 1–12.

Hord, R. M. (1982). "Digital image processing of remotely sensed data". Elsevier.

Hu, X., & Tao, V. (2007). "Automatic extraction of main road centerlines from high resolution satellite imagery using hierarchical grouping". *Photogrammetric Engineering and Remote Sensing*, 73(9), 1049.

Huang, H., Chen, Y., Clinton, N., Wang, J., Wang, X., Liu, C., Gong, P., Yang, J., Bai, Y., Zheng, Y. and Zhu, Z. (2017). "Mapping major land cover dynamics in Beijing using all Landsat images in Google Earth Engine". *Remote Sensing of Environment*, 202, 166-176.

Huang, X., Han, X., Zhang, L., Gong, J., W. Liao, J. A. Benediktsson, (2016). "Generalized Differential Morphological Profiles for Remote Sensing Image Classification", *IEEE Journal of Selected Topics in Applied Earth Observations and Remote Sensing,* vol. 9, no. 4, pp. 1736-1751.

Huang, X., Xie, C., Fang, X., and Zhang, L., (2015) "Combining Pixel- and Object-Based Machine Learning for Identification of Water-Body Types From Urban High Resolution Remote Sensing Imagery", *IEEE Journal of selected topics in applied earth observations and remote sensing*, Vol. 8, No. 5, pp: 2097- 2109.

Huang, X., Xuehua, G., Benediktsson, J. A., Zhang, L., Li Jun, (2014). "Multiple morphological profiles from multicomponent base images for hyperspectral image classification", *IEEE Journal of Selected Topics in Applied Earth Observations and Remote Sensing,* pp. 4653-4669.

Huang, X., Zhang, L., and Wang, L., (2009). "Evaluation of morphological texture features for mangrove forest mapping and species discrimination using multispectral IKONOS imagery", *IEEE Geosci. Remote Sens. Lett.*, vol.6, no. 3, pp. 393–397.

Huggel C., Kaeaeb, A., Haeberli, W., Teysseire, P., Paul, F., (2002). "Remote sensing based assessment of hazards from glacier lake outbursts: a case study in the Swiss Alps". *Canadian Geotechnical Journal,* 39, 316–330.

Igbinosa, I. (2013). "Comparison of edge detection technique in image processing techniques". *International Journal of Information Technology and Electrical Engineering*, 2(1), 25-29.

Ives J., Shresta, R., Mool, P., (2010). "Formation of Glacial Lakes in the Hindu Kush–Himalayas and GLOF Risk Assessment". International Centre for Integrated Mountain Development (ICIMOD), Kathmandu, Nepal.

Jawak, S.D., Kulkarni, K., and Luis, A.J., (2015). "A Review on Extraction of Lakes from Remotely Sensed Optical Satellite Data with a Special Focus on Cryospheric Lakes", *Advances in Remote Sensing*, 4, 196-213.

Jensen, J.R. (1986). Introductory Digital Image Processing: A Remote Sensing Perspective.

Jishuang, Q., & Chao, W., (2002). "A multi-threshold based morphological approach for extraction coastal line feature in remote sensed images", Pecora 15/L& Satellite Information IV Conference (Denver, Colorado), ISPRS Commission I/FIEOS (pp. 319–338).

Joshi, S. R., & Koju, R. (2012). "Study and comparison of edge detection algorithms". In Internet (AH-ICI), 2012 *Third Asian Himalayas International Conference* (pp. 1-5). IEEE.

Kääb, A., & Leprince, S. (2014). "Motion detection using near-simultaneous satellite acquisitions". *Remote sensing of environment*, 154, 164-179

Kampouraki, M., Wood, G. A., & Brewer, T. R. (2008). "Opportunities and limitations of object based image analysis for detecting urban impervious and vegetated surfaces using true-colour aerial photography". In Object-Based Image Analysis (pp. 555-569). Springer, Berlin, Heidelberg.

Kar, S. A., & Kelkar, V. V. (2013). "Classification of Multispectral satellite images". International Conference, In Advances in Technology and Engineering (ICATE*), (*pp. 1-6). IEEE.

Kettig, R. L., & Landgrebe, D. A. (1976). "Classification of multispectral image data by extraction and classification of homogeneous objects". *IEEE Transactions on geoscience Electronics*, 14(1), 19-26.

Kim, M., Madden, M., & Warner, T. A. (2009). "Forest type mapping using object-specific texture measures from multispectral Ikonos imagery". *Photogrammetric Engineering & Remote Sensing*, 75(7), 819-829.

Kowalczyk, M., Koza, P., Kupidura, P., Marciniak, J., (2008). "Application of mathematical morphology operations for simplification and improvement of correlation of image in close-range photomography". *The International Archives of the Photogrammetry, Remote Sensing and Spatial Information Sciences*, XXXVII -Part B5.

Kuleli, T., Guneroglu, A., Karsli, F., & Dihkan, M., (2011). "Automatic detection of shoreline change on coastal Ramsar wetlands of Turkey", *Ocean Engineering*, 38, 1141–1149.

Kumar, D. N. (2002). "Remote sensing applications to water resources". In Research Perspectives in Hydraulics and Water Resources Engineering (pp. 287-316).

Kumar, D. N., & Reshmidevi, T. V. (2013). Remote sensing applications in water resources. Journal of the Indian Institute of Science, 93(2), 163-188.

Kumar, M., Singh, R. K., Raju, P. L. N., & Krishnamurthy, Y. V. N. (2014). Road network extraction from high resolution multispectral satellite imagery based on object oriented techniques. ISPRS annals of the photogrammetry, Remote sensing and spatial information sciences, 2(8), 107.

Kupidura, P., (2013). "Distinction of lakes and rivers on satellite images using mathematical morphology", Biuletyn WAT Vol. LXII, Nr 3, 57-69.

La Monica G.B., Petrocchi E., Salvatore M. C., Salvatori R., Casacchia R., (2008). " A new approach to detect shoreline from satellite images'. In: Beach erosion monitoring: results from BEACHMED-e/OpTIMAL project, Enzo Pranzini & Lilian WetzelEds., Nuova grafica fiorentina, Firenze.

Lafferty J., McCallum A., and Pereira, F. C. N. (2001). "Conditional Random Fields: Probabilistic Models for Segmenting and Labeling Sequence Data," *ICML '01 Proceedings of the Eighteenth International Conference on Machine Learning,* vol. 8, no. June, pp. 282-289.

Ledda, A. (2007). "Mathematische morfologie in de beeldverwerking Mathematical Morphology in Image Processing" (Doctoral dissertation, Ghent University).

Lee J.S.J., Haralick R.M., and Shapiro L.G., (1987) "Morphological Edge Detection," *IEEE J. Robot. Automat*, vol. 3, pp. 142–156.

Lee, J. S., & Jurkevich, I. (1990). "Coastline detection and tracing in SAR images". *IEEE Transactions on Geoscience and Remote Sensing*, 28(4), 662-668.

Li, E., Femiani, J., Xu, S., Zhang, X., & Wonka, P. (2015). "Robust rooftop extraction from visible band images using higher order CRF". *IEEE Transactions on Geoscience and Remote Sensing*, 53(8), 4483-4495.

Li, M., Xu, L., Tang, M., (2011). "An Extraction of water body of remote sensing image based on oscillatory network", *Journal of Multimedia*, Vol. 6, No. 3. 252-260.

Li, Y., Yong, B., Wu, H., An, R. and Xu, H., (2014). "An improved top-hat filter with sloped brim for extracting ground points from airborne lidar point clouds". *Remote Sensing*, 6(12), pp.12885-12908.

Lillesand, T. M. and Kiefer, R.W., (1994), "*Remote Sensing and Image Interpretation*", 3rd Ed., John Wiley and Sons

Lillesand, T. M., Kiefer, R. W., & Chipman, J. W. (2000). Remote sensing and image interpretation. John Willey & Sons. New York, 724.

Liu, D., & Xia, F. (2010). "Assessing object-based classification: advantages and limitations". *Remote Sensing Letters*, 1(4), 187-194.

Liu, H., & Jezek, K. C. (2004). "A complete high-resolution coastline of Antarctica extracted from orthorectified Radarsat SAR imagery". *Photogrammetric Engineering & Remote Sensing*, 70(5), 605-616.

Liu, H., & Jezek, K. C. (2004). "Automated extraction of coastline from satellite imagery by integrating Canny edge detection and locally adaptive thresholding methods". *International Journal of remote sensing*, 25(5), 937-958.

Lu, D., & Weng, Q. (2007). "A survey of image classification methods and techniques for improving classification performance". *International journal of Remote sensing,* 28(5), 823-870.

Luo, J., Sheng, Y., Shen, Z., Li, J., (2010). "High-precise water extraction based on spectral-spatial coupled remote sensing information", *IGARSS (2010),* 2840-2843.

Maini, R., & Aggarwal, H. (2010). "A comprehensive review of image enhancement techniques". arXiv preprint arXiv:1003.4053.

Maiti, S., & Bhattacharya, A. K., (2009). "Shoreline change analysis and its application to prediction: A remote sensing and statistics based approach", *Marine Geology*, 57, 11–23.

Maragos, P. (1996). Differential morphology and image processing. IEEE Transactions on Image Processing, 5(6), 922-937.

MarketsandMarkets, (2013). "Unmanned Aerial Vehicle Market" (2013–2018). Technical Report. MarketsandMarkets. Dallas, TX, USA

Mason, D. C., & Davenport, I. J. (1996). "Accurate and efficient determination of the shoreline in ERS-1 SAR images". *IEEE Transactions on Geoscience and Remote Sensing*, 34(5), 1243-1253.

Mather, P. M. (2004). "*Computer Processing of Remotely-Sensed Images: An Introduction* (3rd ed.)", Chichester, England: John Wiley & Sons.

Matheron, G. (1975). *Random sets and integral geometry.* John Wiley & Sons, New York.

MathWorks. (2010). Image Processing Toolbox Page. Retrieved 2010, from The MathWorks, Inc: http://www.mathworks.com/index.html.

MathWorks. (2011). Image Processing Toolbox, Examples and Webinars, Detecting a Cell Using Image Segmentation. Retrieved 2011, from The MathWorks, Inc. WebSite:http://www.mathworks.com/products/image/demos.html?file=/products/demos/shipping/images/ipexcell.html.

http://www.dca.fee.unicamp.br/~lotufo/cursos/ia-870-2002/html/

Mayr, W., (2013). "Unmanned aerial systems—for the rest of us". *In: 54th Photogrammetric Week*. The Institute for Photogrammetry of the University of Stuttgart, pp. 151–163.

McCabe, M. F., Rodell, M., Alsdorf, D. E., Miralles, D. G., Uijlenhoet, R., Wagner, W., Lucieer A, Houborg R, Verhoest NE, Franz T.E.,& Shi, J. (2017). "The future of Earth observation in hydrology". *Hydrology and Earth System Sciences*, 21(7), 3879.

McFeeters, S. K., (1996). "The use of Normalized Difference Water Index (NDWI) in the delineation of open water features". *International Journal of Remote Sensing*, 17, 1425–1432.

Mena, J. B. (2003). "State of the art on automatic road extraction for GIS update: a novel classification". *Pattern recognition letters*, 24(16), 3037-3058.

Mergili, M., Schneider, D., Worni, R., Schneider, J.F., (2011). "Glacial Lake Outburst Floods (GLOFs): challenges in prediction and modelling". Proceedings of the 5th International Conference on Debris-Flow Hazards Mitigation: Mechanics, Prediction and Assessment, Padova, pp. 14–17.

Mishra, K., & Prasad, P. (2015). Automatic extraction of water bodies from Landsat imagery using perceptron model. Journal of Computational Environmental Sciences, 2015.

Mohajerin, N., Histon, J., Dizaji, R., & Waslander, S. L. (2014).'Feature extraction and radar track classification for detecting UAVs in civillian airspace". *In Radar Conference, IEEE* (pp. 0674-0679).

Mohammadzadeh, A., Tavakoli, A., & Zoej, M. V. (2004). "Automatic linear feature extraction of Iranian roads from high resolution multi-spectral satellite imagery". *The International Archives of the Photogrammetry, Remote Sensing and Spatial Information Sciences,* 35(3), 764-767.

Mokhtarzade, M., & Zoej, M. V. (2007). "Road detection from high-resolution satellite images using artificial neural networks". *International journal of applied earth observation and geoinformation,* 9(1), 32-40.

Möller, M., Lymburner, L., & Volk, M. (2007). "The comparison index: A tool for assessing the accuracy of image segmentation". *International Journal of Applied Earth Observation and Geoinformation,* 9(3), 311-321.

Möller, M., Lymburner, L., & Volk, M. (2007). The comparison index: A tool for assessing the accuracy of image segmentation. International Journal of Applied Earth Observation and Geoinformation, 9(3), 311-321.

Momm, H. G., and Easson, G. (2010). "Population restarting: a study case of feature extraction from remotely sensed imagery using textural information", GECCO'10: Proceedings of the 12th annual conference on Genetic and evolutionary computation, ACM, New York, NY, USA, pp. 973–974.

Momm, H., & Easson, G. (2011). Feature extraction from high-resolution remotely sensed imagery using evolutionary computation (pp. 423-442). INTECH Open Access Publisher.

Moser, G., Zerubia, J., Serpico, S. B., & Benediktsson, J. A. (2018). "Mathematical Models and Methods for Remote Sensing Image Analysis: An Introduction". In Mathematical Models for Remote Sensing Image Processing (pp. 1-36). Springer, Cham.

Mukhopadhyay S, Chanda B., (2002). "An edge preserving noise smoothing technique using multi-scale morphology". *J. Signal Processing*, 82, 527-544.

Munyati, C., (2000). "Wetland change detection on the kafue flats, zambia, by Classification of a multitemporal remote sensing image dataset", *International Journal of Remote Sensing* 21(9): 1787–1806.

Mura, D. M., (2011). "Advanced techniques based on mathematical morphology for the analysis of remote sensing images" (Doctoral dissertation, University of Trento).

Mura, M. D., Benediktsson, J.A., Waske, B. and Bruzzone, L., (2010). "Morphological attribute profiles for the analysis of very high resolution images". *IEEE Transactions on Geoscience and Remote Sensing,* 48(10), pp.3747-3762.

Naegel B., (2007). "Using mathematical morphology for the anatomical labeling of vertebrae from 3D CT-scan images". *J. Computerized Medical Imaging and Graphics,* 3,141-156.

Najman, L., & Talbot, H. (2010). "Introduction to mathematical morphology. Mathematical morphology": From theory to applications, 1-33.

Nguyen, Hai-Hoa, McAlpine, Clive, Pullar, David, Johansen, Kasper and Duke, Norman C. 2013, "The relationship of spatial-temporal changes in fringe mangrove extent and adjacent land-use: case study of Kien Giang coast, Vietnam". *Ocean & Coastal Management,* 76 12-22.

Ohlhof, T., Gulch, E., Muller, H., Wiedemann, C., & Torre, M. (2004). "Semi-automatic extraction of line and area features from aerial and satellite images". The International Archives of the Photogrammetry, Remote Sensing and Spatial Information Sciences, 34(B3), 471-476.

Ononye, A. E., Vodacek, A., & Saber, E. (2007). "Automated extraction of fire line parameters from multispectral infrared images". *Remote Sensing of Environment*, 108(2), 179-188.

Ortiz, F. Torres, E. De Juan, and N. Cuenca, (2002). "Colour mathematical morphology for neural image analysis," Real Time Imaging, vol. 8, no. 6, pp. 455–465.

Otsu, N. (1979). "A threshold selection method from gray-level histograms". *IEEE transactions on systems*, man, and cybernetics, 9(1), 62-66.

Feature Extraction Strategies Based on Mathematical Morphology for the Analysis of Remotely Sensed Imagery, PhD Thesis, 2019, NITK Surathkal, India.

143

Ouzounis, G, Soille, P., and Pesaresi, M., (2011). "Rubble detection from VHR aerial imagery data using differential morphological profiles", *inProc. 34th Int. Symp. Remote Sens. Environ*. Sydney, Australia, 1–4.

Parker, J., (1997). *Algorithms for image processing and computer vision*. Wiley.

Pesaresi, M. and Benediktsson, J.A., (2001). "A new approach for the morphological segmentation of high-resolution satellite imagery". IEEE transactions on Geoscience and Remote Sensing, 39(2), pp.309-320.

Petrie, G., (2013). "Commercial operation of lightweight UAVs for aerial imaging and mapping", *GEOInformatics*, 16, 28–39.

Ping Tian, D. (2013). A review on image feature extraction and representation techniques. International Journal of Multimedia and Ubiquitous Engineering, 8(4), 385-396.

Plaza, A., Martinez, P., Plaza, J. and Perez, R., (2005). "Dimensionality reduction and classification of hyperspectral image data using sequences of extended morphological transformations". *IEEE Transactions on Geoscience and remote sensing,* 43(3), pp.466-479.

Powers, D. M. (2007). Evaluation: From precision, recall and F-factor to ROC, informedness, markedness & correlation (Tech. Rep.). Adelaide, Australia.

Powers, D.M.W., (2011). "Evaluation: from Precision, Recall and F-measure to ROC, Informedness, Markedness and Correlation". *Journal of Machine Learning Technologies*, 2(1), 37-63.

Puissant, A., S. Lefèvre, J. Weber, 2008. "Coastline extraction in VHR imagery using mathematical morphology with spatial and spectral knowledge", The International Archives of the Photogrammetry, Remote Sensing and Spatial Information Sciences. Vol. XXXVII. Part B8. Beijing, pp-1305-1309.

Quackenbush, L. J. (2004). A review of techniques for extracting linear features from imagery. Photogrammetric Engineering & Remote Sensing, 70(12), 1383-1392.

Ramiya, A. M., Nidamanuri, R. R., & Krishnan, R. (2016). Object-oriented semantic labelling of spectral–spatial LiDAR point cloud for urban land cover classification and buildings detection. Geocarto International, 31(2), 121-139.

Ramiya, A. M., Nidamanuri, R. R., & Krishnan, R. (2016). Object-oriented semantic labelling of spectral–spatial LiDAR point cloud for urban land cover classification and buildings detection. Geocarto International, 31(2), 121-139.

Rathi, V. G. P., & Palani, D. S. (2012). "A novel approach for feature extraction and selection on MRI images for brain tumor classification". In Int Conf Comp Sci Eng Appl (pp. 225-234).

Richards J. A. and Jia, X., (2013). *Remote Sensing Digital Image Analysis: An Introduction*, Springer-Verlag Berlin Heidelberg.

Robert, A. S. (2007). Remote sensing: Models and methods for image processing. By Elsevier Inc. All rights reserved, p300-304.

Ronse, C., Najman, L., & Decencière, E. (Eds.). (2006). Mathematical morphology: 40 years on: proceedings of the 7th International Symposium on Mathematical Morphology, April 18-20, 2005 (Vol. 30). Springer Science & Business Media.

Rosenfield A. and Davis L. S., (1979). "Image segmentation and image model," Proceedings of IEEE, vol. 67, no. 5, pp. 764-772,

S. Beucher, (1992). "The Watershed Transformation Applied to Image Segmentation," in *Proceedings of the 10th Pfefferkorn Conference on Signal and Image Processing in Microscopy and Microanalysis*, pp. 299-314.

Sabins, F.F., (1997), *Remote Sensing—Principles and Interpretation*. 3rd Edition, W.H. Freeman, New York, NY.

Saini, S., & Arora, K. (2014). "A study analysis on the different image segmentation techniques". *International Journal of Information & Computation Technology*, 4(14), 1445-1452.

Sebari I. and Dong-Chen, (2013). "Automatic fuzzy object-based analysis of VHSR images for urban objects extraction", *ISPRS Journal of Photogrammetry and Rem. Sensing*, 79, 171–184

Serra, J. C., (1988). "Image Analysis and Mathematical Morphology", vol.2: Theoretical Advances. Academic Press, London.

Serra, J., (1982). *Image Analysis and Mathematical Morphology*, Academic Press, London.

Seul, M., O'Gorman, L., and Sammon, M., (2001). *Practical algorithms for image analysis*. Cambridge.

Sghaier, M. O., & Lepage, R. (2016). "Road extraction from very high resolution remote sensing optical images based on texture analysis and beamlet transform". *IEEE Journal of Selected Topics in Applied Earth Observations and Remote Sensing*, 9(5), 1946-1958.

Sharma, O., Mioc D., Franc¸ Anton F. O., (2008), "Polygon feature extraction from satellite imagery based on Colour image segmentation and medial axis", The International Archives of the Photogrammetry, Remote Sensing and Spatial Information Sciences. Vol. XXXVII. Part B3a. Beijing, 235-240.

Shaw, G. A., & Burke, H. H. K. (2003). "Spectral imaging for remote sensing". *Lincoln laboratory journal*, 14(1), 3-28.

Shih, F. Y., King, C. T. and Pu, C. C., (1995). "Pipeline architectures for recursive morphological operations", *IEEE Transactions on Image Processing*, vol. 4, no. 1, pp. 11–18.

Singh, P. P., & Garg, R. D., (2013). A hybrid approach for information extraction from high resolution satellite imagery. International Journal of Image and Graphics, 13(02), 1340007.

Sklansky, J. (1978). "Image segmentation and feature extraction". *IEEE Transactions on Systems, Man, and Cybernetics*, 8(4), 237-247.

Soille P., (1999). *Morphological image analysis: principles and applications*, Springer-Verlag, Berlin Heidelberg, ISBN 978-3-662-05088-0.

Soille, P (2008). "Constrained connectivity for hierarchical image partitioning and simplification", *IEEE Trans. Pattern Anal. Mach. Intell.*, vol. 30, no. 7, pp. 1132–1145.

Soille, P. (2009, September). Recent developments in morphological image processing for remote sensing. In Image and Signal Processing for Remote Sensing XV (Vol. 7477, p. 747702). International Society for Optics and Photonics.

Soille, P., & Talbot, H. (1998, August). Image structure orientation using mathematical morphology. In Proceedings. Fourteenth International Conference on Pattern Recognition (Cat. No. 98EX170) (Vol. 2, pp. 1467-1469). IEEE.

Soille, P., (2003). *Morphological Image Analysis: Principles and Applications*, 2nd ed. Berlin, Germany: Springer-Verlag.

Soille, P., and Pesaresi, M., (2002), "Advances in mathematical morphology applied to geoscience and remote sensing," *IEEE Trans. Geosci. Remote Sens.,* vol. 40, no. 9, pp. 2042–2055, Sep. 2002

Song C., Bo Huang, Linghong Ke, Richards K. S., (2014). "Remote sensing of alpine lake water environment changes on the Tibetan Plateau and surroundings: A review", *ISPRS Journal of Photogrammetry and Remote Sensing*, 92, 26–37.

Stankov K. and He D. C., (2013). "Building detection in very high spatial resolution multispectral images using the hit-or-miss transform", *IEEE Geosci. Remote Sens. Lett.,* vol. 10, no. 1, pp. 86–90.

Stroppa, R. G., Leonardi, F., & da Silva, E. A. (2010)."Digital Image Processing using techniques of mathematical morphology". In *Proceedings of 3rd International Mutil-Conference on Engeneering and Technological Innovation. International Institute of Informatics and Systemics, Orlando*.

Tarabalka, Y., Chanussot, J. and Benediktsson, J. A. (2010). "Segmentation and classification of hyperspectral images using watershed transformation*", Pattern Recognit.*, vol. 43, no. 7, pp. 2367–2379.

Thakur, R. S., & Dikshit, O. (1997). "Contextual classification with IRS LISS-II imagery. ISPRS journal of photogrammetry and remote sensing", 52(2), 92-100.

Tian, Y., Guo, P., & Lyu, M. R. (2005). "Comparative studies on feature extraction methods for multispectral remote sensing image classification". In Systems, Man and Cybernetics, 2005 IEEE International Conference on (Vol. 2, pp. 1275-1279). IEEE.

Transon, J., d'Andrimont, R., Maugnard, A., & Defourny, P. (2018). "Survey of Hyperspectral Earth Observation Applications from Space in the Sentinel-2 Context". *Remote Sensing*, 10(2), 157.

Valero, S., Chanussot, J., Benediktsson, J. A., Talbot, H., & Waske, B. (2010). "Advanced directional mathematical morphology for the detection of the road

network in very high resolution remote sensing images". *Pattern Recognition Letters,* 31(10), 1120-1127.

Valero, S., Chanussot, J., Benediktsson, J. A., Talbot, H., & Waske, B. (2010). Advanced directional mathematical morphology for the detection of the road network in very high resolution remote sensing images. Pattern Recognition Letters, 31(10), 1120-1127.

Van Droogenbroeck, M., & Buckley, M. J. (2005). "Morphological erosions and openings: fast algorithms based on anchors". *Journal of Mathematical Imaging and Vision*, 22(2-3), 121-142.

Velasco-Forero S and Angulo J. (2010). "Hit-or-miss transform in multivariate images", in Proc. Adv. Concepts Intell. Vis. Syst., Sydney, Australia, pp. 452–463.

Velasco-Forero, S., & Angulo, J. (2010). "Parameters selection of morphological scale-space decomposition for hyperspectral images using tensor modelling". In Algorithms and Technologies for Multispectral, Hyperspectral, and Ultraspectral Imagery XVI (Vol. 7695, p. 76951B). International Society for Optics and Photonics.

Vincent, L. (1993) Morphological grayscale reconstruction in image analysis: "Applications and efficient algorithms". *IEEE Transactions on Image Processing,* 2, 176-201,

Vincent, L., & Soille, P. (1991). "Watersheds in digital spaces: an efficient algorithm based on immersion simulations". *IEEE Transactions on Pattern Analysis & Machine Intelligence*, (6), 583-598.

Wang C, Jie Zhang and Yi Ma, (2010). "Coastline interpretation from multispectral remote sensing images using an association rule algorithm", *International Journal of Remote Sensing* Vol. 31, No. 24, 6409–6423.

Wang, H., Pan, L., Zheng H., (2008). "Multi-texture-model for water extraction based on remote sensing image", *Proc. of 2008 Congress on Image and Signal processing*. IEEE computer society.

Wang, J., Cheng, W., Luo, W., Zheng, X. and Zhou, C., (2017). "An Iterative Black Top Hat Transform Algorithm for the Volume Estimation of Lunar Impact Craters". *Remote Sensing*, 9(9), pp.952.

Wang, W., Yang, N., Zhang, Y., Wang, F., Cao, T., & Eklund, P. (2016). "A review of road extraction from remote sensing images". *Journal of Traffic and Transportation Engineering (English Edition)*, 3(3), 271-282.

Weszka, J. S., (1978). "A Survey of Threshold Selection Techniques," *Computer Graphics and Image Processing*, vol. 7, no. 2, pp. 259-265.

White, K., & El Asmar, H., 1999. "Monitoring changing position of coastlines using Thematic Mapper imagery, and example from the Nile Delta". *Geomorphology*, 29, 93–105.

Woodcock C. E., and Strahler A. H., (1987). "The Factor of Scale in Remote Sensing," *Remote Sensing of Environment*, vol. 21, no. 3, pp. 311-332.

Xiao, Y., Lim, S. K., Tan, T. S., & Tay, S. C. (2004). "Feature extraction using very high resolution satellite imagery". In Geoscience and Remote Sensing Symposium, IGARSS'04. Proceedings, (Vol. 3). IEEE.

Xu, H., (2006). "Modification of normalized difference water index (NDWI) to enhance open water features in remotely sensed imagery". *International Journal of Remote Sensing,* 27, 3025–3033.

Yan, L., Roy, D.P., (2014), "Automated crop field extraction from multi-temporal Web Enabled Landsat Data", *Remote Sensing of Environment*, 144, 42–64.

Yang, Y., & Newsam, S. (2010, November). Bag-of-visual-words and spatial extensions for land-use classification. *In Proceedings of the 18th SIGSPATIAL international conference on advances in geographic information systems, ACM*, pp. 270-279.

Zadeh L. A., (1965). "Fuzzy sets", *Information and Control*, vol. 8, no. 3, pp. 338-353.

Zanin, R. B., Martins, E.F.O., Poz, A.P., (2013). "Automatic extraction of rivers in satellite images using geometric active contours", *Geografia,* vol. 38, 171-190.

Zhang, L., Zhang, L., Tao, D., & Huang, X. (2012). "On combining multiple features for hyperspectral remote sensing image classification", *IEEE Transactions on Geoscience and Remote Sensing*, 50(3), 879-893.

Zhou, Jiancheng L., Zhanfeng S., Xiaodong Hu, and Yang, H., (2014). "Multiscale Water Body Extraction in Urban Environments from Satellite Images", *IEEE Journal of selected topics in applied earth observations and remote sensing,* vol. 7, no.10, pp- 4301

Zhu, X. X., Tuia, D., Mou, L., Xia, G. S., Zhang, L., Xu, F., & Fraundorfer, F. (2017). Deep learning in remote sensing: A comprehensive review and list of resources. IEEE Geoscience and Remote Sensing Magazine, 5(4), 8-36.

I.   SHORELINE EXTRACTION

```matlab
%% Initialization
    SE1 = 40;        % SE declaration/ initialization
    SE2 = 15;
    SE3 = 1;
    P = 100          % Variable for unwanted object or noise removal

%% Input imagery

    I  = uigetfile({'*.*'},'Load Matlab File');
    fg = imread(I);
%       fg = imread ('cart2_mang_shore.tif'); % For direct read

%% Reading size of the image
    [R,C] = size (fg);
%% PreProcessing
    f1 = medfilt2 (fg, [3, 3]);

%% resolution

    prompt = 'Please mention spatial resolution of the input
    image?\n, enter 1 if Veryhigh(>1m), 2 if  high(1-5m), 3 if
    moderate(5-25m), 4 if sparse(>25)\n, Plaease enter any value 1
    to 4\n';

    Resln = input (prompt);

%% MM operations
    SE = strel ('disk', SE1);
    FTB = (f1 + imtophat (f1, SE))-imbothat (f1, SE);
    f3 = mmopenrec (FTB, mmsedisk (SE2), mmsebox);

%% Auto thresholding,
%% 'otherwise' section will consider image size into account

  switch Res
     case '1'
      X1 = im2bw (f3, 0.995);
     case '2'
      X1 = im2bw (f3, 0.9);
     case '3'
      X1 = im2bw (f3, 0.70);
     case '4'
      X1 = im2bw (f3, 0.45);
     Otherwise
      if(Resln == 1 ) ||(C < 3000)|| (R< 3000)
          X1 = im2bw (f3, 0.975);
      end
```

```
    if (Resln == 2) && (C < 5000)||(R< 5000)
     X1 = im2bw (f3, 0.9);
    end
     if (Resln==3||4)&& (C < 9000)||(R< 9000 )&&(C > 5000)&&(R >
    5000))
         X1 = im2bw (f3, 0.6);
    end
    if ((Res==3||4)&&(C < 5000)||R <15000)&&(C > 9000)&& R > 9000))
         X1 = im2bw (f3, 0.5);
    end
    if (Resln == 4)||(C > 15000)|| (R > 15000))
         X1 = im2bw (f3, 0.45);
    End


%% Mannual Thresholding
    prompt = 'Please input the threshold value'
         th = input(prompt);
         X1 = im2bw (f3, th);
%% MM operations
         X = mmcloserec(X1,mmsedisk(SE3),mmsebox);
         X = bwareaopen(X, P);
%% Display and output file writing
    Figure, imshow(X), title('Extracted shoreline');
    imwrite(X, 'Shoreline_map.tif');
```


II.   WATERBODY EXTRACTION


```
%% Initialization
    B1 = 1;
    B2 = 1;
    B3 = 1;
%% Data
    I = uigetfile({'*.*'},'Load Matlab File');
    f = imread(I);
%   f = imread ('c2_mang.jpg');    % image: direct read

%% Get spatial resolution information

prompt = 'Please mention resolution of the input image?\n enter 1 for
Veryhigh(>1m), 2 for high(1-5m), 3 for high(5-25m), 4 for
moderate(25-60m) and 5 for sparse\n, if unspecified/unknown
resolution then use dynamic SE size\n';
Resln = input(prompt);
if(Resln == 1)
    B1 = 4;        % SE 1 size for VHR images
    B2 = 10;       % SE 2 size for VHR images
    B3 = 20;       % SE 3 size for VHR images
end
if(Resln == 2)
    B1 = 4;        % SE 1 size for HR images
    B2 = 10;       % SE 1 size for HR images
    B3 = 18;       % SE 1 size for HR images
```

Feature Extraction Strategies Based on Mathematical Morphology for the Analysis of Remotely Sensed Imagery, PhD Thesis, 2019, NITK Surathkal, India.

152

```matlab
end
if(Resln == 3)
    B1 = 2;          % SE 1 size for MR images
    B2 = 8;          % SE 1 size for MR images
    B3 = 12;         % SE 1 size for MR images
end
if(Resln == 4)       % SE 1 size for low-resolution images
    B1 = 1;
    B2 = 5;
    B3 = 10;
end
if(Resln == 5)       % SE 1 size for Sparse resolution images
    B1 = 1;
    B2 = 0.25;
    B3 = 1;
End

%% SE programming / Dynamic SE values

prompt = 'Do you want to Specify dynamic SE kernel size? \n enter 1
for Yes and 0 for No (input 0 for optimal default values) \n';
result = input(prompt);

if(result == 1)
Prompt = 'Please enter the SE size for B1, B2 and B3? \n recommended
range B1(2-4),B2(0.15-5), B3(1-20)\n specify greater value for High
resolution images';
    B1 = input(prompt);
    B2 = input(prompt);
    B3 = input(prompt);
end

%% Pre-processing for noisy images

Prompt = 'Input 1 for pre-processing, 0 to skip this step';

    Pre = input (prompt);
    If (Pre == 1)
    f1= medfilt2 (f, [3, 3]);
    End
%% core MM operations
    SE = strel('disk',B1);
    CF = (f1 + imtophat(f1,SE))-imbothat(f1,SE);
    f3 = mmopenrec (CF, mmsedisk (B2));
    f4 = mminfrec(f,f3,mmsebox);
    level = graythresh (f4);
    X1 = im2bw (f4, level);
    X = mmcloserec(X1, mmsedisk (B3));

%% Display of outcome and output file writing
    imshow(X);imwrite(X,'Extracted_waterbody.tif');
```

III.   URBAN FEATURE EXTRACTION


```matlab
%% read Aerial/satellite Data

    I = uigetfile({'*.*'},'Load Matlab File');
%   f = mmreadgray ('NITK_Surathkal_54.jpg');   % direct read
    f = imread(I);
    f = im2uint8(f);

%%   SE size specifications / Initialization of variables

    T = mean2 (f);
    B1 = round (0.1* T);  % 10 percentage value for SE1
    B2 = round (0.01* T); % 1 percentage of value for SE2
    Pixel_Limit = T/B2;

%% core operations
    se1 = strel('square',B1);
    se1 = strel('disk',B1); % for irregular features
    TH = imtophat(f,se1);
    BH = imbothat(f,se1);
    CF = ((f + TH) - BH);
    OR = mmopenrec (CF, mmsedisk (B2));
    count = 0;
    Mn = mean2(OR);
    done = false;
    while ~done
    count = count + 1;
    g = OR > Mn;
    Tnext = 0.5*(mean(OR(g))+ mean(OR(~g)));
    done  = abs(Mn-Tnext)<0.5;
    Mn = Tnext;
    end
    Th = Mn;
    g = im2bw (OR, Th/255); % binarization
%   g = mmneg(g);           % Optional step
    ope = mmero(g,mmsedisk(1));
    Fnl = mmareaopen (g, Pixel_Limit);    % area opening
    fin = mmshow(Fnl, ope);

%% Display & print outcome
    mmshow(Fnl,ope),title('Extracted urban features');
    imwrite (fin ,'Extracted urban features.jpg');
```


* * * * * * * * * * *

INTERNATIONAL JOURNALS

1. **Rishikeshan, C.A.,** & Ramesh, H. (2018). "An automated mathematical morphology driven algorithm for water body extraction from remotely sensed images." *ISPRS journal of photogrammetry and remote sensing,* 146, 11-21. Elsevier. **doi.org/10.1016/j.isprsjprs.2018.08.014**

2. **Rishikeshan, C.A.,** & Ramesh, H. (2017). "A novel mathematical morphology based algorithm for shoreline extraction from satellite images." *Geo-spatial Information Science*, 20(4), pp.345-352. (Taylor & Francis). **DOI: 10.1080/10095020.2017.1403089.**

3. **Rishikeshan C.A.,** & Ramesh, H. (2017). "An ANN supported mathematical morphology based algorithm for lakes extraction from satellite images." *ISH Journal of Hydraulic Engineering*, pp.1-8. (Taylor & Francis). **doi.org/10.1080/09715010.2017.1408040**

INTERNATIONAL CONFERENCES

1. **Rishikeshan, C.A.,** Ramesh, H. & Anjali, V. (2017), "An MM based approach for glacial lakes extraction". Extended abstract has been peer reviewed and presented in the *3rd International Conference on the Status and Future of the World's Large Rivers*, 18-21 April 2017, New Delhi, India.

2. **Rishikeshan, C.A.,** & Ramesh, H. "Automated extraction of road networks in urban areas from remote sensing imageries using mathematical morphology", has been presented in the *International conference on Urban Geoinformatics (ICUG)-2017*, TERI University, New Delhi, February 2017.

----

3. **Rishikeshan C.A.,** & Ramesh, H. "A mathematical morphology assisted approach for shoreline extraction from satellite imageries." Abstract has been reviewed and presented as a poster in the *ISRS-ISG national symposium*, held at IIRS Dehradun, December 2016.

RESUME

Name	:	Rishikeshan C A
Date of Birth	:	10.05.1988
Address	:	Gayathri Bhavan, Kattipoil Post, Nileshwar, Kasaragod – 671 314 Kerala.
Mobile	:	+91-9846952919
E-mail	:	rishikesh.ca@gmail.com
Qualifications	:	Bachelor of Engineering (Computer science and Engineering), M.Tech (Remote sensing and GIS)
Publications	:	

International journals	: 3
International conferences	: 3

Feature Extraction Strategies Based on Mathematical Morphology for the Analysis of Remotely Sensed Imagery, PhD Thesis, 2019, NITK Surathkal, India.

157